GL04004

# GEOPHYSICAL INVESTIGATION OF THE BALTAZOR HOT SPRINGS KNOWN GEOTHERMAL RESOURCE AREA AND THE PAINTED HILLS THERMAL AREA, HUMBOLDT COUNTY, NEVADA

by

Ronald K. Edquist

An abstract of a thesis submitted to the faculty of The University of Utah in partial fulfillment of the requirements for the degree of

Master of Science

in

Geophysics

Stanley H. Ward — Chairman, Supervisory Committee

Professor of Geophysics

Department of Geology and Geophysics

The University of Utah

March 1981

## ABSTRACT

This report describes geophysical investigations of the Baltazor Hot Springs KGRA and the Painted Hills thermal area, Humboldt Co., Nevada. The study includes a gravity survey of 284 stations covering 750 sq km, numerical modeling and interpretation of five detailed gravity profiles, numerical modeling and interpretation of 21.8 line-km of dipole-dipole electrical resistivity data along four profiles, and a qualitative interpretation of 38 line-km of self-potential data along eight profiles. The primary purpose of the investigation is to try to determine the nature of the geologic controls of the thermal anomalies at the two areas.

At Baltazor KGRA, the control is interpreted to be a narrow, north-trending Basin and Range structure which has as much as 610 m of alluvial fill in a narrow graben. The faulting associated with this Basin and Range structure is interpreted as tapping aquifers in the Steens Basalt which contain thermal fluids at elevated temperatures. The main thermal activity at Baltazor KGRA is localized along the west side of Continental Lake Valley by a north-trending, range-bounding fault zone. This fault zone has expression in the gravity and resistivity data, as well as being coincident with an approximately 100 mv self-potential anomaly.

The primary geologic features at the Painted Hills area are, 1) a thick sequence (up to 760 m) of low density, low resistivity, tuffaceous rocks (Thousand Creek Formation) bordering the Rock Spring

Table on the east, and 2) a high density zone marginal to the Table which is interpreted as an area of intense alteration or possibly a rhyolitic intrusive. The data are insufficient to determine a likely cause of the thermal anomaly here, but one good possibility is that the thermal gradient is related to the intensity of alteration. The physiography of the Painted Hills area is more typical of the plateau regions to the west and north rather than of the Basin and Range Province. This change of physiography within the study area is apparent in the gravity maps.

The gravity data cover a sufficient area such that features of a more regional scale have expression in gravity maps encompassing both Baltazor KGRA and the Painted Hills thermal area. A 30 mgal gravity low in Thousand Creek Valley is modeled in cross section as up to 3 km of post-Miocene tuffaceous volcanic and sedimentary basin fill. This fill overlies Steens Basalt which dips approximately 10° to the southwest from the surface exposure in the Pueblo Mountains. From the cross section modeling, Bog Hot Springs, like Baltazor Hot Springs, appears to be controlled by the location of recent faults which tap aquifers in the Steens Basalt. A low in the gravity data that extends northeast from the Painted Hills area through the narrow playa valley containing Baltazor Hot Springs is interpreted as the extension of a prominent topographic linear that begins 104 km to the southwest at the Soldier Meadow Hot Springs. This suggests that the thermal anomalies at these areas may be generically related and that this linear may be a good geothermal exploration target.

Similarly, the Eugene-Denio fault zone, a proposed belt of transform faulting marginal to the Basin and Range province, projects

through the northeastern portion of the study area. The fault zone appears to have expression in the gravity data and it has been noted in previous geologic work. The fault zone appears to be important at Baltazor Hot Springs and hence it may be an important exploration guide elsewhere.

# GEOPHYSICAL INVESTIGATION OF THE BALTAZOR HOT SPRINGS KNOWN GEOTHERMAL RESOURCE AREA AND THE PAINTED HILLS THERMAL AREA, HUMBOLDT COUNTY, NEVADA

by

Ronald K. Edquist

A thesis submitted to the faculty of The
University of Utah in partial fulfillment of the requirements
for the degree of

Master of Science

in

Geophysics

Department of Geology and Geophysics

The University of Utah

March 1981

ABSTRACT

This report describes geophysical investigations of the Baltazor Hot Springs KGRA and the Painted Hills thermal area, Humboldt Co., Nevada. The study includes a gravity survey of 284 stations covering 750 sq km, numerical modeling and interpretation of five detailed gravity profiles, numerical modeling and interpretation of 21.8 line-km of dipole-dipole electrical resistivity data along four profiles, and a qualitative interpretation of 38 line-km of self-potential data along eight profiles. The primary purpose of the investigation is to try to determine the nature of the geologic controls of the thermal anomalies at the two areas.

At Baltazor KGRA, the control is interpreted to be a narrow, north-trending Basin and Range structure which has as much as 610 m of alluvial fill in a narrow graben. The faulting associated with this Basin and Range structure is interpreted as tapping aquifers in the Steens Basalt which contain thermal fluids at elevated temperatures. The main thermal activity at Baltazor KGRA is localized along the west side of Continental Lake Valley by a north-trending, range-bounding fault zone. This fault zone has expression in the gravity and resistivity data, as well as being coincident with an approximately 100 mv self-potential anomaly.

The primary geologic features at the Painted Hills area are, 1) a thick sequence (up to 760 m) of low density, low resistivity,

tuffaceous rocks (Thousand Creek Formation) bordering the Rock Spring Table on the east, and 2) a high density zone marginal to the Table which is interpreted as an area of intense alteration or possibly a rhyolitic intrusive. The data are insufficient to determine a likely cause of the thermal anomaly here, but one good possibility is that the thermal gradient is related to the intensity of alteration. The physiography of the Painted Hills area is more typical of the plateau regions to the west and north rather than of the Basin and Range Province. This change of physiography within the study area is apparent in the gravity maps.

The gravity data cover a sufficient area such that features of a more regional scale have expression in gravity maps encompassing both Baltazor KGRA and the Painted Hills thermal area. A 30 mgal gravity low in Thousand Creek Valley is modeled in cross section as up to 3 km of post-Miocene tuffaceous volcanic and sedimentary basin fill. This fill overlies Steens Basalt which dips approximately 10° to the southwest from the surface exposure in the Pueblo Mountains. From the cross section modeling, Bog Hot Springs, like Baltazor Hot Springs, appears to be controlled by the location of recent faults which tap aquifers in the Steens Basalt. A low in the gravity data that extends northeast from the Painted Hills area through the narrow playa valley containing Baltazor Hot Springs is interpreted as the extension of a prominent topographic linear that begins 104 km to the southwest at the Soldier Meadow Hot Springs. This suggests that the thermal anomalies at these areas may be generically related and that this linear may be a good geothermal exploration target.

Similarly, the Eugene-Denio fault zone, a proposed belt of transform faulting marginal to the Basin and Range province, projects through the northeastern portion of the study area. The fault zone appears to have expression in the gravity data and it has been noted in previous geologic work. The fault zone appears to be important at Baltazor Hot Springs and hence it may be an important exploration guide elsewhere.

CONTENTS

LIST OF ILLUSTRATIONS

Figures

## Tables

ACKNOWLEDGEMENTS

I wish to thank Dr. Stan Ward for his suggestion of this project and his guidance during the work. Dr. Howard Ross provided most of the supervision for this work and in the process taught me a great deal about professionalism.

All of the staff at ESL deserve my thanks, but in particular, Jeff Hulen for a wide range of contributions on the geology of the study area; Claron Mackleprang, Ted Glenn, Kip Smith and Bill Sill for their many helpful discussions on aspects of the geophysical surveys; Carleen Nutter for help with computer programming; Connie Pixton who did the bulk of the drafting and provided excellent guidance on various questions of presentation; and Elizabeth Bird who did most of the typing.

Ronald Greek and Laura Serpa provided valuable assistance during the data reduction phase of the study, while Ted Dustman and James Huber assisted in the collection of the data. The project was supported under Department of Energy contract number DE-AC07-80ID12079.

# INTRODUCTION

This report describes geophysical investigations at the Baltazor Hot Springs Known Geothermal Resource Area (KGRA) and the Painted Hills thermal area located, respectively, ten and twenty-nine kilometers southwest of Denio, in northwest Humboldt County, Nevada (Figure 1). The study includes a gravity survey of 284 stations covering 750 sq km, numerical modeling and interpretation of five detailed gravity profiles, numerical modeling and interpretation of 21.8 line-km of dipole-dipole electrical resistivity data, and qualitative interpretation of 38 line-km of self-potential profiles. Survey line locations are shown on Figure 2. This study was conducted under the sponsorship of the Earth Science Laboratory (ESL), University of Utah Research Institute, as part of the Industry Coupled Program of the Department of Energy/Division of Geothermal Energy.

Geothermal leases for the two thermal areas are currently held by Earth Power Production Company (EPPC) of Tulsa, Oklahoma. In 1977, EPPC initiated geothermal exploration at the Baltazor and Painted Hills areas. To date, their exploration program has consisted of a microearthquake study (Senturion Sciences, 1977), groundwater appraisal (Klein and Koenig, 1977), literature review and photogeologic mapping (Gardner and Koenig, 1978) and shallow- to moderate-depth thermal gradient drilling (EPPC, 1979, 1980; Langenkamp, 1977). In addition, Hulen (1979) completed detailed geologic and hydrothermal alteration mapping at the two thermal areas as part of the Industry Coupled Case

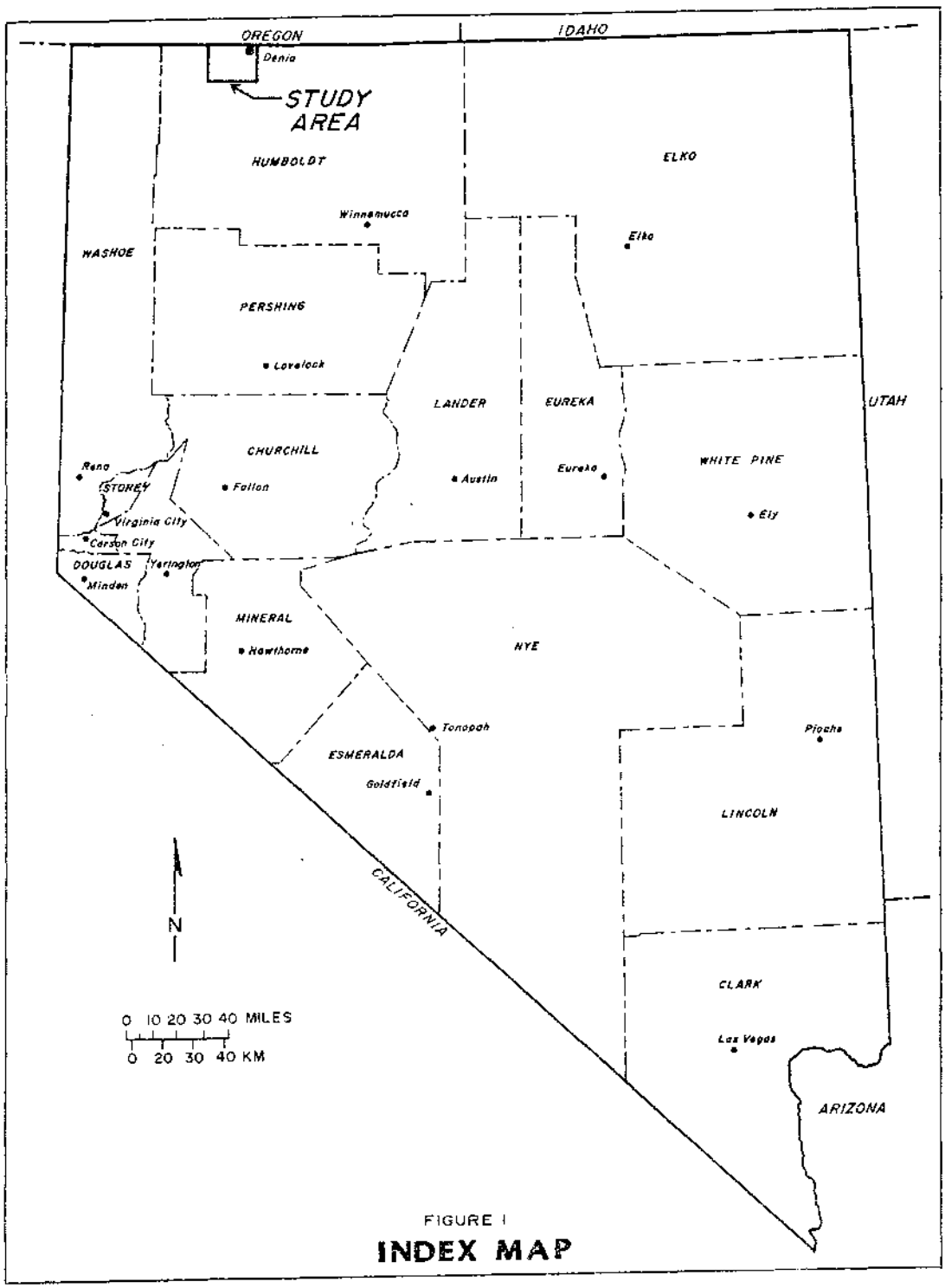


FIGURE 1

**INDEX MAP**

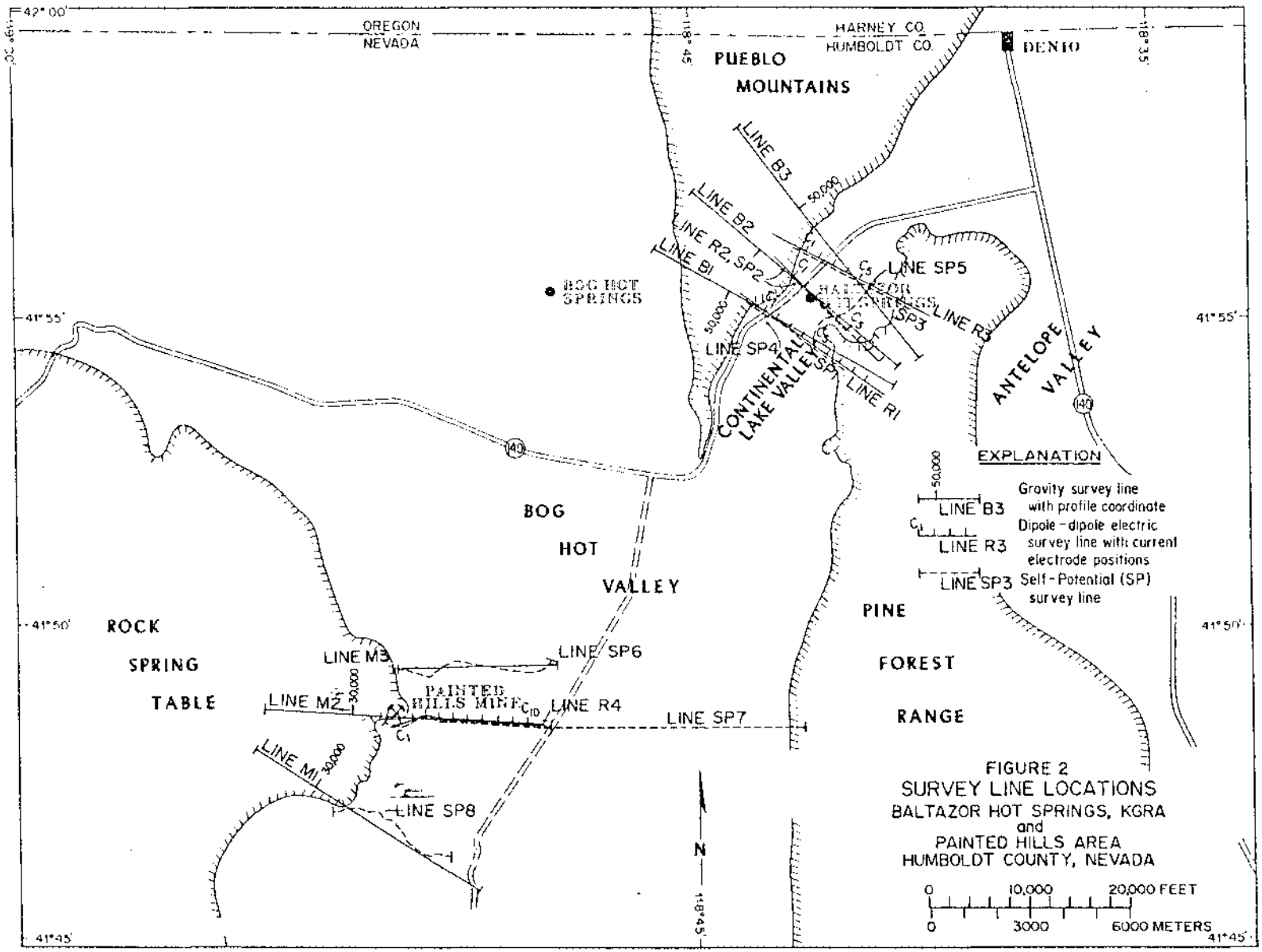
42° 00'
OREGON
NEVADA
HARNEY CO.
HUMBOLDT CO.
DENIO
PUEBLO
MOUNTAINS
118° 45'
118° 35'
LINE B3
50,000
LINE B2
LINE R2, SP2
LINE B1
LINE SP5
BOG HOT SPRINGS
BALTAZOR HOT SPRINGS
LINE SP3
LINE R3
LINE SP4
CONTINENTAL
LAKE VALLEY
LINE R1
ANTELOPE
VALLEY
140
41° 55'
EXPLANATION
Gravity survey line with profile coordinate
Dipole-dipole electric survey line with current electrode positions
Self-Potential (SP) survey line
LINE B3
LINE R3
LINE SP3
BOG
HOT
VALLEY
PINE
FOREST
RANGE
ROCK
SPRING
TABLE
41° 50'
LINE M3
LINE SP6
LINE M2
30,000
PAINTED
HILLS MINE
LINE R4
LINE SP7
LINE M1
LINE SP8
N
41° 45'
FIGURE 2
SURVEY LINE LOCATIONS
BALTAZOR HOT SPRINGS, KGRA
and
PAINTED HILLS AREA
HUMBOLDT COUNTY, NEVADA
0 10,000 20,000 FEET
0 3000 6000 METERS

Study program.

EPPC has completed approximately 12,500 ft (3811 m) of exploration drilling to date. About half of the drilling is in thermal gradient holes 300 ft (91 m) or less in depth and the balance is in four nominally 1500 ft (457 m) deep exploration holes. This work and the results of the microearthquake study are summarized on Figure 3.

The contours of the thermal gradient data on Figure 3 are taken directly from Langenkamp (1977) and this work is not critically examined in this report. Contours of thermal gradient data are ambiguous since thermal gradients can change substantially due to lithologic changes in an area that has essentially constant heat flow. Also, the contouring is poorly constrained, especially to the NE and SW at Baltazor KGRA and to the north and SW at the Painted Hills area. Hence, the contouring on Figure 3 should be used with care and in conjunction with the thermal gradient drilling logs (EPPC, 1979, 1980).

Two gravity surveys by the U.S. Geological Survey (Plouff et al., 1976; Peterson and Hoover, 1977) include stations within the study area and these are used as part of the regional data base. Aeromagnetic coverage flown at a constant barometric elevation of 9000 ft (2.74 km) is available for the area (Scintrex Mineral Surveys, 1972). The survey is regional in nature, primarily reflecting the topography, and is not used in this report. Audio-magnetotelluric data, collected at 12 stations at the Baltazor KGRA by Long and Senterfit (1977), have been open filed by the U.S. Geologic Survey without interpretation. Since the dipole-dipole resistivity survey contained in this report provides more detailed coverage and better resolution of the resistivity structure at the Baltazor KGRA than does this AMT Survey, the AMT data

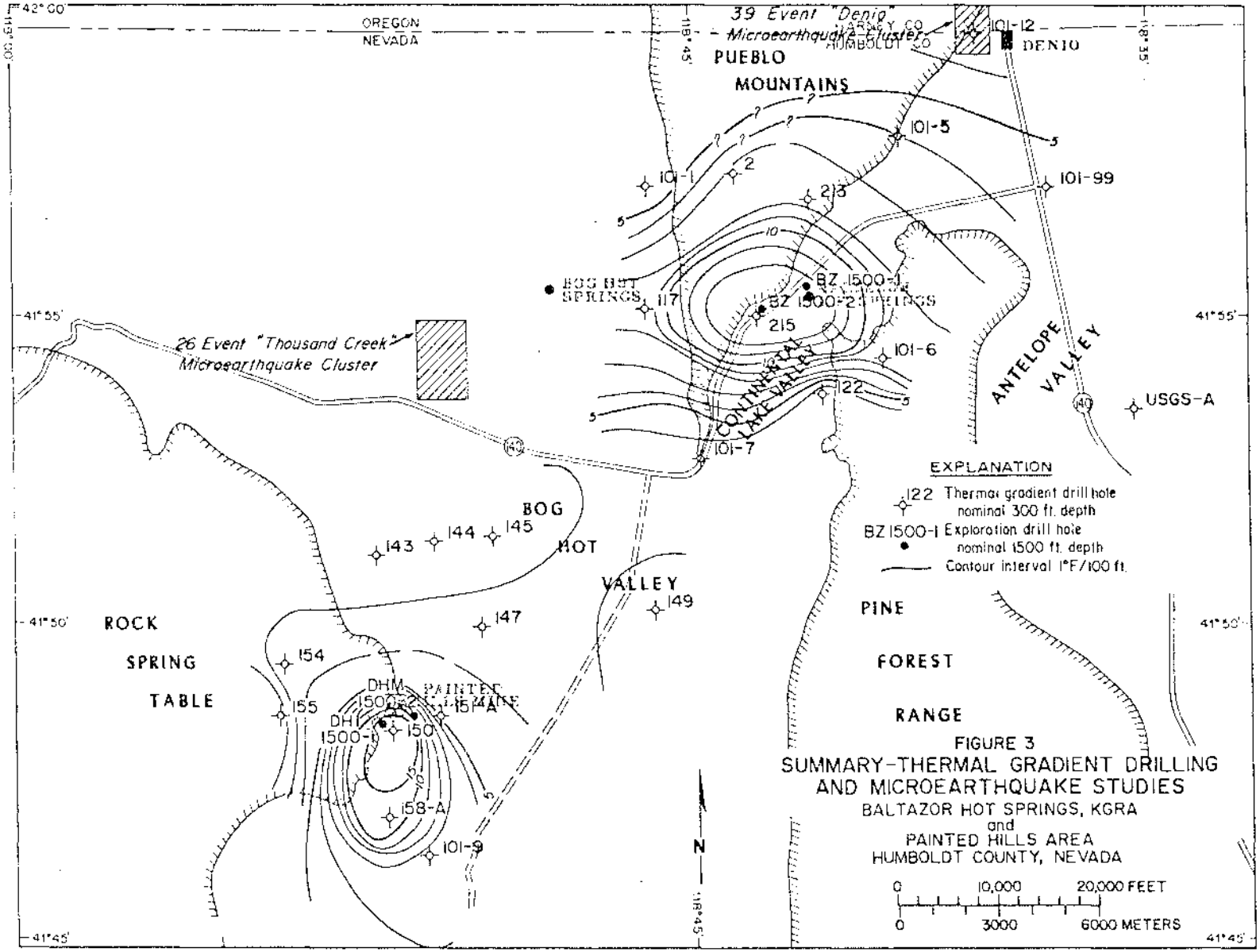
42°00'
OREGON
NEVADA
39 Event "Denio"
Microearthquake Cluster
HUMBOLDT CO
PUEBLO
MOUNTAINS
101-12
DENIO
101-5
101-1
2
213
101-99
BOG HOT SPRINGS
117
BZ 1500-1
BZ 1500-2
215
101-6
41°55'
26 Event "Thousand Creek"
Microearthquake Cluster
CONTINENTAL
LAKE VALLEY
122
ANTELOPE
VALLEY
USGS-A
40
101-7
EXPLANATION
122 Thermal gradient drill hole nominal 300 ft. depth
BZ 1500-1 Exploration drill hole nominal 1500 ft. depth
Contour interval 1°F/100 ft.
BOG
HOT
143
144
145
VALLEY
149
PINE
FOREST
RANGE
41°50'
ROCK
SPRING
TABLE
147
154
155
DHM
1500-2
PAINTED
HILLS
154A
DH
1500-1
150
158-A
101-9
N
118°45'
41°45'
FIGURE 3
SUMMARY-THERMAL GRADIENT DRILLING
AND MICROEARTHQUAKE STUDIES
BALTAZOR HOT SPRINGS, KGRA
and
PAINTED HILLS AREA
HUMBOLDT COUNTY, NEVADA
0 10,000 20,000 FEET
0 3000 6000 METERS

have not been used. However the results of the AMT and dipole-dipole surveys have been qualitatively compared and the results from the two surveys are roughly compatible.

## GEOLOGY

The following synopsis of the geology relies primarily on the work of Hulen (1979) and Gardner and Koenig (1978), to whom the interested reader is referred. Figure 4 is a generalized geologic map of the study area. The Baltazor Hot Springs KGRA and the Painted Hills thermal area are situated at the northwestern margin of the Basin and Range Province within the Battle Mountain heat-flow high (Sass and others, 1971) and about 30 miles (48 km) from the western limit of the McDermitt Caldera. The primary positive topographic features, shown on Figure 2, are the Pueblo Mountains, the Pine Forest Range and the Rock Spring Table. The Pine Forest Range and the Pueblo Mountains are northerly-trending, westward-tilted fault blocks bordered on the east by a large Basin and Range fault. They are the southern extension of the Steens Mountains in southern Oregon and contain the oldest rocks in the area - Permian to Triassic(?) metasedimentary and subordinate metavolcanic rocks. These metamorphic rocks have been intruded by Cretaceous plutonic rocks, predominantly diorite and quartz diorite, which make up the bulk of the outcrop in the Pine Forest Range.

At the Baltazor KGRA these older rocks are unconformably overlain by at least 4000 ft (1220 m) of diverse volcanic and volcaniclastic rocks that range in age from Oligocene to Recent. This sequence includes up to 2800 ft (854 m) of mid-Miocene Steens Basalt.

Recent hydrothermal alteration at Baltazor is primarily restricted to the eastern limit of the Pueblo Mountains and valley areas near the

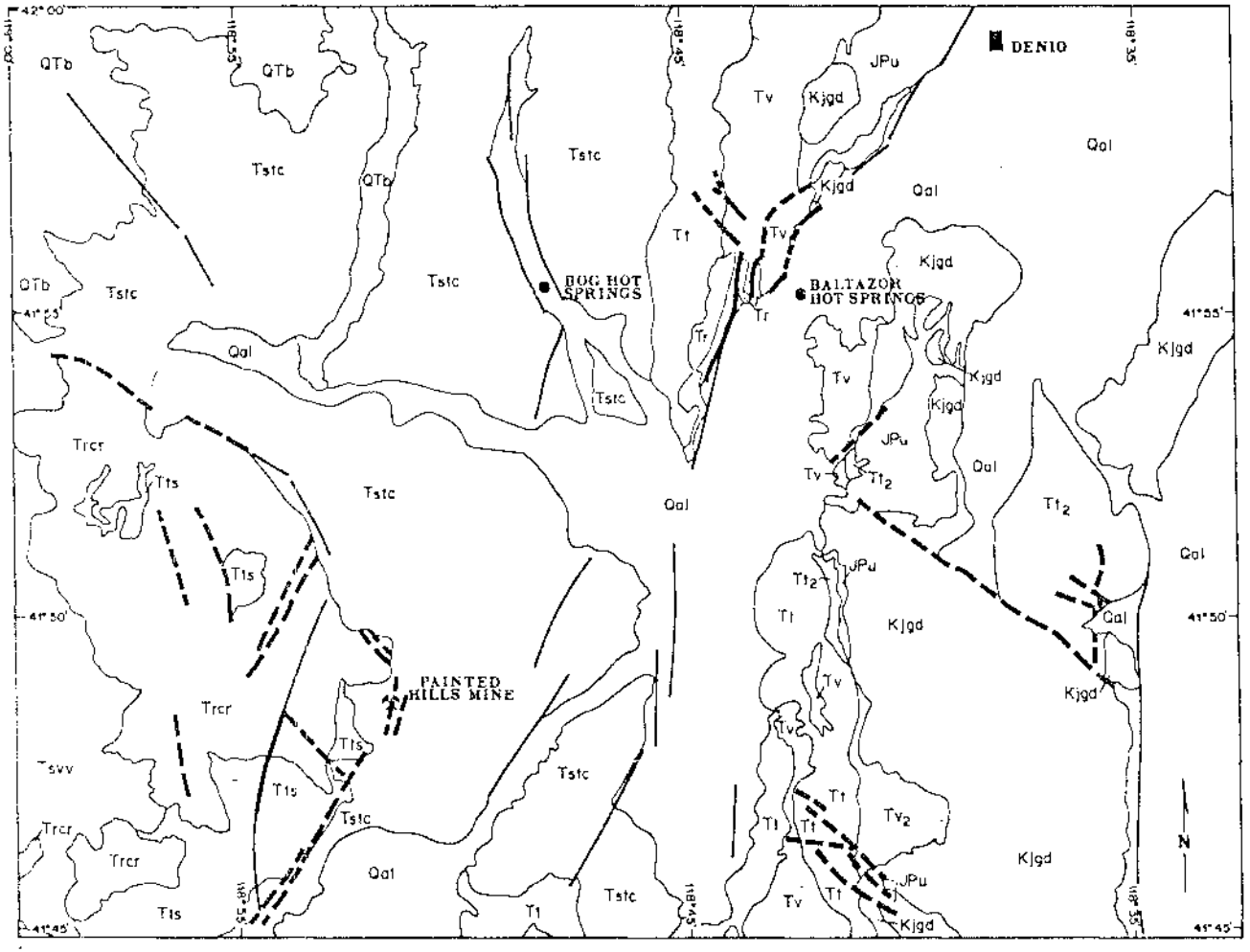


## MAPPED UNITS

QUATERNARY

- Qal — ALLUVIAL AND LACUSTRINE DEPOSITS
- QTb — YOUNGEST BASALT FLOWS
- Tstc — THOUSAND CREEK FORMATION; PREDOMINANTLY TUFFS AND TUFFACEOUS SEDIMENTS

TERTIARY

- Tf — FELSIC ASH FLOW TUFF AND TUFFACEOUS SEDIMENTS
- Tr — RHYOLITE AND RHYOLITE FLOW BRECCIA
- Tv — STEENS BASALT
- Tt2 — OLDER ASH FLOW TUFFS
- Tv2 — OLDER BASALT
- Kjgd — PLUTONIC ROCKS; PREDOMINANTLY DIORITE AND QUARTZ DIORITE, UNDIVIDED

PERMIAN TO CRETACEOUS (?) TRIASSIC (?)

- JPu — METASEDIMENTARY AND METAVOLCANIC ROCKS

(CONFORMABLE / UNCONFORMABLE)

PAINTED HILLS AREA ONLY

- Tsvv — VIRGIN VALLEY FORMATION; PREDOMINENTLY FLUVIOLACUSTRINE TUFFACEOUS SEDIMENTS
- Trcr — CANYON RHYOLITE; RHYOLITE FLOWS, FLOW-BRECCIAS AND TUFFS
- Tts — TUFFS AND TUFFACEOUS SEDIMENTARY ROCKS

## MAP SYMBOLS

- MAJOR MAPPED FAULT; DASHED WHERE APPROXIMATE
- MAJOR PHOTO-LINEAR
- APPROXIMATE CONTACT

*Modified from Hulen (1979) and from compilation by Gardner and Koenig (1978) after Wilden (1961), Wendell (1969), Rowe (1971), Burnham (1971), Bryant (1969), Grolchen (1972) and Smith (1973)*

FIGURE 4
GENERALIZED GEOLOGIC MAP
BALTAZOR HOT SPRINGS, KGRA
and
PAINTED HILLS AREA
HUMBOLDT COUNTY, NEVADA

0 10,000 20,000 FEET
0 3000 6000 METERS

hot springs. Calcite veins, locally accompanied by chalcedony and by bleaching and argillization of the host rocks, characterize the alteration. A few small opaline sinter mounds, locally calcite-bearing, are distributed around Baltazor Hot Springs.

The Painted Hills area is located along the northeast margin of the Rock Spring Table, one of the high volcanic plateaus of northwestern Nevada and south-central Oregon that form a transition zone between the Basin and Range Province and the Columbia Plateau (Bonham, 1969). Only Tertiary (mid-Miocene and younger) volcanic and volcaniclastic rocks are exposed here and correlation with sequences of similar age at Baltazor KGRA is not clear.

Hydrothermal alteration at the Painted Hills area is widespread, primarily occurs in tuffaceous sedimentary rocks, and includes silicification, argillization and hematization. This alteration is most intensely developed in the vicinity of the Painted Hills "Mine", a small fracture-controlled mercury prospect.

## GRAVITY SURVEY

### Data Acquisition and Reduction

A total of 284 gravity stations is included in the survey area, of which 194 are newly collected by the author. Thirty-one stations are from Peterson and Hoover (1977) and 58 are from Plouff et al. (1976). The principal facts are given in Appendix I while Figure 5 shows station locations. Of these new stations, 136 are along six pre-selected gravity profiles, while the balance were selected to augment the regional data base.

At Baltazor KGRA horizontal control was established with chained picket lines with 500 ft (152. m) station spacing. Vertical control was established with a Kern self-leveling level with the exception of eight stations in areas of steep topography where a Kern 30" theodolite was used. At the Painted Hills area, profile points were located on generally east-west roads at either 0.1 mile or 0.2 mile (160 or 320 m) intervals using a truck odometer. The odometer was checked against known distances and was accurate to the degree of readability of the meter (about 0.03 miles or about 50 m). The Kern level was used for vertical control on all points except for the ten most western stations on line M1 and the four most western stations on line M2, in which instances the theodolite was used.

Gravity data was collected with the University of Utah LaCoste and Romberg model G no. 264 gravity meter which has an accuracy of 0.001 mgal, a reading precision of about 0.005 mgal and essentially no

instrument drift. Using two field base stations, readings were tied to a master base station at Denio, Nevada. Gravity loops on base stations were closed on most points, including all profile points, in less than 2 1/2 hours. The exceptions, stations in relatively inaccessible areas, are A37 through A46 and A09 through A22 (see Appendix I).

Reduction of the gravity data was made with the University of Utah Univac 1108 computer using standard routines available at the Department of Geology and Geophysics. The simple Bouguer anomaly values were calculated by assuming linear drift between gravity base station ties, subtracting the theoretical gravity at sea level which was calculated using the International Gravity Formula (Swick, 1942), and, finally, correcting for elevation relative to a datum using the free air correction of 0.09406 mgal/ft and a Bouguer slab correction based on a selected density. The datum chosen in this study was sea level and Bouguer densities of 2.67 and 2.45 g/cc were used. The software was modified to reduce the 89 stations selected from other surveys using the observed gravity listed in the principal facts publications noted above.

Terrain-corrected values for all stations were computed utilizing a computer algorithm modified by R. H. Godson (U.S.G.S.) from the original program of Plouff (1977). It has been adapted by Serpa (1980) for use on the University's system. Gabbert (1980) gives a good discussion of this program. The corrections were calculated for radial distances of 0 to 104 miles (167 km) and of 0.56 to 104 miles (0.895 to 167 km) and tabulated as inner zone, outer zone and total terrain correction. Hand-calculated inner zone terrain corrections (zones A through F) using a Hammer Chart template were then made on all profile

points with a machine-calculated terrain correction of more than 0.1 mgal. In cases of less than 0.1 mgal, inner zone corrections by machine were essentially the same as by hand. For regional data base points, all stations in areas of significant topography or with an inner zone machine correction of more than a few tenths of a milligal were checked by hand.

## Accuracy

The instrument drift of the LaCoste and Romberg gravimeter is negligible, about 0.1 to 0.2 mgals per month (K. L. Cook, pers. com.). Hence, drift correction served to compensate for earth tide variations. The maximum change due to tidal effects is about 0.3 mgals in 6 hours (Nettleton, 1976). Using a linear drift correction and a loop time of 2 1/2 hours or less, the maximum possible error is about 0.06 mgals, although it is almost always much less. Since the instrument has a repeatability of about 0.005 mgal, reading errors on the order of 0.02 mgal are not expected in normal circumstances. In the survey area gravity changes with latitude at a rate of 1.30 mgal/mile. On the profiles, horizontal control is relatively high and the profiles trend westerly, so mislocation errors are small ($<<$0.1 mgal). Precision in level surveys varied from about 0.1 to 0.3 vertical feet per mile (0.02 to 0.06 m per km) of traverse. Hence, there is no appreciable error in gravity values due to vertical control for profile stations on level lines. The level was used in areas of subdued topography. Hence, inner-zone terrain corrections for these stations were small and not liable to errors in excess of about 0.05 mgals. The accuracy of outer-zone corrections done by computer is debatable, but as they are precise no error is attributed to them.

Elevation accuracy deteriorated in steeper areas on the ends of profiles where the theodolite was used for vertical control and terrain corrections were large. Vertical control was probably good to within a few feet (± 1 m) especially at the Painted Hills area, but a five- to ten-foot (1 to 3 m) error would have been hard to detect in a few cases at Baltazor KGRA where topographic features were used as elevation checks. Hand-calculated terrain corrections can vary appreciably. Ten percent is a commonly used figure, but 15 to 20% is probably more appropriate in very rugged areas. Assuming a maximum error of 0.6 mgals due to elevation errors (about 10 ft or 3 m) and as much as a 0.4 mgal error for the largest terrain correction, the worst possible combined error at the ends of profile lines could be as much as 1 mgal.

The accuracy of vertical and horizontal control of other points varies substantially, as in most regional surveys. Hence, the principal facts for the gravity survey, presented in Appendix I, include a four-digit accuracy code assigned to each station.

In summary, the accuracy of the gravity values is determined by the vertical control and the inner zone terrain correction. The accuracy of centrally located stations on level lines is probably within 0.1 mgal and certainly within 0.3 mgals. At the edges of profiles the accuracy is somewhat less, especially at Baltazor, and the worst error could be as much as 1 mgal in an area that has substantial relief. The accuracy of regional data points varies greatly. Points located at survey benchmarks are highly accurate, but points in inaccessable areas using topographic features for location and barometric altimeters for elevation control could be in error by more than 1 mgal.

## Density Determinations

Bulk wet density determinations were made on 81 samples from the study area. Table 1 summarizes these results and includes applicable results from other sources, while Appendix II describes procedures and lists individual results.

For reduction purposes a specific gravity of 2.67 g/cc (typical of crystalline basement rocks) was used for gravity plan maps covering the entire study area and for gravity profile interpretations at the Baltazor area. This is slightly higher than the average density of 2.61 g/cc obtained for surficial grab samples of Cretaceous intrusive rocks. It is, however, within one standard deviation of the average and probably better represents the fresh rock at depth. It is also the standard value used in most regional work.

For gravity profile interpretation at the Painted Hills area, Bouguer values were determined using a specific gravity of 2.45 g/cc. No pre-Tertiary rocks are exposed here, and the exposed volcanic units generally have low densities; hence a typical value for Tertiary volcanics of 2.45 g/cc was judged to be appropriate.

## Interpretation

a) Regional. The complete Bouguer gravity anomaly map is presented in Figure 5. There are three principal features. The first ((1) of Figure 5) is a strong north-south elongate gravity high associated with the north Pine Forest Range and part of the Pueblo Mountains, herein referred to as the Strawberry Butte gravity high. The nigh extends out of the mapped area to the north and broadens to the south. It is about 8 miles (13 km) wide east-west, and has about 11 mgal of closure within the study area. The peak gravity values are

# TABLE 1

## SELECTED DENSITIES

| | PAINTED HILLS | | BALTAZOR | | CLARK (1966) | | HEALY (1966) | RATTE et al (1976) | | CARRIER (1969) |
|---|---|---|---|---|---|---|---|---|---|---|
| | Density, g/cc @ % porosity | Number of Samples | Density, g/cc @ % porosity | Number of Samples | Density g/cc | Number of Samples | Density g/cc | Density g/cc | Number of Samples | Density g/cc |
| Rhyolite | 2.25 @ 12 | 20 | 2.42 @ 10.4 | 19 | 2.37 (glass) | 15 | 2.37 | 2.37 | 20 | 2.46 (domes) 2.29 (flows) |
| Basalt, dense | - | - | 2.80 @ 3.1 | 9 | 2.77 | 11 | 2.68 | 2.61 | 30 | 2.73 |
| vesicular | - | - | 2.30 @ 16.3 | 4 | (glass) | - | - | - | - | 2.37 |
| Tuff, unaltered | 1.61* | 9 | 1.72 @ 44.4 | 1 | - | - | 1.94 | - | - | - |
| hematized | 2.01* | 5 | - | - | - | - | - | - | - | - |
| water worked | 1.76 @ 32.3 | 1 | - | - | - | - | - | - | - | - |
| hematized | 2.29 @ 3.4 | 1 | - | - | - | - | - | - | - | - |
| welded | 2.31 @ 14.5 | 1 | - | - | - | - | - | 2.26 | 27 | - |
| Intrusive (felsic) | - | - | 2.61 @ 4.0 (Qtz. diorite) | 9 | 2.67 (granite) | 155 | 2.61 (Qtz. monz.) | - | - | - |
| Metamorphic | - | - | 2.72 @ 4.3 | 3 | 2.82 (Qtz. Sercite) | 76 | - | - | - | - |
| Alluvium | - | - | - | - | 1.93 @ 45.4 | 81 | 1.94 | - | - | - |

* Dry bulk density; all others wet bulk density.

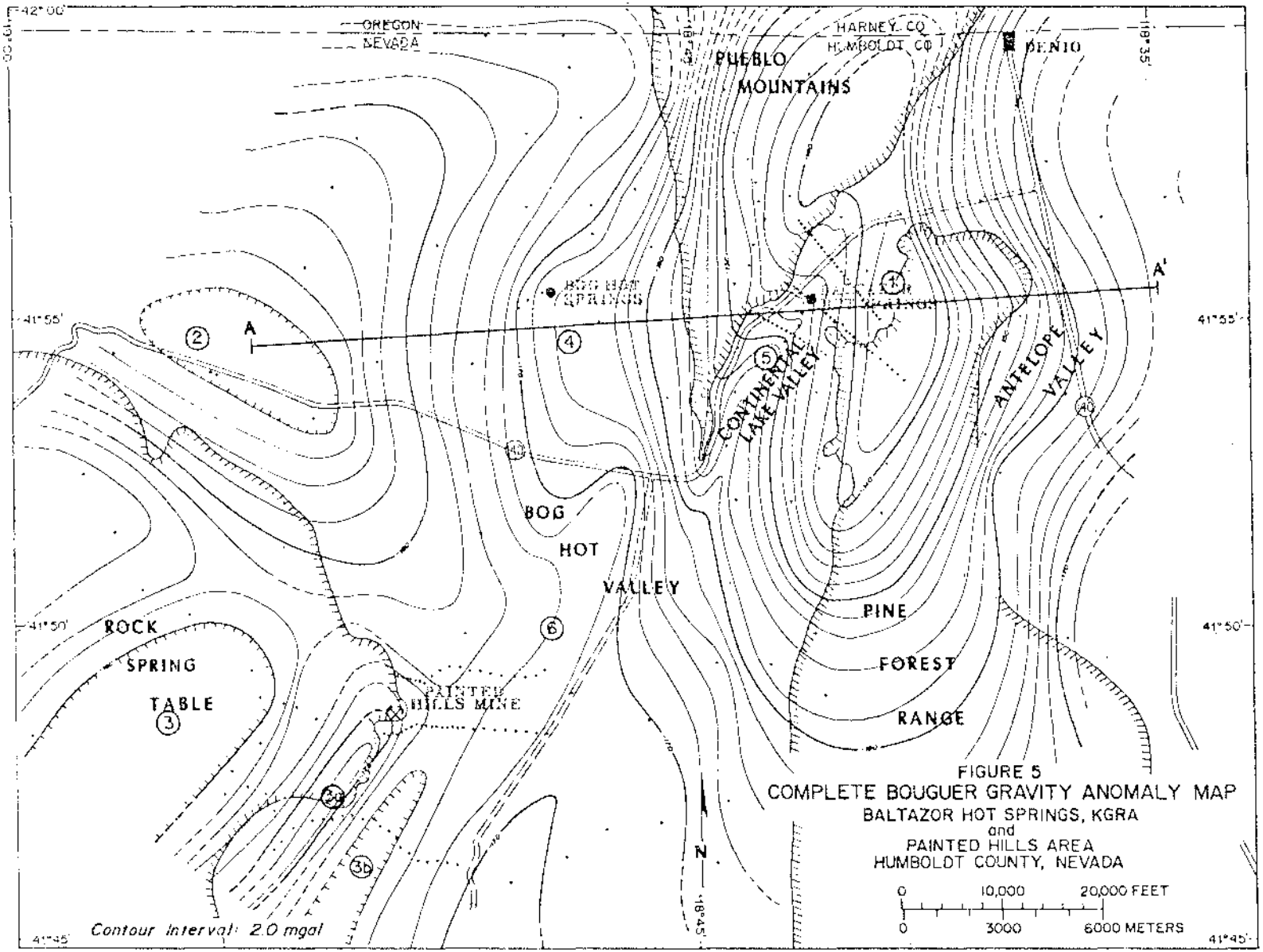


FIGURE 5
COMPLETE BOUGUER GRAVITY ANOMALY MAP
BALTAZOR HOT SPRINGS, KGRA
and
PAINTED HILLS AREA
HUMBOLDT COUNTY, NEVADA

spatially related to the surface exposure of metamorphic rocks. The high is bordered on the west by a steep gradient (up to 20 mgals in 1.5 miles or 2.4 km) that roughly parallels the west side of the Pueblo Mountains. It is bordered on the east by a steep gravity gradient (about 10 mgal/mile) associated with the range-bounding fault on the east side of the Pine Forest Range (Bryant, 1969; Gardner and Koenig, 1978).

The second principal feature, (2) of Figure 5, is a broad gravity low centered on the northwest border of the mapped area, herein called the Thousand Creek gravity low. This feature grades to the east into the Strawberry Butte high and there is a relief of about 50 mgals between the maximum and the minimum of these two features. The low is open to the northwest and bounded on the southwest by faulting associated with the northern limit of the Rock Spring Table (Wendell, 1969; Gardner and Koenig, 1978). The nature of the southeast boundary of the Thousand Creek low is not clear, but the contours indicate a continuation of the NNE-trending gravity low, (3b), that parallels the southeast boundary of the Rock Spring Table, herein called the McGee fault zone (see also (6) below).

The third feature, (3) of Figure 5, is the area of subdued gravity relief in the southwest portion of the mapped area associated with the Rock Spring Table and extending southeast to about longitude 118°45'. Imposed on this even regime is a sharp gravity high, (3a), herein referred to as the McGee gravity high. It is parallel to and on the plateau side of the McGee fault zone. It has about 8 mgal of relief, is about 1.5 mile (2.4 km) wide, and has at least 5 miles (8 km) of strike length.

Other smaller but significant features that appear on Figure 5 are:

(4) - a shelf or bench in the gravity data located in the center of the mapped area and spatially related to Bog Hot Springs.

(5) - a sharp NNE-trending gravity trough centered on Continental Lake Valley and including Baltazor Hot Springs. It is superimposed on the steep gradient on the west side of the Strawberry Butte High and, to the southwest, in Bog Hot Valley, it is truncated in this gradient. The northeast extension is poorly defined due to lack of data.

(6) - a second NE-trending gravity trough that, as mentioned above, is apparently the southeast boundary of the Thousand Creek gravity low and an extension of the McGee fault zone. This trough could be a continuation of (5) that has been offset 1 to 2 miles (2 to 3 km) by right lateral movement. If this is the case, then Baltazor Hot Springs KGRA and the Painted Hills thermal area lie in, or near, the same structural trend. This argument should be tested by additional gravity station coverage in Bog Hot Valley.

Figure 6 shows the regional profile, A-A', and the interpreted model. The location of the profile is shown on Figure 5. It extends from Antelope Valley on the east through the Strawberry Butte gravity high, across Baltazor and Bog Hot Springs, and ends in the Thousand Creek gravity low. Total relief is 52 mgal.

This profile, as well as all other gravity profiles in this report, was modeled with a gravity interpretation program package originally developed by Snow (1978). This program has been modified for interactive use and adapted to the ESL system (Nutter, 1980). Although direct search, inversion, and 2 1/2-dimension options are

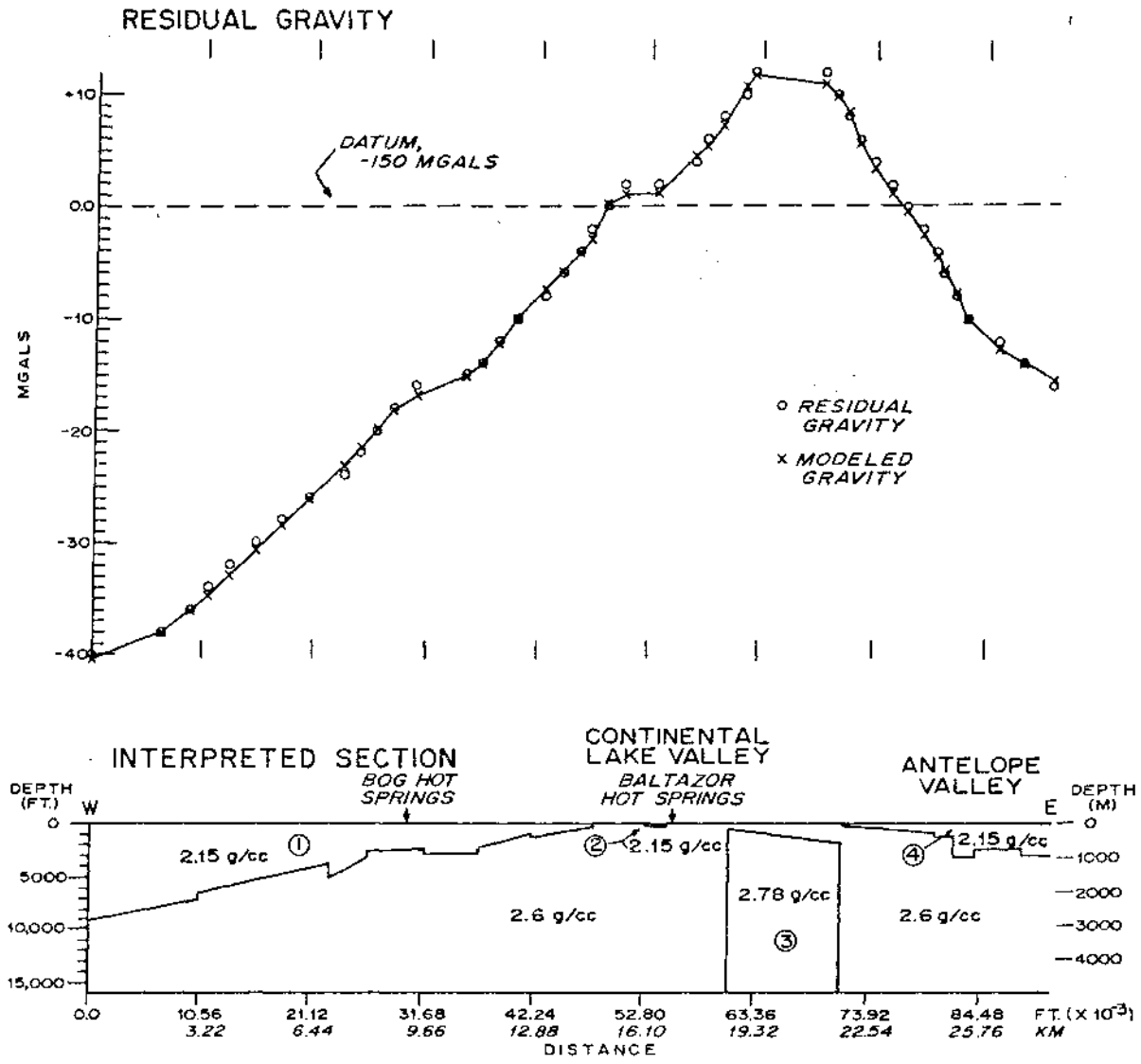


FIGURE 6
GRAVITY INTERPRETATION
REGIONAL PROFILE A-A'
BALTAZOR AREA
HUMBOLDT COUNTY, NEVADA

available, all of the models in this report are two-dimensional and a simple forward model iterative guess procedure was used to arrive at solutions. The contours of the complete Bouguer gravity anomaly values show that the 2-D assumption is satisfactory for most of the profiles. The exceptions are discussed below along with the particular profiles on which the assumption is violated.

The regional complete Bouguer gravity anomaly value in this area of Nevada is about -150 mgal (Mabey, 1960). This value was used as a datum and was subtracted from the observed gravity to arrive at the residual gravity for modeling purposes. The residual gravity was modeled to within 1 mgal.

Four features were used to model the residual gravity. (1) of Figure 6 is interpreted as a westward-deepening basin of tuffaceous volcanic and volcanic-derived sediments that reach a thickness of over 9000 ft (2.74 km). Although horst and graben features with vertical displacements of up to 1400 ft (427 m) are modeled, the generalized structure is a monocline dipping 10 to 15 degrees westward. The easternmost fault (at 48,000 ft or 14.6 km) corresponds to the mapped contact between the Steens Basalt and overlying younger tuffaceous rocks (Burnham, 1971; Hulen, 1979; Gardner and Koenig, 1978); hence the modeled surface is interpreted as the top of the Steens Basalt. The position and relative movement of the modeled faults located at 42,000 ft (12.9 km) and 37,000 ft (11.3 km) on the profile compare well with NNW-trending linears interpreted as faults from photogeologic mapping (Gardner and Koenig, 1978) and shown on Figure 4. It is also interesting to note that Bog Hot Springs occurs over the center of a horst structure. An alternate possibility to a horst structure is locally

increased density of the tuffaceous rocks, perhaps due to hydrothermal densification or alteration.

(2) of Figure 6 represents the low-density alluvium in Continental Lake Valley. It is a small feature on the regional scale.

(3) of Figure 6 represents the pre-Tertiary intrusive and metamorphic rocks making up the Pine Forest Range. The high density of about 2.75 to 2.85 g/cc indicates that metamorphic or possibly mafic phases of the intrusive rocks predominate in this section of the range.

(4) of Figure 6 models the structure of Antelope Valley. It is typical of the Basin and Range Province. The maximum valley fill is about 3200 ft (976 m) with 1950 ft (595 m) of vertical displacement on the largest fault. From geology, Willden (1964) calculated a minimum of 3000 ft (915 m) of throw in this range-front fault zone.

Figure 7 is a third-order polynomial surface that was removed from the complete Bouguer gravity anomaly values to form the residual gravity surface presented in Figure 8. A two-dimensional polynomial fitting routine developed by Montgomery (1973) was used. Although fits through order ten were generated, a third-order polynomial was selected because it was the minimum order that would approximate the east-west gravity relief (see for example Figure 6). The densely grouped profile points were removed prior to fitting so that the regional surface would not be biased to the detailed areas; however, anomalies and steep gradients near the borders of the residual map should be ignored due to edge effects caused by truncating the data.

The residual gravity map of Figure 8 enhances and helps to explain some of the features of the complete Bouguer gravity anomaly map of Figure 5. The Strawberry Butte gravity high, (1) of Figure 8, is

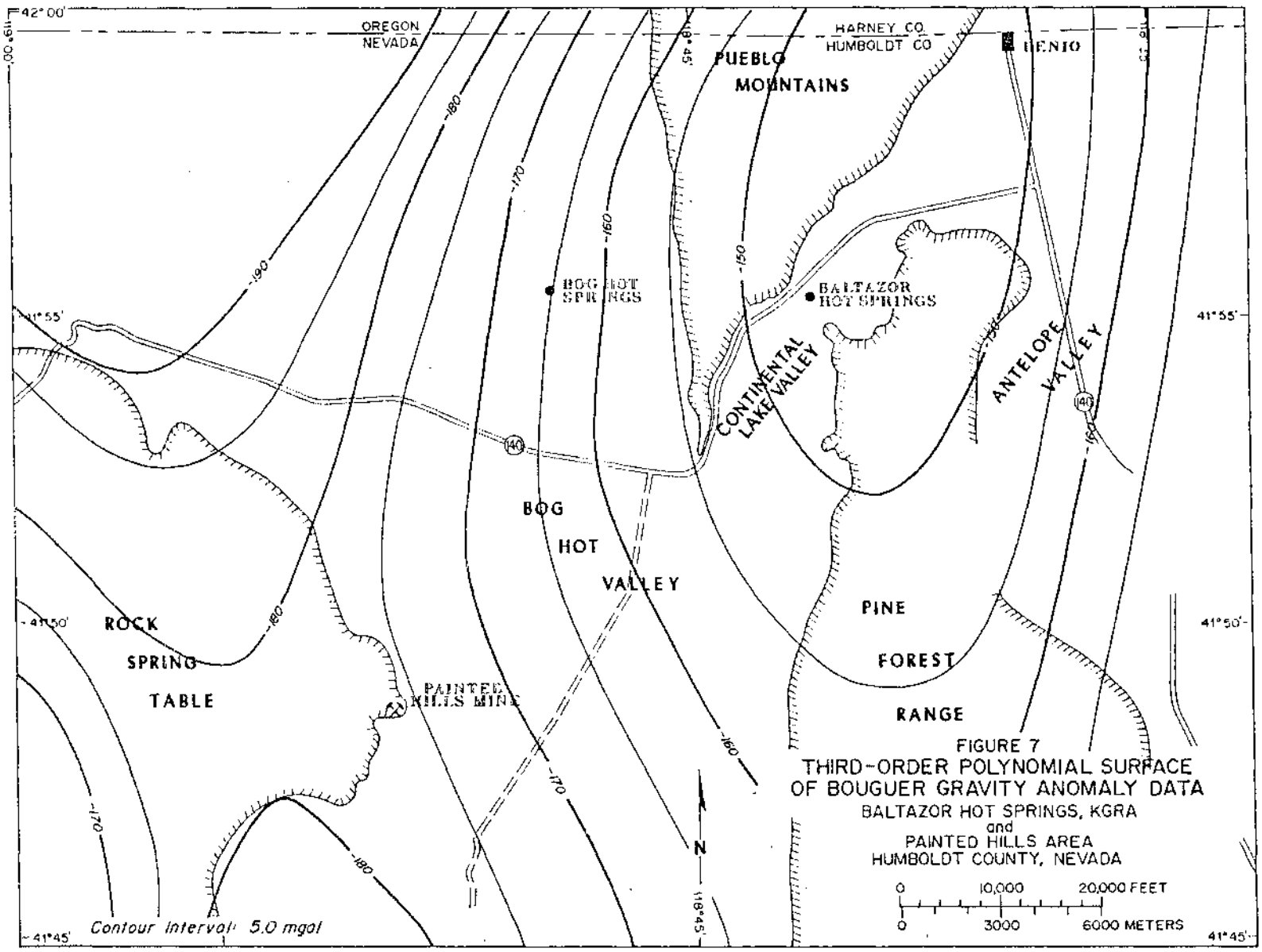


FIGURE 7
THIRD-ORDER POLYNOMIAL SURFACE
OF BOUGUER GRAVITY ANOMALY DATA
BALTAZOR HOT SPRINGS, KGRA
and
PAINTED HILLS AREA
HUMBOLDT COUNTY, NEVADA

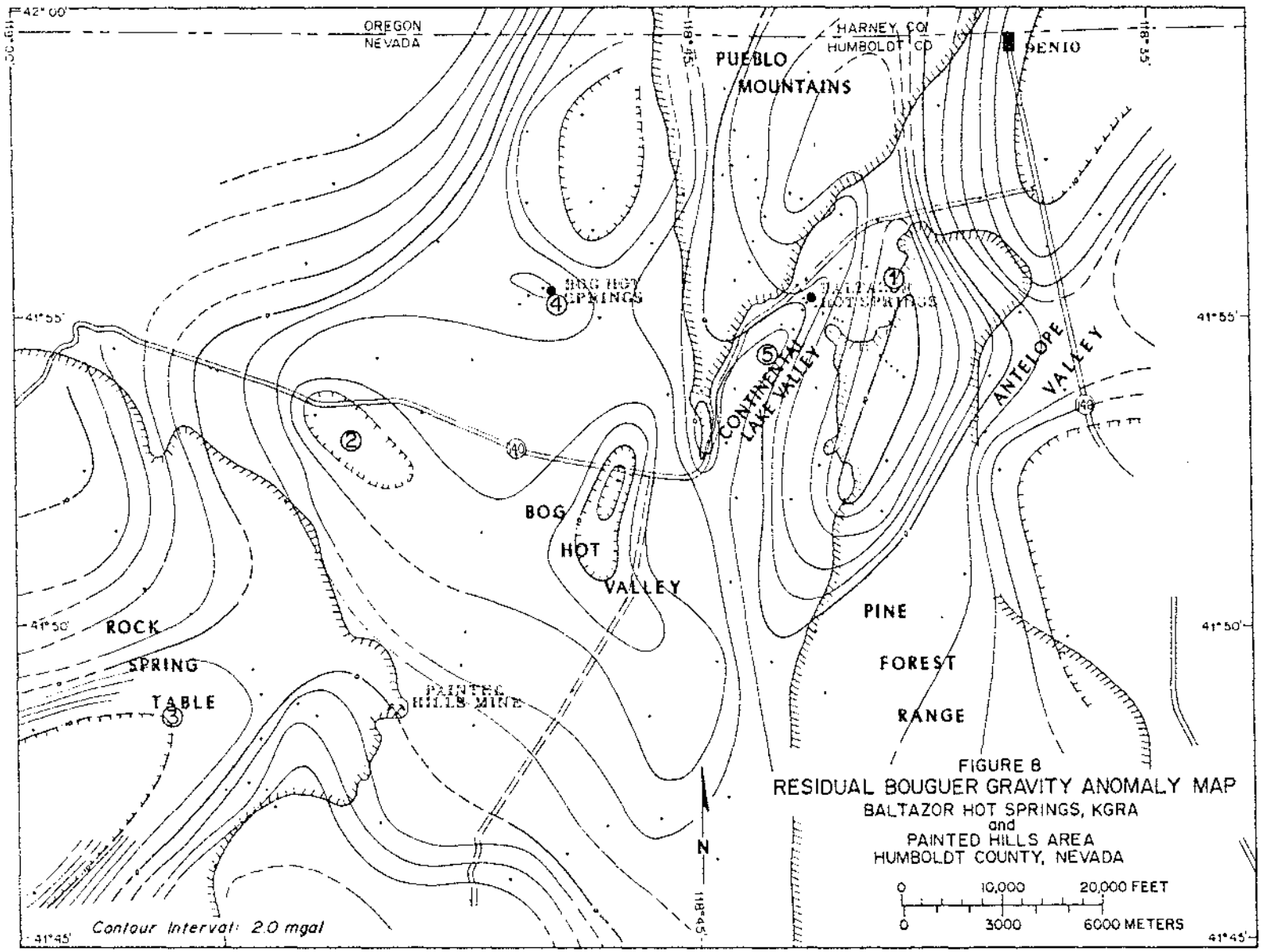


FIGURE 8
RESIDUAL BOUGUER GRAVITY ANOMALY MAP
BALTAZOR HOT SPRINGS, KGRA
and
PAINTED HILLS AREA
HUMBOLDT COUNTY, NEVADA

sharper and more closely overlays the mapped outcrop of metamorphic rocks. The remaining residual gravity gradient on the west side of the Pueblo Mountains supports the interpretation of north-south-trending normal faulting associated with the mapped contact of Steens Basalt with younger tuffaceous rocks. It also suggests that faulting continues south into Bog Hot Valley, although the interpretation here is complicated by a northwest trend in the gravity data that is perhaps the extension of the recent faulting at Bog Hot Spring mapped with photogeology.

The Thousand Creek gravity low, (2) of Figure 8, is now enclosed, but the bounding gradient on the northwest map boundary is probably spurious. However, the southwest bounding fault clearly extends southeast into the Pine Forest Range and is a demarcation between the Rock Spring Table and the geologic regime to the north. Unfortunately, as a consequence the fitted polynomial surface does not well represent the Rock Spring Table area and, combined with edge effects, causes false anomalies in the southwest portion of the map.

The gravity trough in Continental Lake Valley, (5) on Figure 8, is essentially unchanged although it extends somewhat more sharply into the Strawberry Butte gravity high. At Bog Hot Springs, a small closed residual high, (4) of Figure 8, is coincident with the hot springs and the modeled horst of the regional profile.

b) Detailed gravity profiles. One of the prime objectives of this study was to determine the local structure and the depth to basement at the Baltazor and Painted Hills areas; hence the three detailed gravity profiles at each area shown on Figure 2. At Baltazor KGRA the profiles were dominated by a very steep "regional" gradient. The following

procedure was used to extract the residual gravity. The profile lines were graphically extended to the limits of the mapped area and a profile was constructed from the gravity contours. Smoothed curves were then drawn to these regional gradients to eliminate high-frequency features. Since the detail surveys used nominal 500 and 1000 foot (152 to 305 meters) station spacing, and the Continental Lake Valley is a small feature (see for example Figure 6), the regional gradients could not be removed graphically with sufficient accuracy. Therefore a third-order polynomial was fitted to the regional gradients and then removed analytically from the observed gravity. The relatively shallow gradients at the Painted Hills area were removed using the same procedure.

The observed gravity, removed regional gradient, residual gravity, and interpreted gravity model of each profile are presented in Figures 9 through 11, 13 and 14. Interior points of the profiles were modeled to within 0.1 mgal, except that single-point variations of a few tenths of a milligal were sometimes accepted. Modeling at the limits of the profiles should be considered qualitative due to the reduced accuracy of the observed gravity and, at Baltazor KGRA, the steep gradient that was removed. These profiles were modeled using the same algorithm and procedures as discussed for the regional profile. The northernmost profile line at the Painted Hills area (Line M3) was not modeled because a two-dimensional approximation is not applicable at that location.

The three Baltazor KGRA profiles (Figs. 9-11) are closely modeled with typical Basin and Range high-angle normal faults. Each profile has a central graben, ranging from 1500 to 2000 ft (457 to 580 m) of

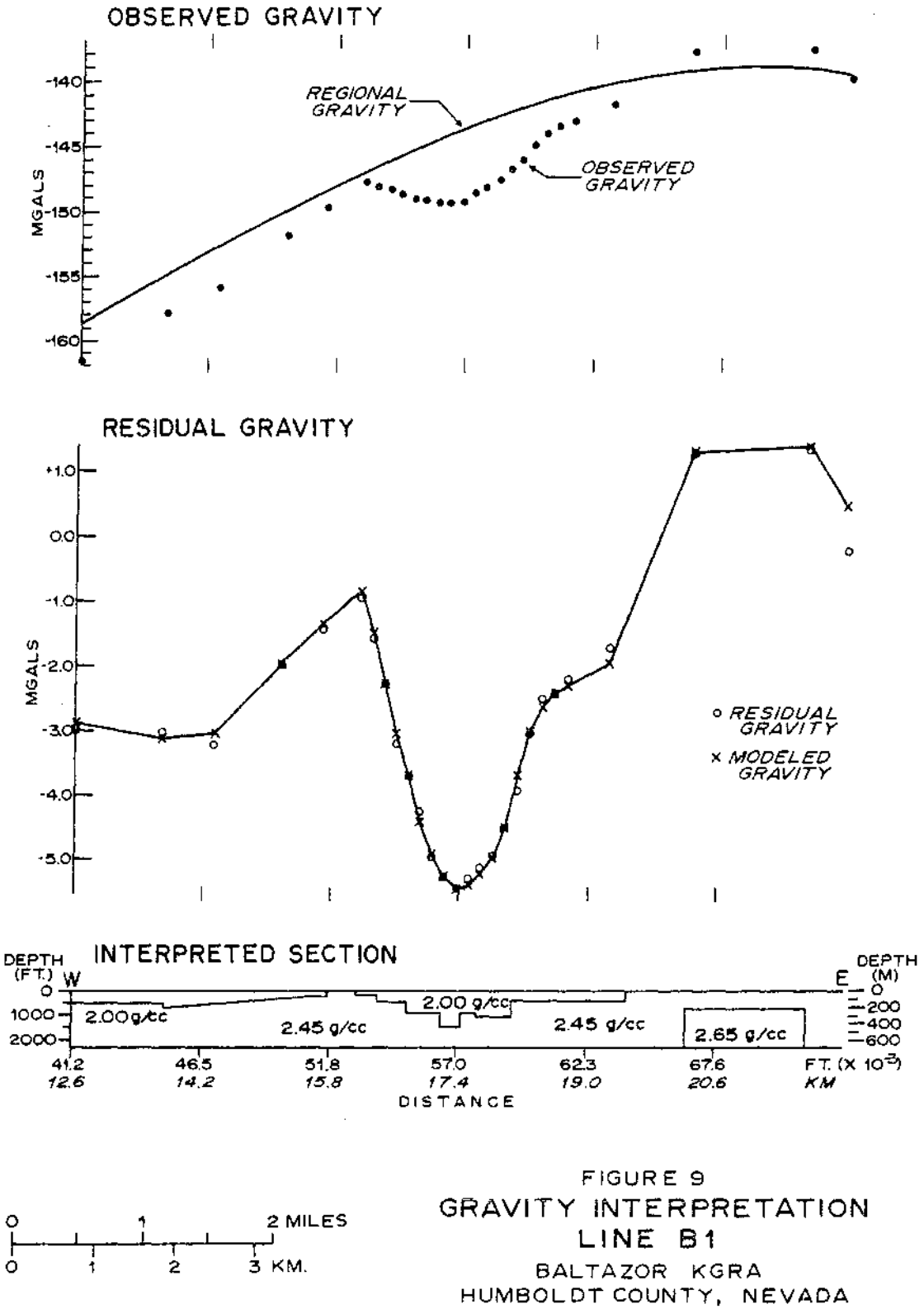


FIGURE 9
GRAVITY INTERPRETATION
LINE B1
BALTAZOR KGRA
HUMBOLDT COUNTY, NEVADA

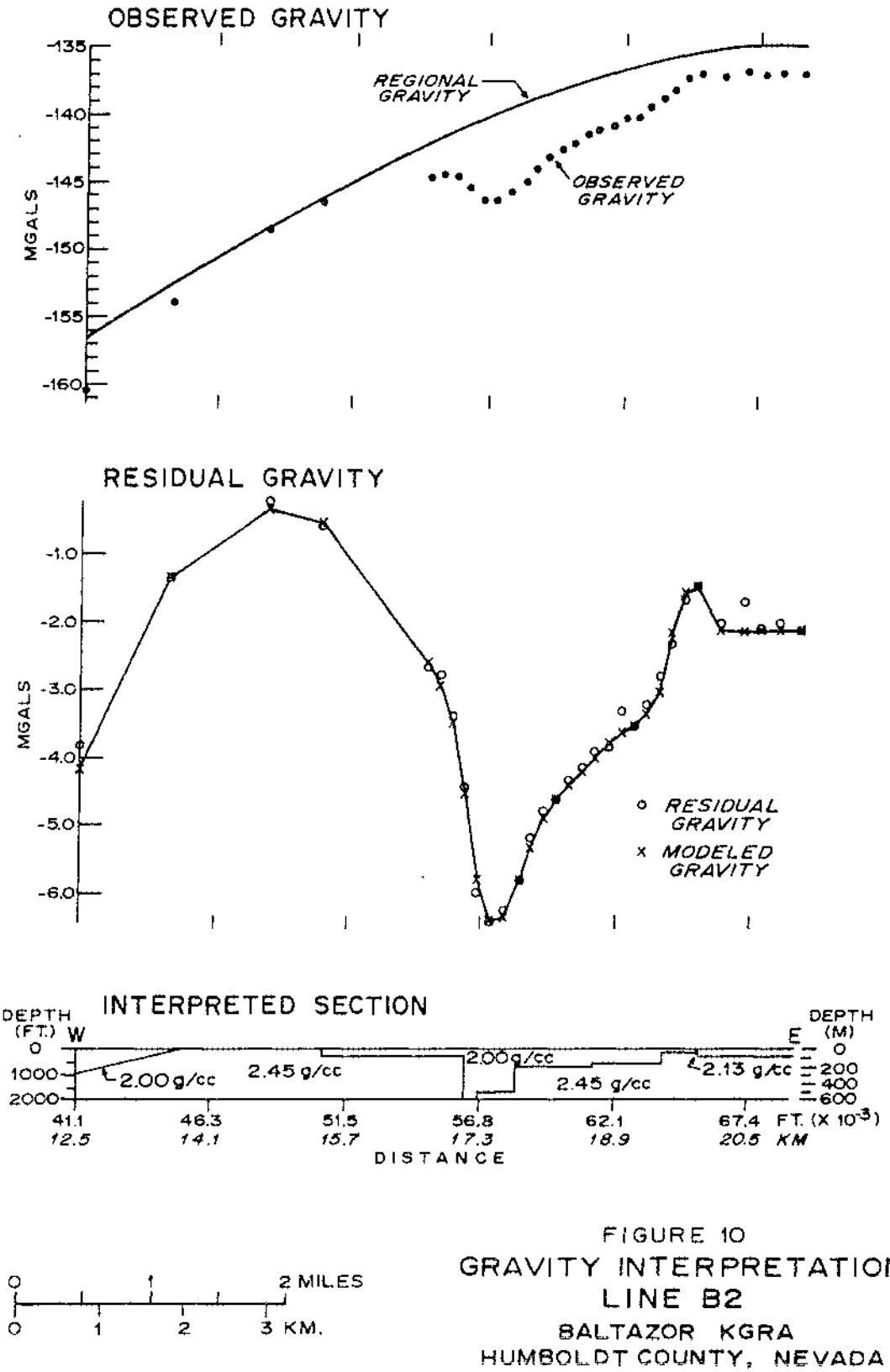


FIGURE 10
GRAVITY INTERPRETATION
LINE B2
BALTAZOR KGRA
HUMBOLDT COUNTY, NEVADA

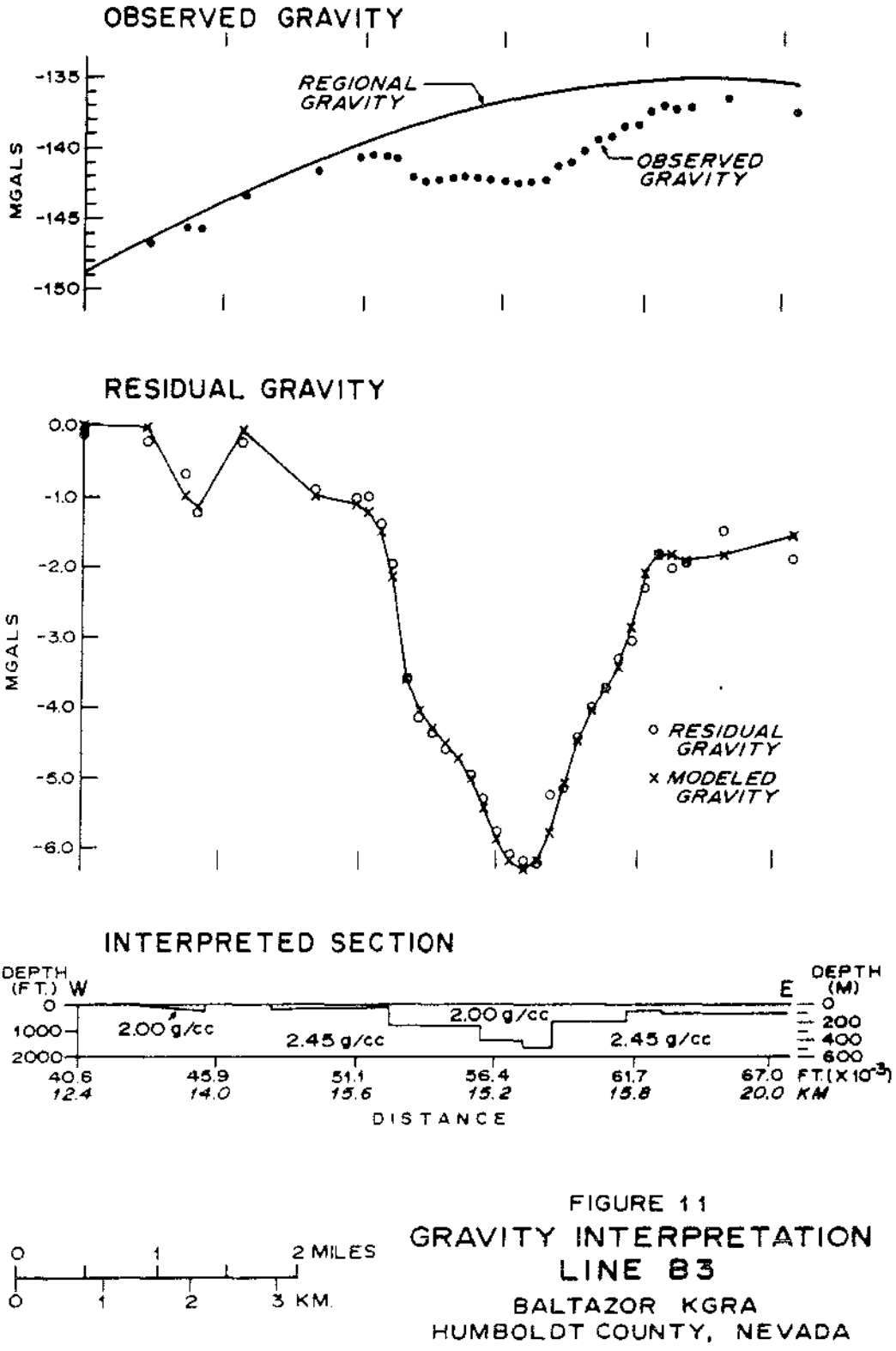


FIGURE 11

GRAVITY INTERPRETATION

LINE B3

BALTAZOR KGRA

HUMBOLDT COUNTY, NEVADA

total alluvial fill, with a series of step faults up to the bordering range.

A density contrast of -0.45 g/cc was used in the models for the alluvial valley fill. In the regional model, high-density pre-Tertiary rocks did not extend under Continental Lake Valley. Assuming the valley is underlain by the volcanic rocks of the south Pueblo Mountains with a composite density of about 2.45 g/cc, the alluvial valley fill would have a density of 2.0 g/cc, which is a typical value. However, drill hole BZ 1500-1 is located on line B2 and provides an opportunity to estimate the maximum density contrast. The hole was drilled to 1584 ft (483 m) but the log is sketchy and cuttings are not available below 320 ft (98 m). However, it does not appear that bedrock was encountered. Therefore, line B2 was re-modeled with 1585 ft (483 m) of alluvial fill at the location of the drill hole. A close match was obtained for -0.5 g/cc, suggesting that the density contrast is not greater than this.

Figure 12 is a plan map showing the modeled depth of alluvial fill along the Baltazor KGRA profile lines and the outline of Continental Lake Valley. Also shown are interpreted faults from the geophysical data and selected faults from geologic mapping (Hulen, 1979). The main valley-forming faults (1a and 1b of Figure 12) are represented on all three profiles. On the northwest side, displacement varies from 450 ft (137 m) to 2000 ft (579 m), while on the southeast side the displacements vary from 140 ft (43 m) to 710 ft (216 m). A graben, 2 of Figure 12, extends through the center of the valley coincident with the topographic lows of Baltazor Hot Springs and the valley drainage. However, the structure of the central graben as modeled on line B2 is

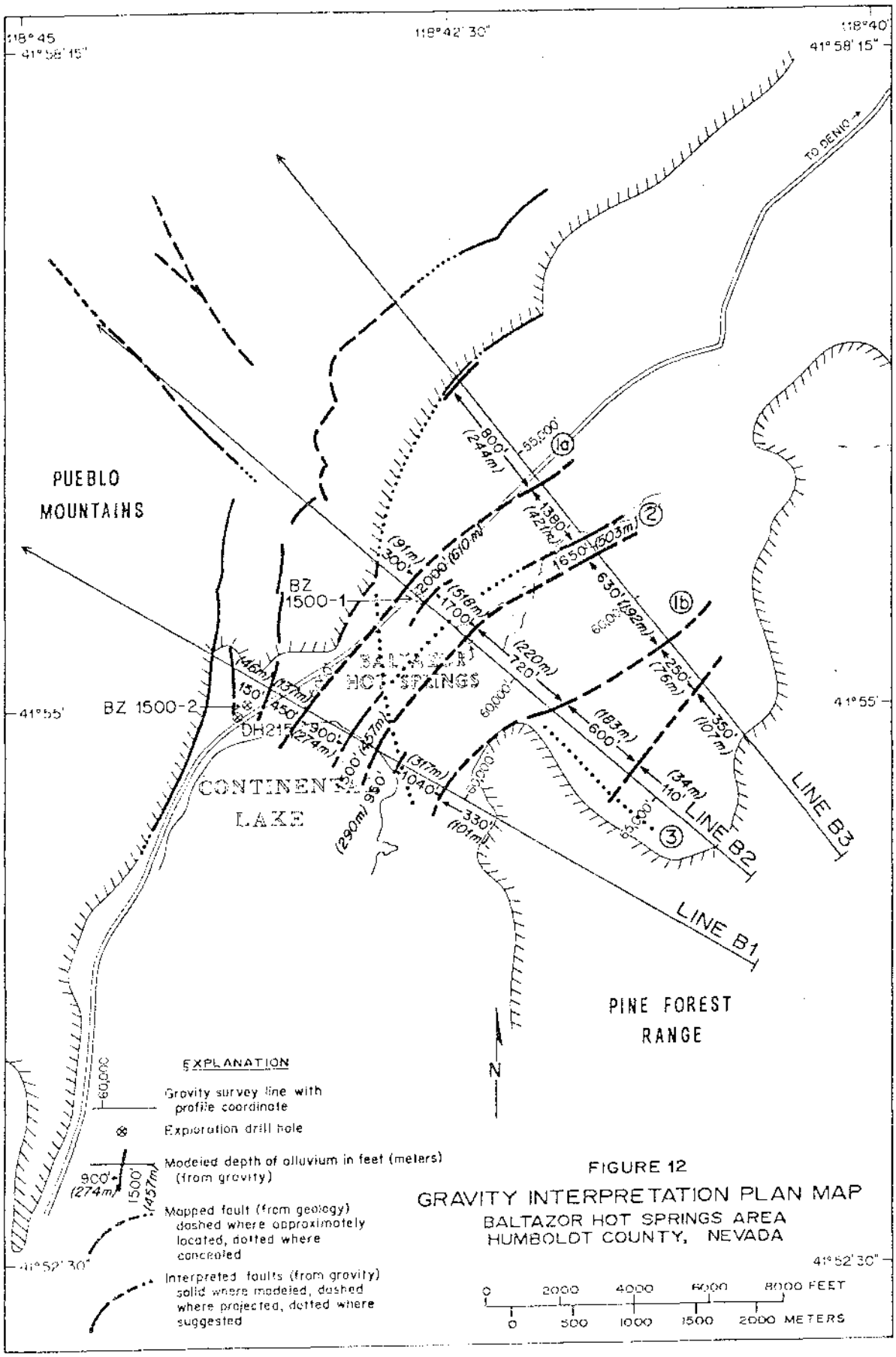


FIGURE 12

GRAVITY INTERPRETATION PLAN MAP
BALTAZOR HOT SPRINGS AREA
HUMBOLDT COUNTY, NEVADA

more complex. The graben is wider, about 1.05 miles (1.69 km) versus about 0.5 miles (0.81 km) on the other profiles, and there is subsidiary down-faulting along Fault (1a).

Relatively deep alluvial fill is modeled east of Fault (1b) on line B2. The structure here is 2 1/2 dimensional, so 600 ft (183 m) is a minimum depth of the alluvium. Because of the juxtaposition of this alluvium with the positive topography directly to the south, a NW-trending fault, (3) of Figure 12, is suggested. This could be the extension of NW-trending faulting mapped in the Pueblo Mountains and would support Hulen's suggestion of intersecting NNE and NW faulting at Baltazor Hot Springs (Hulen, 1979).

Finally, the small horst modeled on line B3 suggests that the arcuate fault on the NW valley perimeter extends into Continental Lake Valley and intersects line B3.

Figures 13 and 14 present the observed gravity, removed regional gradient, residual gravity and the interpreted models for lines M1 and M2 which are located at the Painted Hills area. Both profiles cross the McGee fault zone and the McGee gravity high. Line M1 has 10.6 mgal of relief and line M2 has 7.5 mgal of relief. Both models have a high-density body on the west side of the McGee fault zone, 300 to 1400 ft (92 to 427 m) beneath the surface of the Rock Spring Table. The gravity low to the east of the plateau is modeled on both lines as a graben 1220 to 2500 ft (372 to 762 m) deep, flanked to the east by step faulting and to the west by a sloping contact.

Exploration drill holes DHM 1500-1 and 1500-2, located on line M2, are shown on Figure 14. Information for drill hole DHM 1500-1, drilled to a total depth of 1581 ft (482 m), was not available apparently due

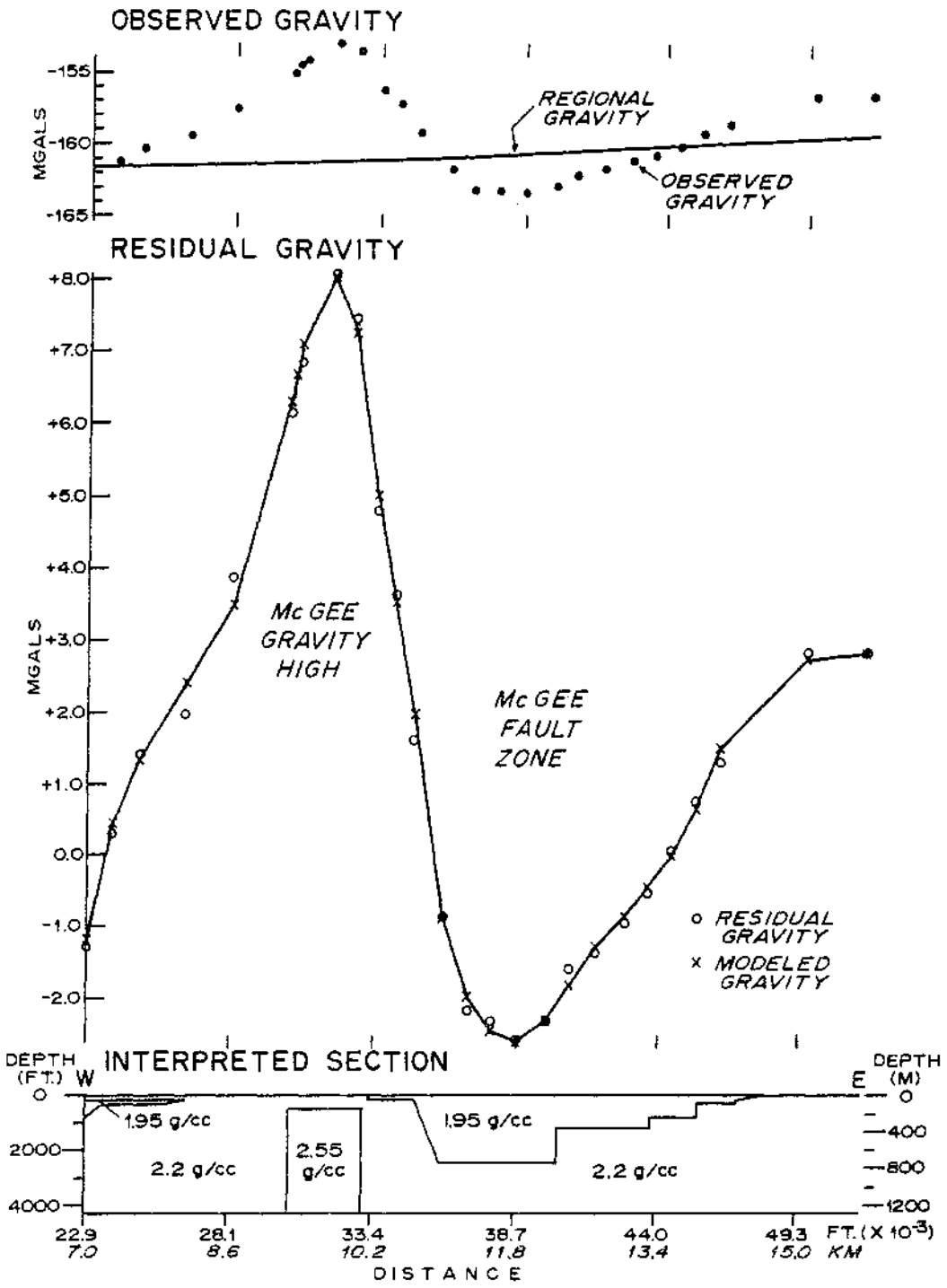


FIGURE 13

GRAVITY INTERPRETATION
LINE M1

PAINTED HILLS AREA
HUMBOLDT COUNTY, NEVADA

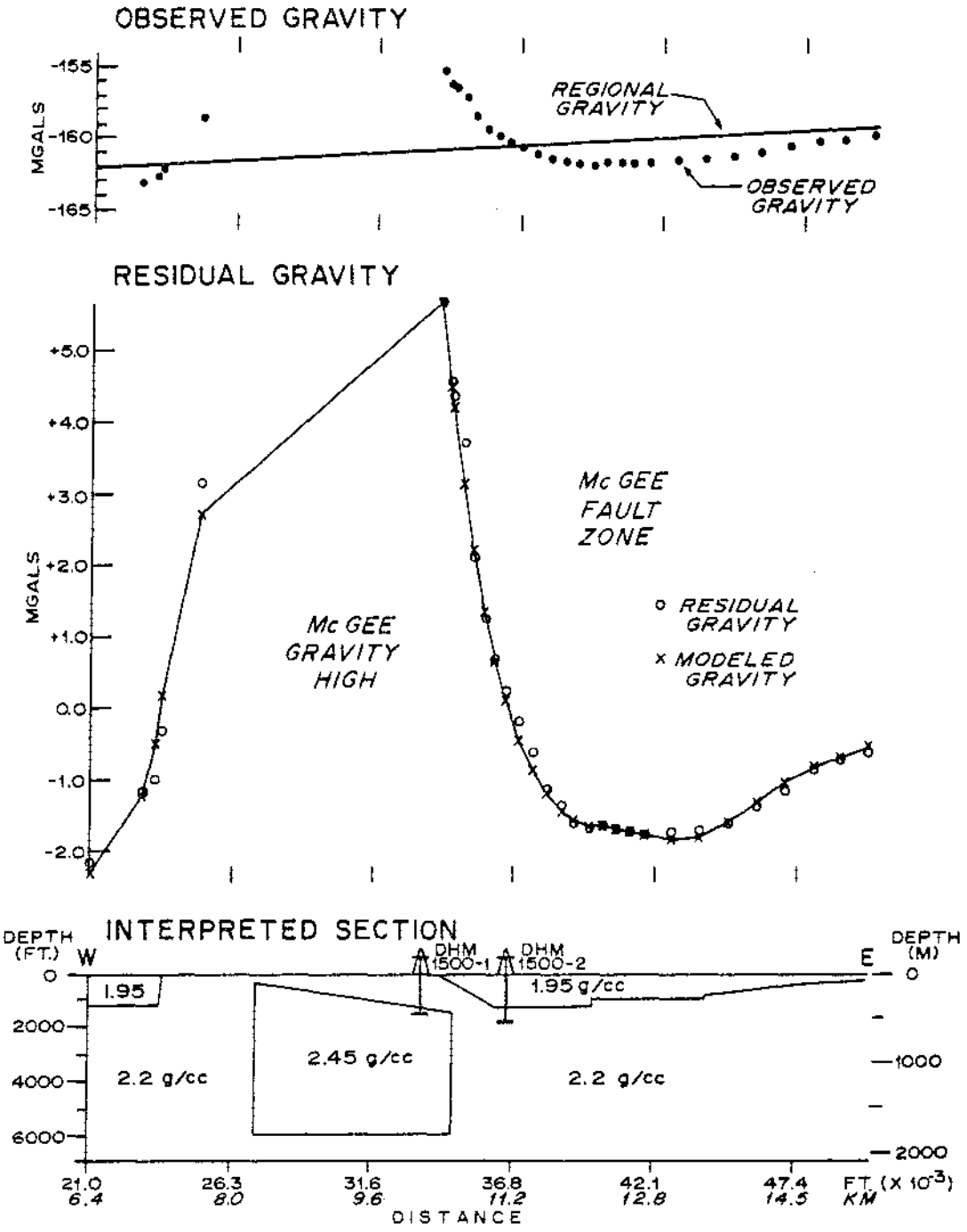


FIGURE 14

GRAVITY INTERPRETATION

LINE M2

PAINTED HILLS AREA

HUMBOLDT COUNTY, NEVADA

to loss of circulation below 125 ft (38 m). DHM 1500-2 was drilled to a depth of 1684 ft (513 m) through alluvial debris and tuffaceous rocks of the Thousand Creek Formation. The intense hematitic and argillic alteration that gives the Painted Hills their name was intersected at 1300 ft (396 m) while the modeled contact was 1200 ft (366 m). The measured density contrast between the altered and unaltered tuffaceous rocks ranged from 0.2 to 0.5 g/cc (see Table 7). Therefore, the low-density body on both profiles is interpreted as the Thousand Creek Formation, with a wet bulk density of about 1.95 g/cc, bordered in the western portion by altered tuffaceous rocks with a density of about 2.2 g/cc. Hence the sloping contact on both lines is not necessarily a fault but may represent the limit of alteration. This agrees well with the mapping and cross section by Hulen (1979). It is unlikely that the alteration extends far out into the valley and so at some point the modeled contact probably represents the upper surface of the Canyon Rhyolite, which has a density of about 2.25 g/cc.

Based on this information, the high-density body would have a density of 2.45 to 2.55 g/cc. This could represent a rhyolitic body intruded along the structural weakness of the McGee fault zone which would be in keeping with the eruptive centers in the Canyon Rhyolite noted by Wendell (1969, p. 29) and Gardner and Koenig (1978, p. 12). However, an intrusion of this size would probably cause deformation of overlying rocks, and there is no documentation of this. The preferred explanation is that this is a zone of intense silicification and hematization of the tuffaceous rocks underlying the Canyon Rhyolite, such as that mapped by Hulen (1979) in an area between lines M1 and M2.

# ELECTRICAL RESISTIVITY SURVEY

## Data Acquisition

A dipole-dipole electrical resistivity survey was conducted by Mining Geophysical Surveys, Inc. (1980) on contract to Earth Power Production Company (EPPC) along four lines specified by EPPC. This work, along with the self-potential survey discussed below, was made available to the Earth Science Laboratory by EPPC through the DOE/DGE Industry Coupled Program. The reader is referred to that report for a more detailed discussion of procedures of both the resistivity and self-potential surveys.

A conventional in-line dipole-dipole "seven" spread (seven current electrodes) with 1500 ft (457 m) dipoles was used throughout the survey. Dipole separation factors (n) of 1/2 and 1 through 6 were read and the apparent resistivity values were plotted in conventional pseudo-section manner.

A 10 amp transmitter was used with a 2 second on/off reversed polarity cycle. The signal at the potential electrode was observed with an analog voltmeter and averaged over at least two cycles. In cases of low signal strength a digital voltmeter was substituted.

## Accuracy

Some question exists as to the exact location of receiving electrodes outside of the current electrode spread. Current electrodes were plotted by the contractor but the locations of receiving electrodes, often in areas of steep topography, were not. These locations

are important in cases where the topography is included for modeling. The solution was to position the receiving electrodes on 1500 ft (457 m) slope distances along the projection of the lines.

The repeat stations on the Baltazor KGRA profiles raise questions about the quality of the data. For the eight repeat stations at Baltazor the average of the ratio of the higher values to the lower value was 3.4 to 1. The worst case was 86 Ω-m versus 8 Ω-m (10.8 to 1), and only one case was better than 3 to 2.

The contractor was asked to review his field notes in regard to this, and reported verbally and in a follow-up memorandum that: 1) difficulties of low input current had been encountered, especially in the morning, on some dipoles due to frozen ground; and 2) that the low wet area along the north end of Continental Lake may have further contributed to a low signal level due to current leakage. The combination of low current input and a moderate to high noise level results in a low signal-to-noise (S/N) ratio and poor data, especially when observations are made manually from an analog voltmeter over a limited number of cycles. Thus the comparison of a reading from a dipole with a low S/N ratio to a reading from a high S/N ratio dipole could explain the poor repeats. Working with the field notes, the contractor identified transmitting dipoles and specific pseudo-section apparent resistivity values that were questionable. These points were then ignored in modeling.

## Interpretation

The electrical resistivity data are modeled with a 2-dimensional forward finite element computer program originally developed by Rijo (1977). The program has been modified to include topography, made

interactive and adapted to the ESL facility (Fox et al., 1978; Killpack and Hohmann, 1979). A good qualitative description of the program and the interpretative procedure used at ESL is given in an electrical resistivity and IP study by Ross (1979).

All of the final numerical models were tested for depth sensitivity. The highest resistivity that had been used in the model was extended at depth across the entire model. This basement was then made successively shallower until the apparent resistivities associated with separation factors of 5 and 6 were substantially affected. All models were found to be sensitive in this sense to a model depth of at least 2a, or 3000 ft (915 m). In areas where the overlying model intrinsic resistivities were relatively high, the model was sensitive to depths of as much as 3.5a. These examples reflect the effect of conductive overburden; with a relatively resistive basement, most of the current will remain in the overlying low-resistivity rocks. Similarly, the experience gained during the modeling indicated that for resistivity contrasts greater than about 10 to 1, the higher resistivity is not well resolved. Once a resistor has an intrinsic resistivity about ten times greater than the surrounding rock, additional large increases in the resistivity of that body do not cause a correspondingly large increase in the apparent resistivities. Hence, model resistivity contrasts were constrained to approximately the same magnitude as the contrasts in the observed apparent resistivities.

The interpreted intrinsic resistivity sections and observed apparent resistivities for the three Baltazor KGRA lines (R1 through R3) and the Painted Hills area line (R4) are presented in Figure 15 through 18, respectively. The complexity of the models is a result of

closely matching the observed data with a limited number of discrete resistivities. The resulting geometries are those that gave the best match to the observed data from a sequence of 20 to 30 iterations. Since the modeling is non-unique and the quality of some of the data is questionable, specific model parameters should not be considered well resolved. In general, however, modeled resistivity discontinuities do represent variations in the subsurface. Common features of the resistivity data at Baltazor KGRA are:

1. Low ($\leq$25 Ω-m) resistivities through Continental Lake Valley. The section is about 1500 ft (455 m) thick along line B3, and greater than 3000 ft (915 m) thick along line B1.
2. Resistivities of 22 to 40 Ω-m associated with the exposed volcanics of the Pueblo Mountains.
3. Very low (5 to 7 Ω-m) resistivities beneath the Pueblo Mountains, starting near the range-front and extending to the west.
4. High resistivities associated with the Pine Forest Range. On lines B1 and B2 these values range from 90 to 180 Ω-m and correspond to the Tertiary volcanics that crop out here. On line B3, 700 Ω-m resistivities are modeled along the east and center of the profile and are interpreted as metamorphic rocks.
5. A tabular, near vertical low (15 to 27.5 Ω-m) resistivity zone(s) on the eastern side of the profiles.

Drill hole BZ 1500-1 was drilled to a depth of 1584 ft (483 m) on line B2 and is shown on Figure 16. As discussed in the gravity section, it was drilled in alluvium and apparently did not penetrate bedrock. An aquifer with 100°C fluids was intersected between 100 and

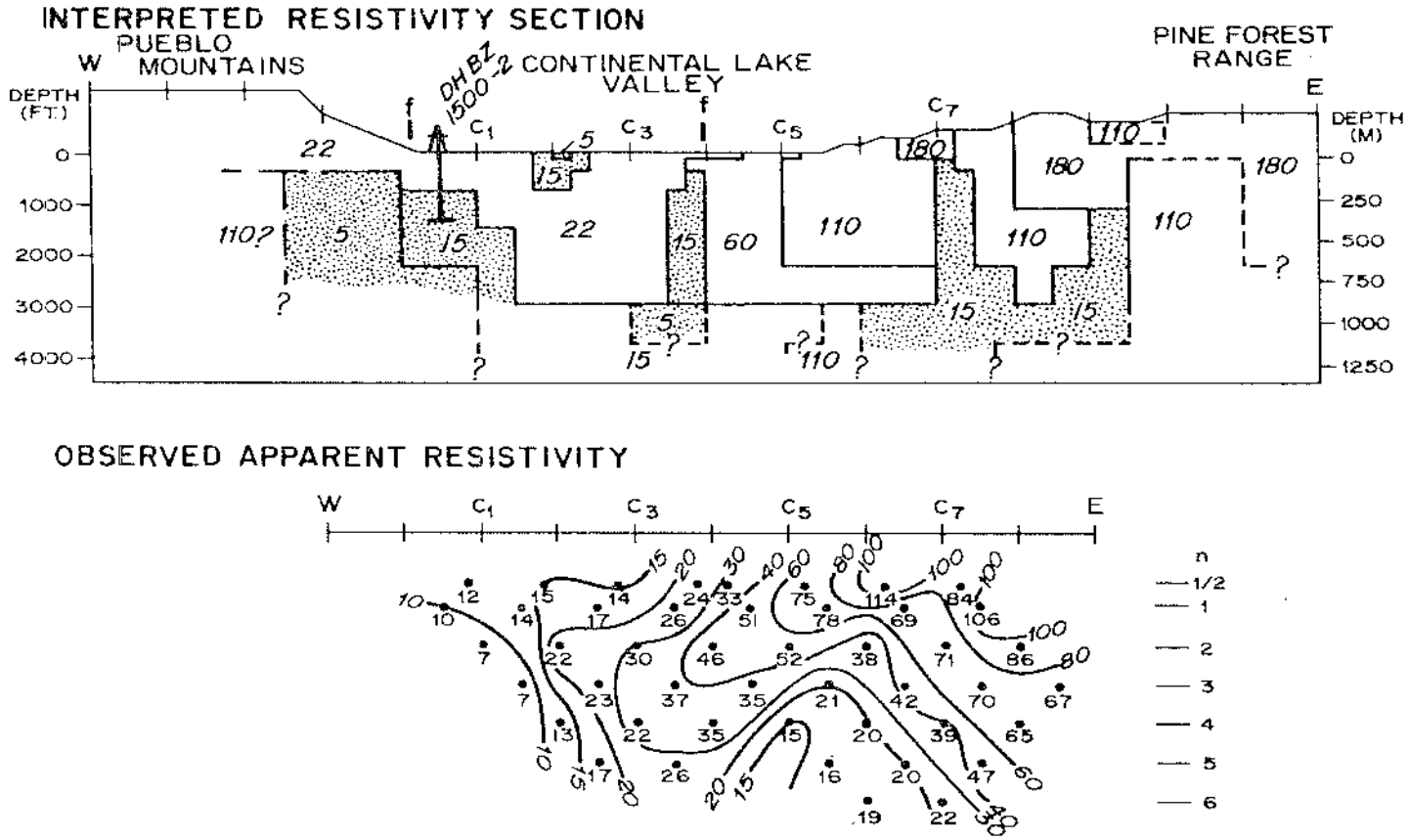


25 – Intrinsic electric resistivity (Ω-m)

$C_5$ – Current electrode

f – Interpreted fault

0 3000 6000 FEET

0 500 1000 1500 METERS

FIGURE 15

INTERPRETED RESISTIVITY SECTION
and
OBSERVED APPARENT RESISTIVITY
LINE R1

BALTAZOR KGRA
HUMBOLDT COUNTY, NEVADA

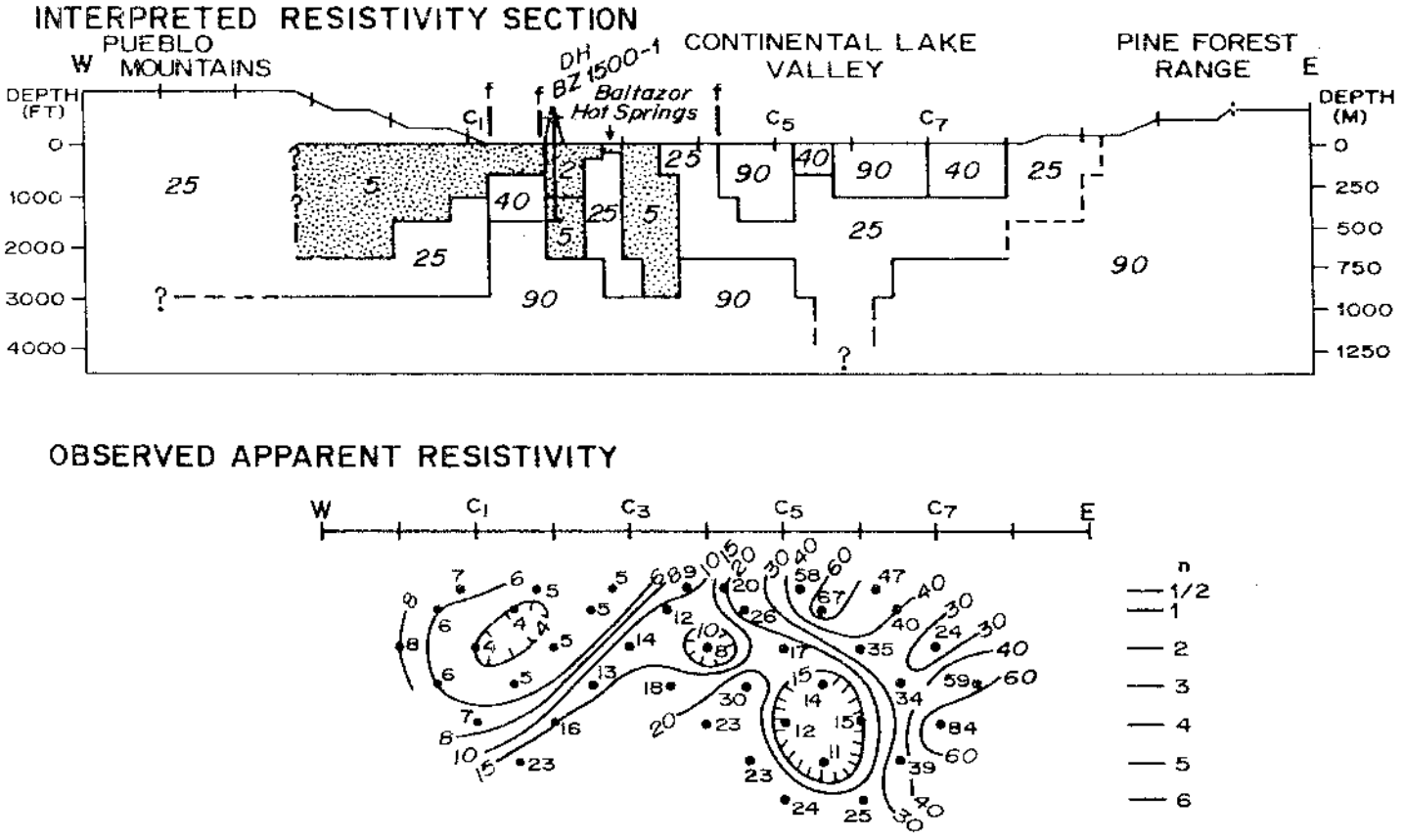


25 – Intrinsic electric resistivity (Ω-m)

$C_5$ – Current electrode

f – Interpreted fault

0 3000 6000 FEET

0 500 1000 1500 METERS

FIGURE 16

INTERPRETED RESISTIVITY SECTION
and
OBSERVED APPARENT RESISTIVITY
LINE R2
BALTAZOR KGRA
HUMBOLDT COUNTY, NEVADA

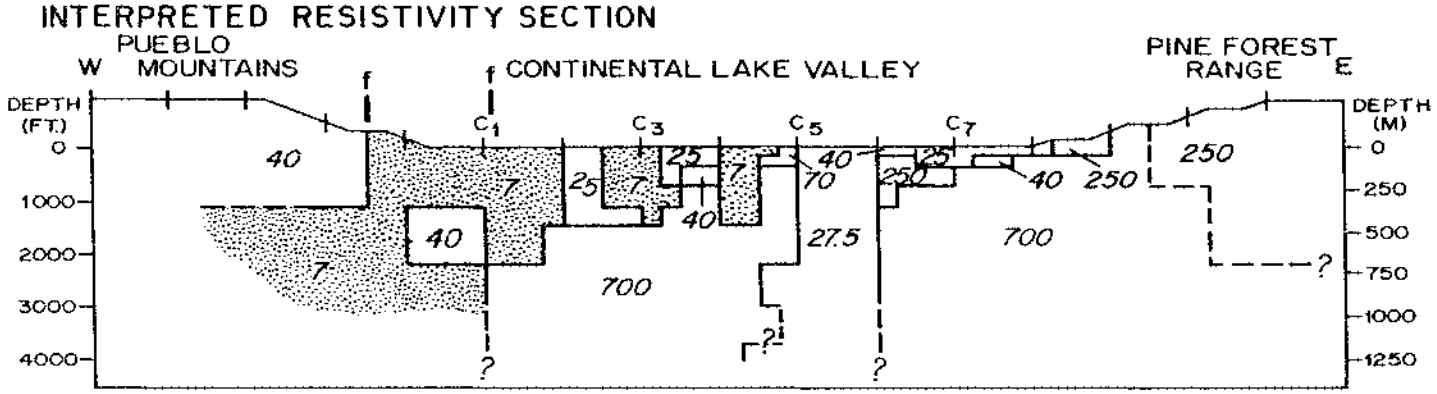


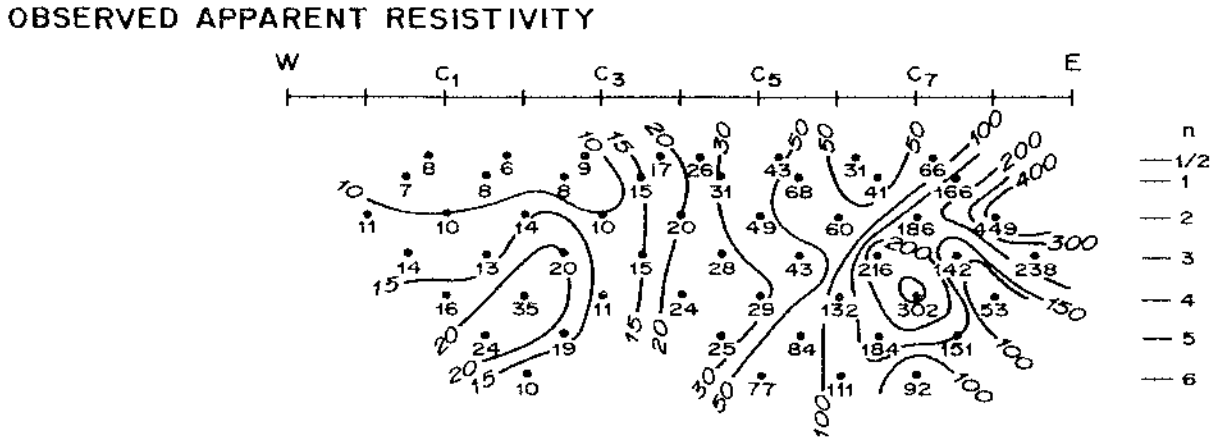


25 – Intrinsic electric resistivity (Ω-m)

$C_5$ – Current electrode

f – Interpreted fault

0 3000 6000 FEET

0 500 1000 1500 METERS

FIGURE 17

INTERPRETED RESISTIVITY SECTION
and
OBSERVED APPARENT RESISTIVITY
LINE R3

BALTAZOR KGRA
HUMBOLDT COUNTY, NEVADA

200 ft (30 and 61 m), and temperatures between 77°C and 82°C were recorded for the remainder of the hole. The resistivity modeled here is 2 to 5 Ω-m. Drill hole BZ 1500-2 was drilled to a depth of 1487 ft (453 m), 700 ft (213 m) south of line B1, and its projected location is shown on Figure 15. The upper 320 ft (98 m) is slide debris, followed by felsic to intermediate volcanics to 620 ft (189 m), and basalt for the remainder of the hole. A sharp increase in the temperature gradient from 36.4°C/km to 139.7°C/km was encountered at about 800 ft (244 m), which is the modeled depth where resistivities dropped to 15 Ω-m. The bottom hole temperature was 67.9°C. Hence, resistivities less than about 15 Ω-m are interpreted as alluvium and/or porous volcanics, generally vesicular or cinder basalt, containing clay alteration products and thermal fluids. Clay alteration must be invoked since, assuming pore fluid at 120°C and 700 ppm total dissolved solids (Klein and Koenig, 1977) in rock with 20% porosity (see Table 1), Archie's Law gives a saturated formation resistivity of 52.5 Ω-m. A good discussion of the presence of clays on resistivity, with reference to geothermal systems, is given by Ward and Sill (1976).

Low resistivities (1.5 to 20 Ω-m) dominate the profile of Figure 18 for the Painted Hills area. The eastern two-thirds of the profile is modeled as a simple layered earth. This layered earth is truncated on the west side by a vertical, low-resistivity (1.5 Ω-m) zone. This low-resistivity zone is bordered on the west by a zone of significantly higher resistivities.

The layered earth is interpreted as generally undisturbed Tertiary and Quaternary tuffaceous volcanic and volcaniclastic rocks. The sequence of higher to lower resistivity with increasing depth may be

INTERPRETED RESISTIVITY SECTION

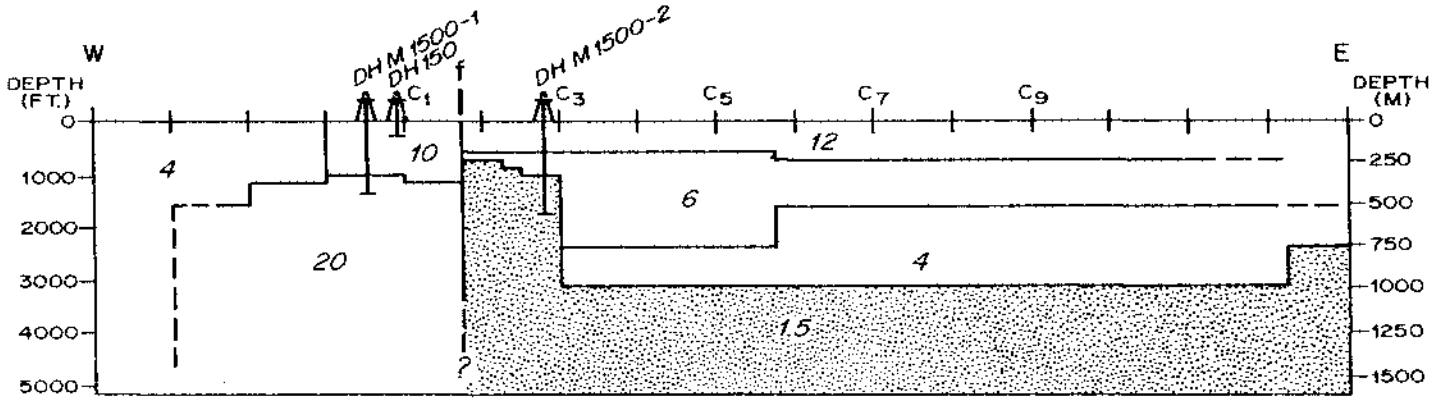


OBSERVED APPARENT RESISTIVITY

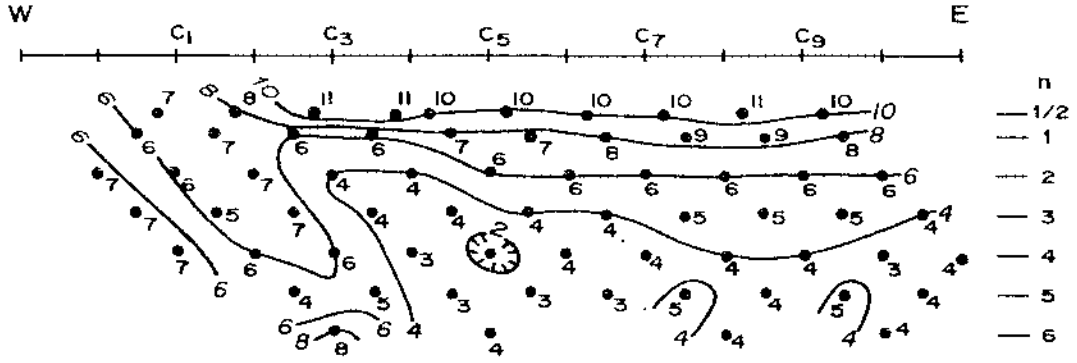


15 – Intrinsic electric resistivity (Ω-m)

$C_5$ – Current electrode

f – Interpreted fault

0 3000 6000 FEET

0 500 1000 1500 METERS

FIGURE 18

INTERPRETED RESISTIVITY SECTION
and
OBSERVED APPARENT RESISTIVITY
LINE R4

PAINTED HILLS AREA
HUMBOLDT COUNTY, NEVADA

associated with increased water content and/or increased water salinity with depth. Another factor may be more advanced devitrification of volcanic glass and corresponding increased development of montmorillonite in the older tuffaceous rock.

The 1500 ft (457 m) wide zone of 1.5 Ω-m material is interpreted as altered tuffaceous rocks containing conductive fluids that migrate up the indicated fault zone of Figure 18 and then circulate down slope to the east. The temperature in drill hole DHM 1500-2 increased from 24°C at the 100 ft (30 m) level to 93°C at the 1680 ft (512 m) level and wet hole conditions were encountered below about 200 feet (61 m) (EPPC, 1980).

Drill hole DH 150 and, apparently, DHM 1500-1 (the data for this hole are incomplete) were drilled through argillized and hematized tuffaceous rocks in the high-resistivity zone to the west of the fault zone and also encountered elevated temperatures and high thermal gradients (EPPC, 1979). These high resistivities are closely related spatially to the high-density zone modeled in the gravity data (Figure 14). The increased resistivity is probably due to decreased porosity associated with the hematitic and, locally, siliceous alteration. However, since this area is at the edge of the profile and the topography is 3-dimensional, the modeling should be considered qualitative.

## SELF-POTENTIAL SURVEY

### Data Acquisition

This survey was conducted in conjuction with the resistivity survey discussed above and the interested reader is referred to the contractor's report, upon which the following discussion is based (Mining Geophysical Surveys Inc., 1980). Approximately 23 line-miles (38 km) of data on eight lines was collected, including coverage along parts of the dipole-dipole resistivity lines. Three lines at the Painted Hills area totaled 14 line-miles (22.5 km), and five lines (including tie-lines) at Baltazor KGRA totaled 9.7 line-miles (15.5 km).

The survey utilized a fixed base station (home pot) with a traveling electrode out to distances of 1.9 miles (3 km) at which point a new base station was established. The station interval was 200 m with additional stations sometimes read at 100 m where SP gradients exceeded about 200 mv/km. Tinker and Rasor non-polarizing electrodes were used - a model 3A "Fat Boy" for central pots at base stations, and Model 88 (cone tipped) for the traveling electrode and for base station satellite pots. In all cases shallow pits were dug in an attempt to place the electrodes in contact with natural moisture. A high-impedance (22 megohm) digital voltmeter was used to observe potential differences.

Base stations consisted of a central pot and three satellite pots, all excavated to natural moisture (about 1 foot or 0.3 m). At the

beginning and end of each spread, the potential from the central electrode to each satellite electrode was observed and the three values averaged. The difference between these averages was considered to be the base station drift. Corrections for base station drift were applied on all eight lines assuming linear drift with time.

At the Baltazor area, closed loops were run tying all the SP lines to a common reference point. The error of closure was distributed incrementally to each station, dividing the total error by the total number of stations to determine the increment, e.g., the fifth station observed in a loop of n stations had an error correction of 5/n of the total error. The three lines at the Painted Hills are not tied to a common point and, hence, there are significant base level differences between them.

## Accuracy

Errors in the data fall into three overlapping catagories -- data scatter, electrode drift, and base station variations. Data scatter, or noise, was estimated to be about ±10 to 20 mv. Included in this would be telluric currents for which corrections were not made, except by averaging the observed potential difference over high-frequency fluctuations.

The potential difference between traveling electrodes and calibration electrodes immersed in a standard solution averaged about 6 mv, indicating some polarization effects in the electrodes. The standard was carried in the field and frequent checks showed the variation to be non-linear. Fluctuation of the potential between the base station and the traveling electrode, again immersed in standard solution, averaged about ±8.4 mv. Finally the fluctuation of potential

difference between base stations averaged ±8.2 mv with a maximum of 21 mv.

Some of these fluctuations are related but, in any instance, the SP technique is quite liable to noise (see for example Sill and Johng, 1979). The SP line profiles, presented in Figures 19 through 21, have a number of single-point anomalies with absolute values in the 20 to 40 mv range. This suggests that anomalies should not be considered significant unless they are multi-point and greater than about 30 mv. However, a threshold value for anomalous response based solely on the above discussion would be questionable since factors such as aliasing due to the large sampling interval, and surface or near-surface lateral and temporal changes are not quantifiable with this data set. Surveys of this design are properly applied only when used to locate gross features in the SP data, and the scope of the resulting qualitative interpretation should reflect this limitation of the survey.

## Interpretation

Figure 19 presents the SP survey results along the dipole-dipole resistivity lines at Baltazor KGRA while Figure 20 shows the results of the two tie-lines there. There is no evidence of a long wave length anomaly such as is sometimes associated with geothermal areas (Corwin and Hoover, 1979). The primary feature is a large, roughly dipolar anomaly occurring on the west side of lines SP-2 and SP-3. The amplitude is 115 mv on line SP-3 and 81 mv on line SP-2, and it is coincident with the valley-bordering fault (Fault (1a)) as determined from the gravity data. Rapidly changing SP values on the west side of Line SP-1 are associated with faulting and elevated temperatures along line B1 (see Figure 22), but the sampling of the SP is too sparse to

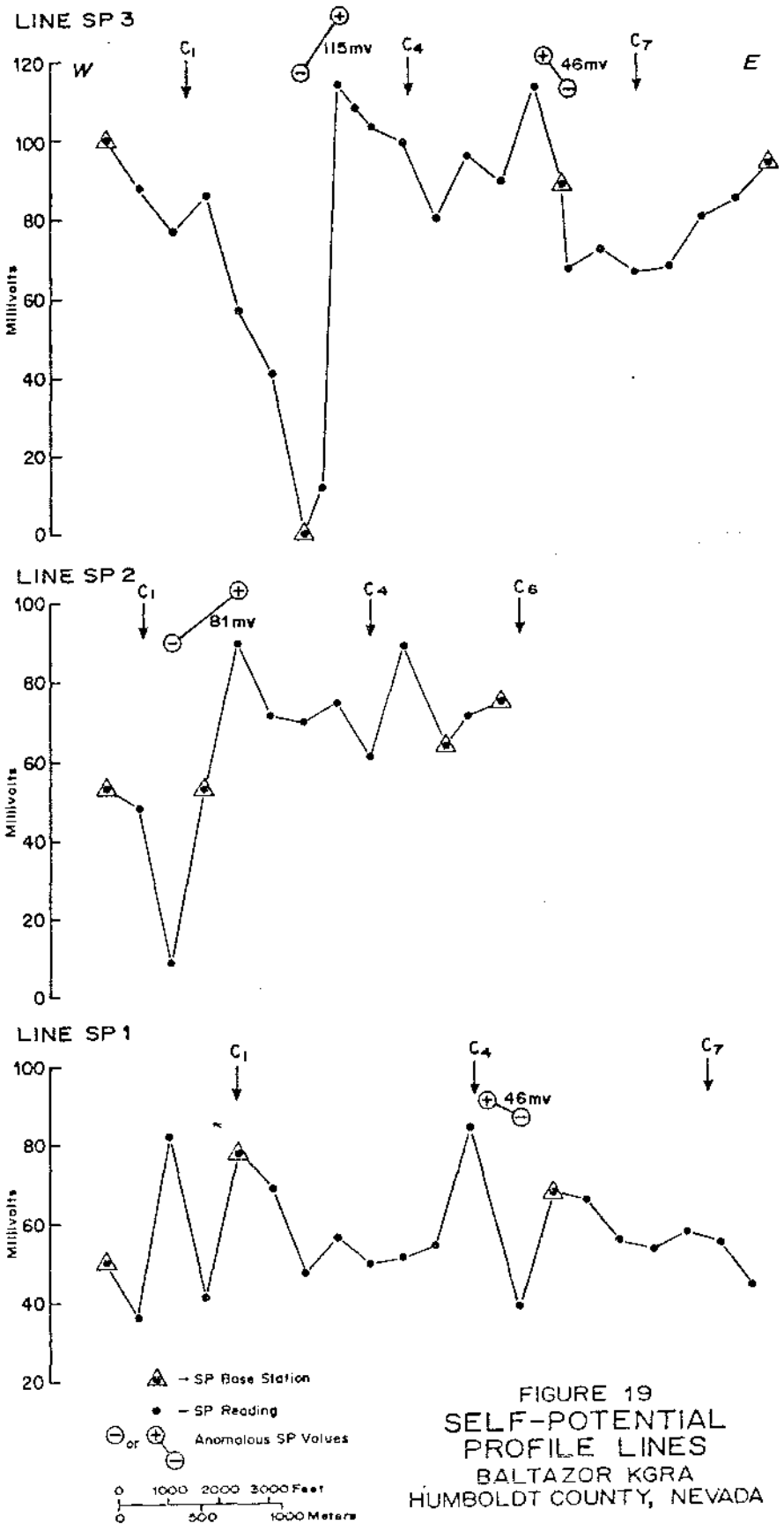


FIGURE 19
SELF-POTENTIAL
PROFILE LINES
BALTAZOR KGRA
HUMBOLDT COUNTY, NEVADA

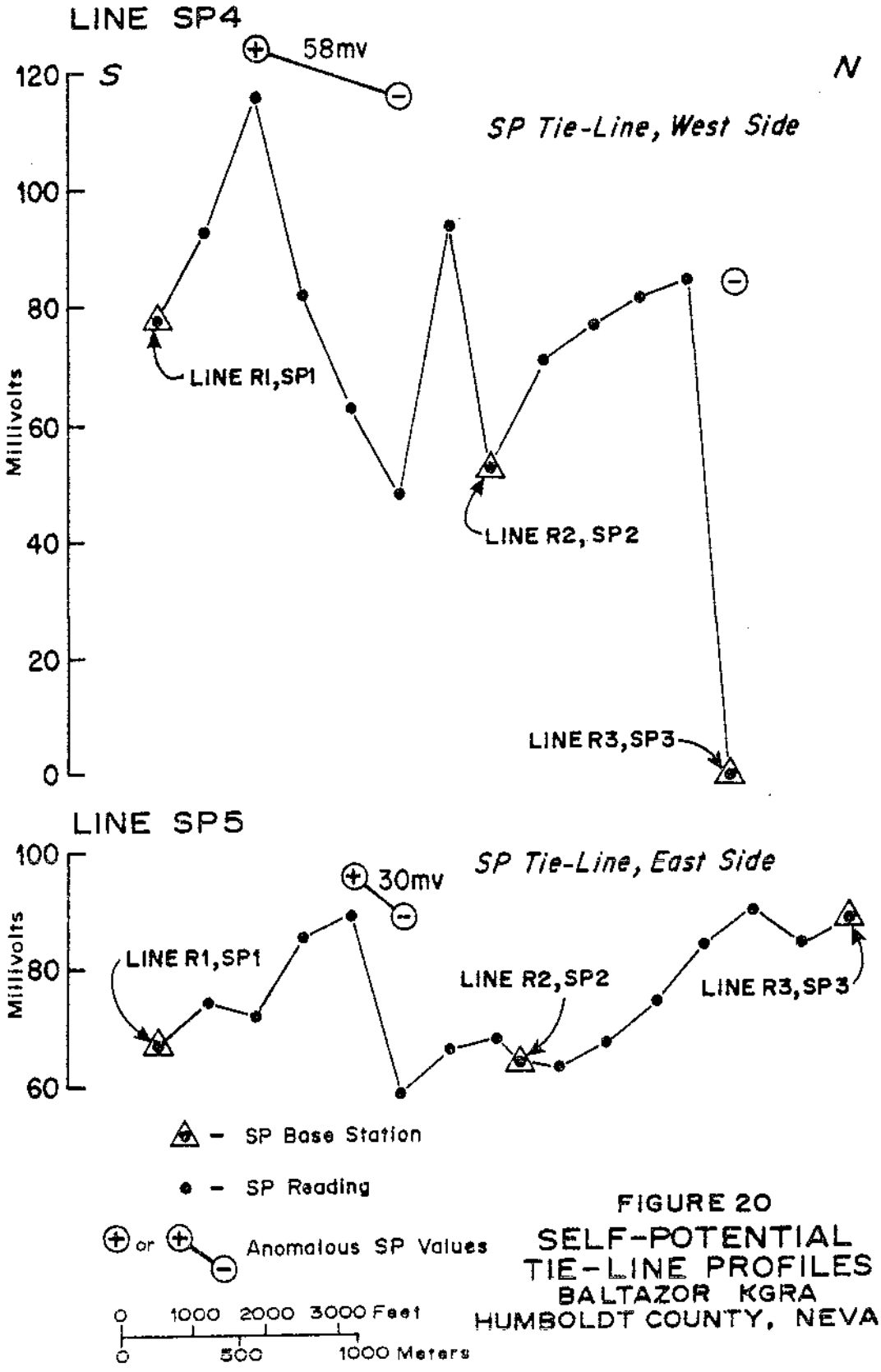


FIGURE 20
SELF-POTENTIAL
TIE-LINE PROFILES
BALTAZOR KGRA
HUMBOLDT COUNTY, NEVADA

draw any conclusions. The tie-lines (Figure 20) are sub-parallel to the structural trends. Line SP-5 is relatively featureless but line SP-4 has sharp gradients where it intersects modeled or projected faults determined with the gravity data. Hence, some of the SP anomalies at Baltazor are probably related to thermoelectric and electrokinetic (streaming potential) effects associated with fault zones and clay alteration in the alluvium.

Figure 21 presents the three profiles for the Painted Hills area. The west side of line SP-7 was observed along dipole-dipole resistivity line 4, and then extended across Bog Hot Valley. SP lines 6 and 8 follow gravity profiles M3 and M1, respectively. Again, a long wave length anomaly is not evident in the data. Multi-point SP anomalies with amplitudes of 20 to 40 mv occur at the west ends of each profile, including areas where lateral contrasts were modeled for the gravity and resistivity data. However, the correlation between lines is ambiguous and the anomalies are weak.

Alternating highs and lows with 40 to 60 mv of relief occur on line SP-8 and appear to be real but do not correspond to any structure in the gravity or resistivity models. The same is true for a roughly dipolar 55 mv anomaly at the east end of line SP-6. The strongest anomaly in the area is a base level change that occurs on line SP-7 on the eastern extension into Bog Hot Valley and beyond the area of detail interest. This line continues to the east 4 km beyond what is shown on Figure 21 and on this extension the SP values fluctuate between 0 and -26 mv.

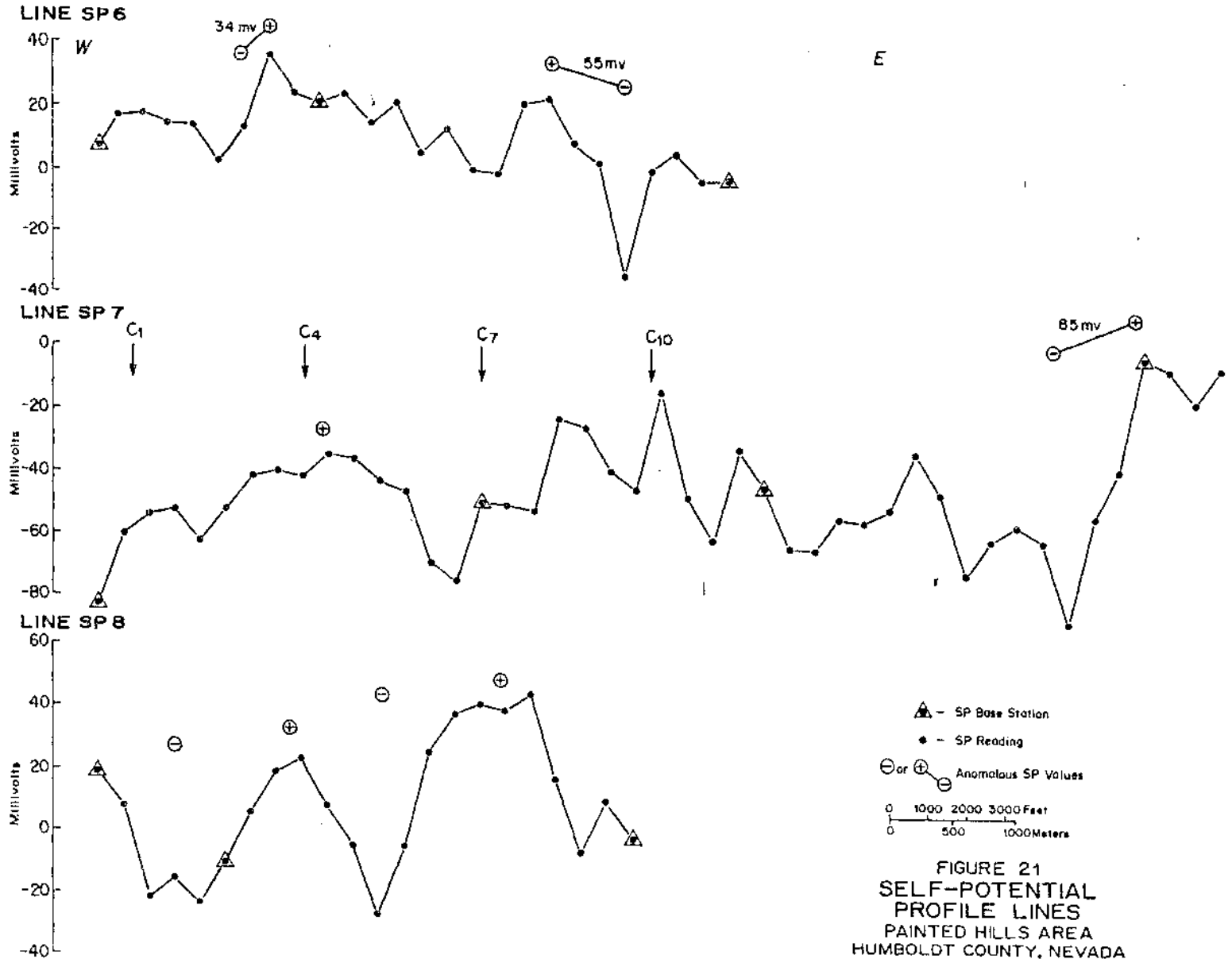


FIGURE 21
SELF-POTENTIAL
PROFILE LINES
PAINTED HILLS AREA
HUMBOLDT COUNTY, NEVADA

## SUMMARY AND DISCUSSION

Figure 22 is a composite interpretation plan map of the Baltazor Hot Springs KGRA. The principal structural features, previously discussed with regard to Figure 12 and shown again on Figure 22, are: 1) two valley-bordering faults labeled (1a) and (1b); and, 2) a central graben labeled (2), although this structure is somewhat more complex on line B2. As shown on Figure 22, the valley drainage and Baltazor Hot Springs lie within or near the surface trace of the central graben, and low (5 to 7 Ω-m) near-surface resistivities occur coincident with this topographic low on the northern two lines. Low (2 to 15 Ω-m) near-surface resistivities are also observed beginning at Fault (1a) and extending to the east toward the center of the valley on each of the lines. An approximately 100 mv dipolar SP anomaly occurs coincident with Fault (1a) on the northern two lines. Drill hole BZ 1500-1, shown on Figure 22, was drilled on line B2 and encountered alluvium saturated with hot fluid.

Figure 23 portrays an interpreted east-west geologic cross section of Continental Lake Valley along line B2. The thermal manifestations at Baltazor KGRA are interpreted to be localized by Fault (1a). This fault zone acts as a conduit for upwardly mobile hot fluids that presumably circulate toward the center of the valley and run off along the valley drainage. Low (5 to 7 Ω-m) resistivities west of Fault (1a) and beneath the Pueblo Mountains are interpreted as due to porous units of the Steens Basalt containing clay alteration products and thermal

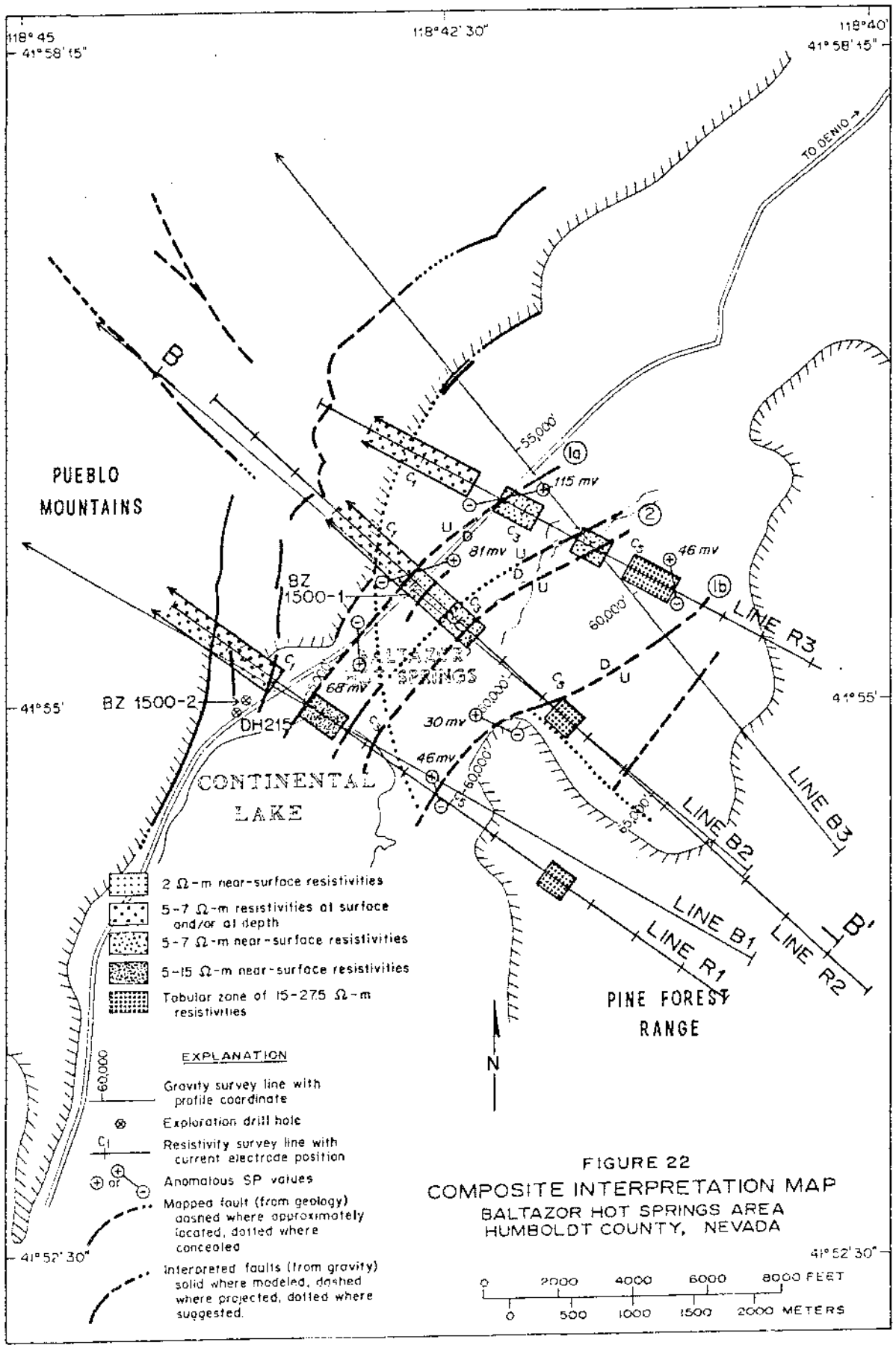


FIGURE 22
COMPOSITE INTERPRETATION MAP
BALTAZOR HOT SPRINGS AREA
HUMBOLDT COUNTY, NEVADA

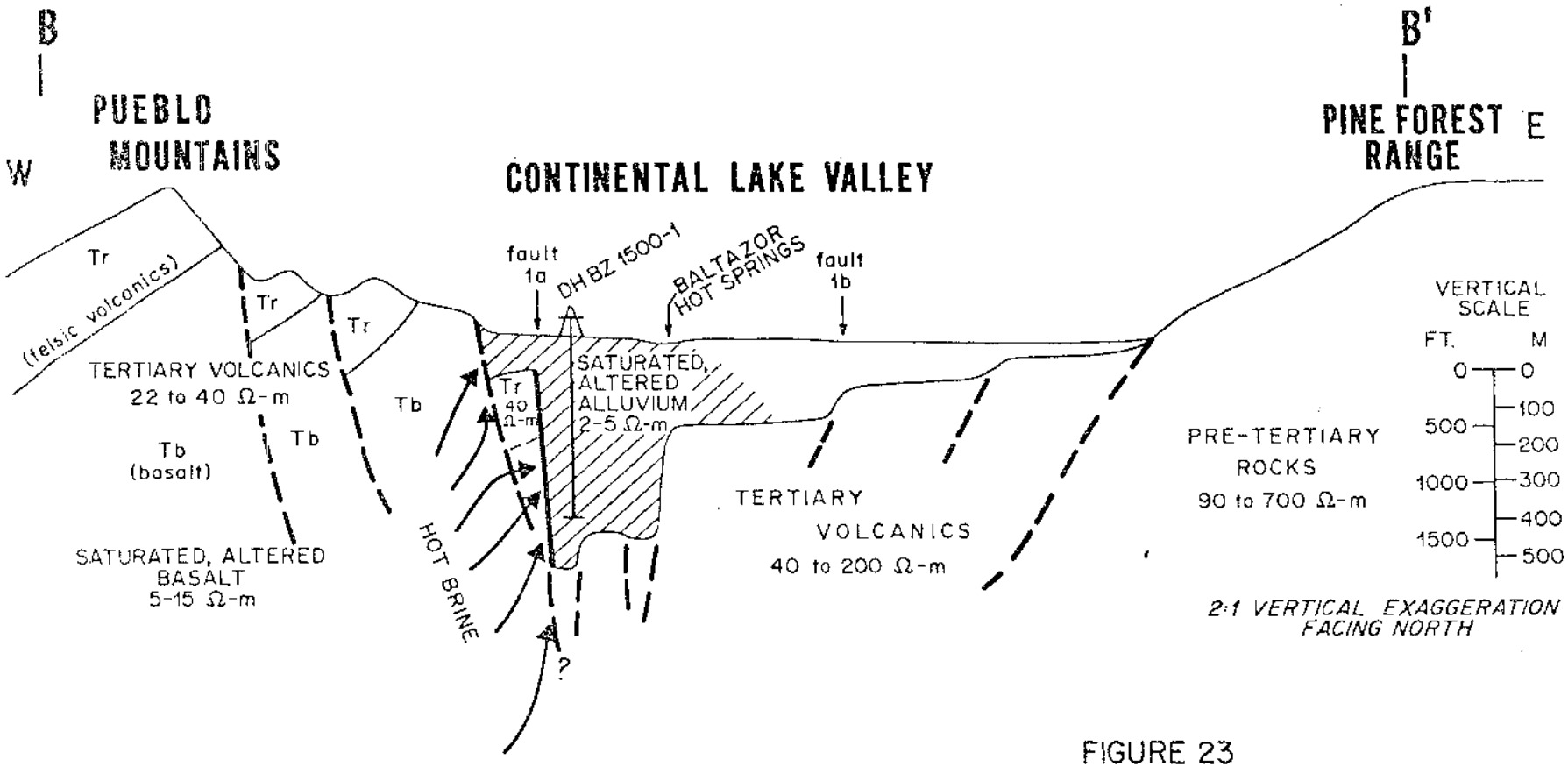


FIGURE 23

INTERPRETED GEOLOGIC CROSS-SECTION
ALONG LINE B2
BALTAZOR HOT SPRINGS KGRA
HUMBOLDT COUNTY, NEVADA

fluids. Fault (1a) may either tap aquifers in the Steens Basalt, or, alternately, leak fluids into the basalt.

As shown on Figure 22, SP anomalies have some correlation with Fault (1b). However, these anomalies are weak and low resistivities are not modeled here, so significant thermal activity is not expected. Also, on the east side of the valley and shown on Figure 22, the tabular zone of low resistivity modeled on each of the resistivity lines is seen to strike roughly due north; however, this trend is not related to any other known structure.

Figure 24 is a composite interpretation plan map of the Painted Hills area, while Figure 25 is a interpreted east-west geologic cross section along line M2. The main features, shown on both figures, are: 1) the high density zone west of the Rock Spring Table margin, 2) a sloping contact bordering the table interpreted as the limit of hematitic and argillic alteration ± silicification, and 3) a graben-like structure on the east side of the plateau margin interpreted as a thick section of unaltered Thousand Creek Formation. As discussed above, the preferred explanation for the high-density body is that it is a zone of higher grade alteration, probably including intense silicification. In this case, the hematitic and argillic alteration that characterize the Painted Hills area would undoubtedly be genetically related. The data are insufficient to determine whether the limit of the hematitic and argillic alteration (best shown on Figure 25) is due to faulting or to some other factor, such as permeability. However, the vertical zone of low resistivities discussed above (Figure 18) and shown on Figures 24 and 25 is marginal to the high-density body and probably is fault controlled, the low resistivity resulting from

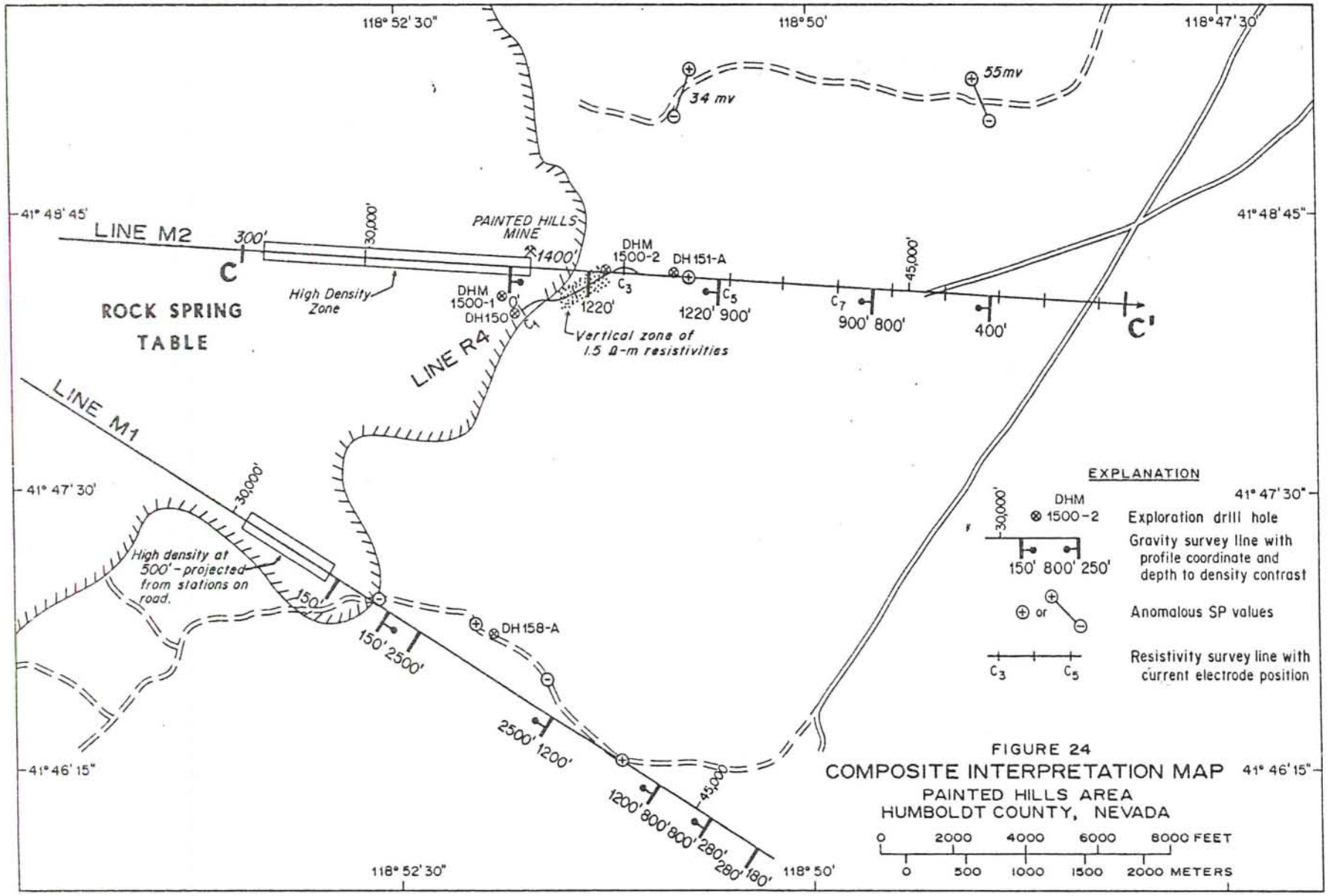


FIGURE 24
COMPOSITE INTERPRETATION MAP
PAINTED HILLS AREA
HUMBOLDT COUNTY, NEVADA

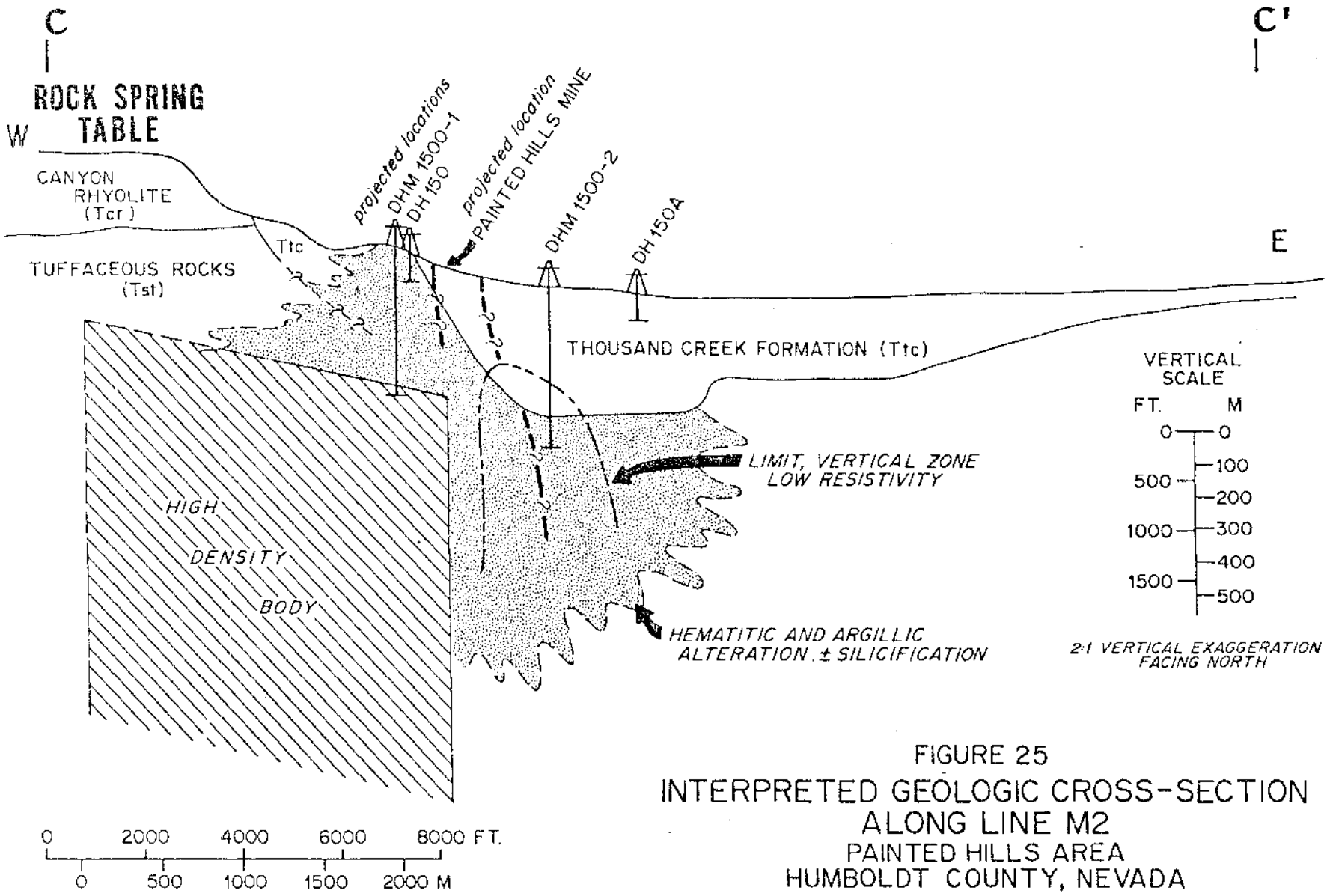


FIGURE 25

INTERPRETED GEOLOGIC CROSS-SECTION
ALONG LINE M2
PAINTED HILLS AREA
HUMBOLDT COUNTY, NEVADA

increased porosity due to fracturing and perhaps the presence of conductive fluids and additional clay alteration.

The low amplitude, short wavelength SP anomalies on the center SP line at the Painted Hills area (line SP-7, Figure 21) can not be correlated with any certainty to SP features one to two miles distant on the other two lines. Also, the resistivity and gravity data are relatively featureless east of about drill holes 151-A and 158-A (Figure 24) and hence do not help to explain the SP data. In summary, the SP survey did not contribute to the geologic interpretation at the Painted Hills area.

The exploration drilling to date at the Painted Hills area (see Figure 3) does not suggest an obvious relation between features in the geophysical data and elevated temperatures. However, the highest thermal gradient encountered (in DH 150, shown on Figures 24 and 25) occurred in strongly altered rocks west of the vertical zone of low resistivities and above the high-density zone modeled with the gravity data. If the high-density feature is due to more intense and/or higher grade alteration than is seen at the surface or in drill cuttings received to date, anomalous temperatures could be associated with the hydrothermal system that caused or is causing this alteration, or with high thermal conductivities due to silicification. Hence, intensity of alteration could be a direct guide to elevated temperatures. If this is tne case, the fault zone suggested by the vertical zone of low resistivities may not be the primary control of the thermal anomaly at the Painted Hills area.

In regard to regional structure, the NE-trending gravity low (⑤ and ⑥ of Figure 5) that appears to relate the Painted Hills area and

Baltazor Hot Springs KGRA lies on a prominent topographic linear that extends over 65 miles (104 km) from the Soldier Meadow Hot Springs to the large fault that forms the eastern boundary of the Pine Forest Range. This linear is briefly discussed by Hose and Taylor (1974) and a modified sketch from their report is given in Figure 26. The intersection of this linear and the range-bounding fault, near Denio, Nevada, is the location of the 39 event Denio microearthquake cluster (Senturion Sciences, Inc., 1977) shown on Figure 3. Given the known thermal anomalies associated with this linear, it is a prime target for geothermal resources.

The Eugene-Denio fault zone, as proposed by Lawrence (1976), is one of three parallel west-northwest-trending belts of apparent transform faulting at the northern margin of the Basin and Range province. This fault zone, trending N60°W, projects through the northeastern portion of the study area. Local expressions of the Eugene-Denio zone may include: 1) "A NW-SE grain...imposed on the topography and drainage" north of the Rock Spring Table (Gardner and Koenig, 1978), 2) a subtle NW-SE trend in the residual gravity data (Figure 8) from the vicinity of Bog Hot Springs to the southern extreme of the Strawberry Butte gravity high ((1) of Figure 8), and 3) NW-SE-trending faults mapped by Hulen (1979) in the southern Pueblo Mountains. Hulen (1979) suggests that Baltazor Hot Springs is controlled by the intersection of one of these faults with the Pueblo Mountains eastern range-front fault zone (Fault (1a) of Figure 22) which forms a segment of the prominent NE-trending topographic linear discussed above and shown on Figure 26. Since the apparent intersection of the Eugene-Denio fault zone with the topographic linear of Figure 26 is

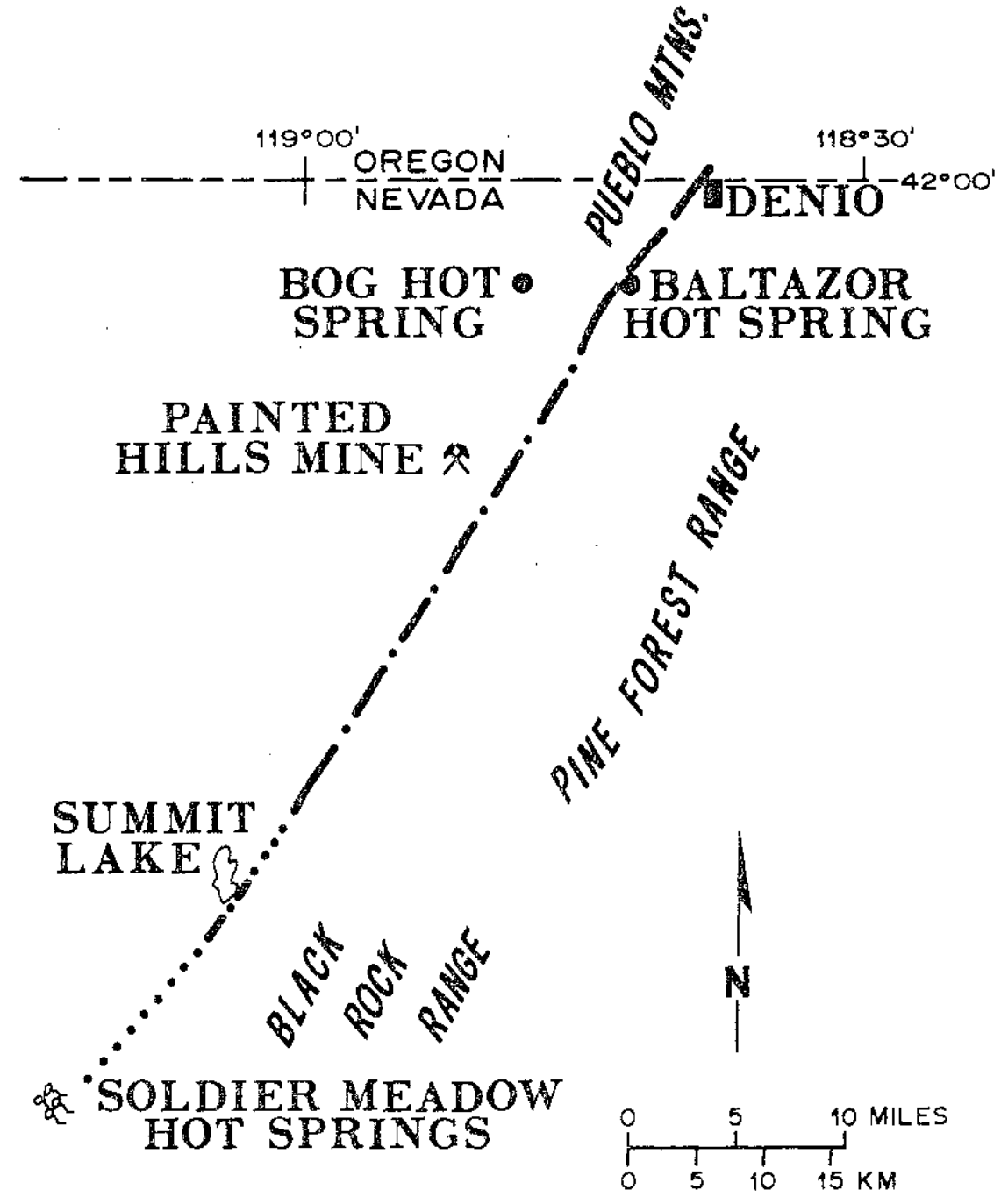


FIGURE 26

RELATION OF TOPOGRAPHIC LINEAR TO HOT SPRINGS
HUMBOLDT COUNTY, NEVADA

important at Baltazor Hot Springs, other such intersections should be investigated for geothermal resources. The most obvious such target is the covered area just south of the Pueblo Mountains in Bog Hot Valley.

APPENDIX I

## Principal Facts of the Gravity Data

Tables 2 through 5 describe a station location accuracy code developed by the U.S. Geological Survey that was assigned to the stations read by the author. These tables were taken from Plouff et al. (1976) and their code assignment is repeated here for stations included from that survey. Modifications of the code for the present survey are indicated by parentheses in Tables 2 through 5.

Table 6 presents the principal facts of the gravity data. The station labels are coded as follows:

| Label | Description |
|---|---|
| DB | Master base station "in Denio, Nevada at the Post Office, 50 meters south of the Oregon-Nevada state line, 1.6 meters south of the door in the southeast corner of the concrete porch, near the mail box...Base value is 979,945.94" (Peterson and Hoover, 1977).<br><br>This site had a monument with a "U.S.A.F. Gravity Station" disc (A.C.I.C. reference no. 2352-1), but in April of 1980 the author noted that the monument had been broken out of the concrete slab. |
| BM67 & BM281 | Bench marks used as the two field base stations. |
| "M" and "B" prefix | Detail profile line stations - M for the Painted Hills area, B for the Baltazor area. Prefix followed by the line number and station number. Observed in September, 1979. |
| "R" prefix | Regional data base point acquired by the author in September, 1979. |

| | |
|---|---|
| "A" prefix | Regional data base point acquired by the author in April, 1980. |
| "CS" prefix | From Plouff et al., 1976. |
| "DE" prefix | From Peterson and Hoover, 1977. |

All gravity values are in milligals. Complete Bouguer gravity values are listed in Table 6 for Bouguer reduction densities of 2.45 and 2.67 gm/cc. The listed terrain corrections are for a density of 2.67 gm/cc. The inner zone correction represents Hammer chart zones A through F.

Table 2. Location description code (digit one).

| Code | Examples |
|---|---|
| B | On level-line bench mark or other permanent marks incorporated into U.S. Geological Survey vertical control system. |
| N | Near level-line bench mark. (Note. In this survey, all profile points on level lines have this classification). |
| V | On vertical angle bench mark. (Note. In this survey, profile points acquired with the KERN theodolile have this classification). |
| H | Near vertical angle bench mark. |
| X | Near location markers such as section corners, wells, or windmills. |
| D | Near assumed location of any of the above markers that was destroyed or not found. |
| F | Near a location with or without a marker at which a surveyed elevation is indicated on a published topographic map. |
| G | Near a location on a manuscript map or a published map at which spot elevations are determined by photogrammetry or near a doubtful F-location. |
| W | Near edge of lake or reservoir, interpolated elevation or elevation given for water or dam frequently at unknown height relative to present level. |
| C | Topographic contour line interpolation not along stream. (Note. In this survey, barometric or topographic control has this classification). |
| Q | Topographic contour line interpolation along stream. |

Table 3. Accuracy of elevations (digit two).

| Code | Accuracy (Feet) | Examples |
|---|---|---|
| 1 | 0.1 | On Bench mark |
| 2 | 0.5 | Elevation difference hand-leveled to nearby bench mark. (Note. In this survey, profile points on level lines.) |
| 3 | 1 | Near bench mark. (Note. In this survey, also vertical angle elevation control.) |
| 4 | 2 | Near assumed location of bench mark that was not found. |
| 5 | 5 | Surveyed spot elevation - "F" for digit one. |
| 6 | 10 | Photogrammetric elevation of precise location such as fence corner. |
| 7 | 20 | Photogrammetric elevation on map with a 40-foot contour interval. |
| 8 | | Primarily barometric altimeter control. |

Table 4. Accuracy of horizontal location (digit three).

| Code | Accuracy (feet) | Examples |
|---|---|---|
| 2 | 84 | Near section corners, bench marks, road intersections, or stream crossings. (Note. Also survey lines.) |
| 3 | 210 | Sharp road curve; uncertain spot elevation location. |
| 4 | 420 | Broad road curve or gentle hillcrest. |

Table 5. Accuracy of observed gravity (digit four).

| Code | Accuracy (mgal) | Examples |
|---|---|---|
| 1 | 0.01 | Principal base station |
| 3 | 0.05 | Repeated reading |
| 4 | 0.10 | Non-repeated reading |

Table 6

Principal facts of the
gravity data

| STAT NO | LATITUDE DEG | LATITUDE MIN | LONGITUDE DEG | LONGITUDE MIN | ELEV FT | OBSERVED GRAVITY | THEORETICAL GRAVITY | TERRAIN COR INNER | TERRAIN COR TOTAL | COMPLETE BOUGUER 2.45 | BOUGUER 2.67 | CODE |
|---|---|---|---|---|---|---|---|---|---|---|---|---|
| BM281 | 41. | 48.99 | 118. | 47.73 | 4281. | 979913.50 | 980342.65 | .01 | .70 | -159.65 | -171.57 | B121 |
| M1-20 | 41. | 46.48 | 118. | 54.26 | 5253. | 979852.34 | 980338.91 | .11 | 1.71 | -155.15 | -169.70 | V323 |
| M1-19 | 41. | 46.61 | 118. | 54.10 | 5227. | 979854.68 | 980339.11 | .12 | 1.71 | -154.60 | -169.08 | V324 |
| M1-18 | 41. | 46.83 | 118. | 53.84 | 5221. | 979855.44 | 980339.45 | .22 | 1.85 | -154.44 | -168.89 | V324 |
| M1-17 | 41. | 46.94 | 118. | 53.43 | 5152. | 979860.58 | 980339.60 | .92 | 2.56 | -153.15 | -167.35 | V324 |
| M1-16 | 41. | 46.97 | 118. | 53.20 | 5137. | 979860.46 | 980339.65 | 1.50 | 3.11 | -153.73 | -167.86 | V324 |
| M1-15 | 41. | 46.96 | 118. | 52.98 | 5152. | 979856.74 | 980339.63 | 1.69 | 3.27 | -156.34 | -170.48 | V324 |
| M1-14 | 41. | 47.02 | 118. | 52.76 | 5070. | 979860.97 | 980339.72 | 1.61 | 3.15 | -157.46 | -171.39 | V324 |
| M1-13 | 41. | 47.03 | 118. | 52.56 | 4938. | 979867.80 | 980339.73 | 1.13 | 2.61 | -159.43 | -173.04 | V324 |
| M1-12 | 41. | 46.97 | 118. | 52.32 | 4859. | 979871.24 | 980339.65 | .22 | 1.57 | -161.81 | -175.28 | V324 |
| M1-11 | 41. | 46.97 | 118. | 52.08 | 4815. | 979872.95 | 980339.65 | .14 | 1.38 | -163.07 | -176.42 | V324 |
| M1-10 | 41. | 46.86 | 118. | 51.95 | 4810. | 979873.04 | 980339.49 | .24 | 1.38 | -163.15 | -176.50 | N224 |
| M1-9 | 41. | 46.78 | 118. | 51.76 | 4748. | 979876.77 | 980339.37 | .12 | 1.19 | -163.33 | -176.53 | N224 |
| M1-8 | 41. | 46.66 | 118. | 51.60 | 4687. | 979880.73 | 980339.18 | .16 | 1.17 | -163.00 | -176.03 | N224 |
| M1-7 | 41. | 46.52 | 118. | 51.51 | 4600. | 979886.78 | 980338.98 | .21 | 1.24 | -162.21 | -174.98 | N224 |
| M1-6 | 41. | 46.42 | 118. | 51.33 | 4542. | 979890.71 | 980338.84 | .09 | 1.12 | -161.89 | -174.50 | N224 |
| M1-5 | 41. | 46.30 | 118. | 51.14 | 4499. | 979893.75 | 980338.64 | .03 | 1.06 | -161.40 | -173.90 | N224 |
| M1-4 | 41. | 46.28 | 118. | 50.94 | 4456. | 979896.87 | 980338.61 | .04 | 1.10 | -160.89 | -173.27 | N224 |
| M1-3 | 41. | 46.30 | 118. | 50.72 | 4425. | 979899.45 | 980338.64 | .04 | 1.12 | -160.26 | -172.56 | N224 |
| M1-2 | 41. | 46.26 | 118. | 50.50 | 4394. | 979902.09 | 980338.58 | .07 | 1.18 | -159.48 | -171.68 | N224 |
| M1-1 | 41. | 46.23 | 118. | 50.28 | 4371. | 979904.07 | 980338.54 | .06 | 1.20 | -158.87 | -171.00 | B123 |
| M2-07 | 41. | 48.42 | 118. | 49.67 | 4392. | 979903.61 | 980341.80 | .01 | .83 | -161.64 | -173.85 | N224 |
| M2-06 | 41. | 48.40 | 118. | 49.43 | 4374. | 979904.92 | 980341.77 | .02 | .81 | -161.42 | -173.59 | N224 |
| M2-05 | 41. | 48.40 | 118. | 49.20 | 4359. | 979906.26 | 980341.77 | .02 | .79 | -161.07 | -173.19 | N224 |
| M2-04 | 41. | 48.39 | 118. | 48.97 | 4344. | 979907.50 | 980341.77 | .01 | .77 | -160.76 | -172.85 | N224 |
| M2-03 | 41. | 48.38 | 118. | 48.74 | 4336. | 979908.40 | 980341.75 | .02 | .77 | -160.37 | -172.44 | N224 |
| M2-02 | 41. | 48.36 | 118. | 48.52 | 4320. | 979909.64 | 980341.72 | .01 | .76 | -160.12 | -172.14 | N224 |
| M2-01 | 41. | 48.35 | 118. | 48.29 | 4288. | 979911.79 | 980341.70 | .00 | .79 | -159.92 | -171.86 | N224 |
| BM 67 | 41. | 55.61 | 118. | 42.50 | 4234. | 979952.44 | 980352.55 | .14 | 1.50 | -132.83 | -144.56 | B121 |
| B3-26 | 41. | 56.64 | 118. | 42.64 | 4583. | 979936.26 | 980354.09 | .85 | 2.02 | -128.18 | -140.84 | V324 |
| B3-25 | 41. | 56.58 | 118. | 42.58 | 4557. | 979938.02 | 980354.00 | .66 | 2.11 | -127.89 | -140.46 | V324 |
| B3-24 | 41. | 56.52 | 118. | 42.51 | 4479. | 979942.49 | 980353.91 | .62 | 2.13 | -128.17 | -140.53 | V324 |

| STAT NO | LATITUDE DEG | LATITUDE MIN | LONGITUDE DEG | LONGITUDE MIN | ELEV FT | OBSERVED GRAVITY | THEORETICAL GRAVITY | TERRAIN COR INNER | TERRAIN COR TOTAL | COMPLETE 2.45 | BOUGUER 2.67 | CODE |
|---|---|---|---|---|---|---|---|---|---|---|---|---|
| B3-23 | 41. | 56.46 | 118. | 42.44 | 4394. | 979947.19 | 980353.83 | .57 | 2.19 | -128.71 | -140.83 | V324 |
| B3-22 | 41. | 56.39 | 118. | 42.37 | 4342. | 979949.02 | 980353.73 | .43 | 2.06 | -130.15 | -142.13 | V324 |
| B3-21 | 41. | 56.32 | 118. | 42.30 | 4313. | 979950.66 | 980353.61 | .23 | 1.80 | -130.46 | -142.39 | N224 |
| B3-20 | 41. | 56.26 | 118. | 42.23 | 4289. | 979952.21 | 980353.52 | .12 | 1.64 | -130.46 | -142.32 | N224 |
| B3-19 | 41. | 56.20 | 118. | 42.16 | 4271. | 979953.34 | 980353.44 | .11 | 1.57 | -130.46 | -142.28 | N224 |
| B3-18 | 41. | 56.13 | 118. | 42.09 | 4250. | 979954.62 | 980353.33 | .09 | 1.51 | -130.41 | -142.17 | N224 |
| B3-17 | 41. | 56.06 | 118. | 42.02 | 4232. | 979955.72 | 980353.23 | .05 | 1.44 | -130.44 | -142.16 | N224 |
| B3-16 | 41. | 56.00 | 118. | 41.95 | 4219. | 979956.30 | 980353.14 | .03 | 1.39 | -130.59 | -142.28 | N224 |
| B3-15 | 41. | 55.94 | 118. | 41.88 | 4211. | 979956.52 | 980353.04 | .02 | 1.34 | -130.84 | -142.52 | N224 |
| B3-14 | 41. | 55.88 | 118. | 41.82 | 4209. | 979956.46 | 980352.95 | .01 | 1.30 | -130.99 | -142.66 | N224 |
| B3-13 | 41. | 55.80 | 118. | 41.74 | 4208. | 979956.54 | 980352.84 | .00 | 1.25 | -130.87 | -142.55 | B124 |
| B3-12 | 41. | 55.74 | 118. | 41.68 | 4208. | 979956.62 | 980352.75 | .01 | 1.24 | -130.71 | -142.39 | N224 |
| B3-01 | 41. | 55.04 | 118. | 40.91 | 4367. | 979950.98 | 980351.70 | .33 | 1.60 | -125.01 | -137.09 | N224 |
| B3-02 | 41. | 55.10 | 118. | 40.98 | 4332. | 979953.26 | 980351.79 | .13 | 1.43 | -125.18 | -137.18 | N224 |
| B3-03 | 41. | 55.16 | 118. | 41.05 | 4310. | 979954.85 | 980351.87 | .09 | 1.39 | -125.08 | -137.02 | N224 |
| B3-04 | 41. | 55.23 | 118. | 41.12 | 4289. | 979955.77 | 980351.99 | .07 | 1.35 | -125.63 | -137.52 | N224 |
| B3-05 | 41. | 55.30 | 118. | 41.19 | 4267. | 979956.38 | 980352.09 | .06 | 1.34 | -126.54 | -138.36 | N224 |
| B3-06 | 41. | 55.36 | 118. | 41.26 | 4246. | 979957.39 | 980352.18 | .06 | 1.34 | -126.93 | -138.69 | N224 |
| B3-07 | 41. | 55.42 | 118. | 41.33 | 4230. | 979957.96 | 980352.27 | .04 | 1.32 | -127.49 | -139.21 | N224 |
| B3-08 | 41. | 55.49 | 118. | 41.40 | 4217. | 979958.48 | 980352.37 | .02 | 1.29 | -127.89 | -139.59 | N224 |
| B3-09 | 41. | 55.55 | 118. | 41.47 | 4209. | 979958.49 | 980352.46 | .04 | 1.30 | -128.48 | -140.14 | N224 |
| B3-10 | 41. | 55.61 | 118. | 41.54 | 4208. | 979957.80 | 980352.55 | .02 | 1.26 | -129.33 | -141.00 | N224 |
| B3-11 | 41. | 55.68 | 118. | 41.60 | 4218. | 979957.11 | 980352.66 | .01 | 1.21 | -129.55 | -141.25 | N224 |
| B1-01 | 41. | 54.48 | 118. | 42.11 | 4313. | 979947.35 | 980350.87 | .59 | 1.48 | -131.31 | -143.26 | N224 |
| B1-02 | 41. | 54.53 | 118. | 42.20 | 4270. | 979949.65 | 980350.94 | .41 | 1.36 | -131.89 | -143.72 | N224 |
| B1-03 | 41. | 54.57 | 118. | 42.30 | 4251. | 979950.55 | 980351.00 | .35 | 1.31 | -132.30 | -144.08 | N224 |
| B1-04 | 41. | 54.61 | 118. | 42.40 | 4229. | 979951.16 | 980351.05 | .30 | 1.28 | -133.16 | -144.89 | N224 |
| B1-05 | 41. | 54.65 | 118. | 42.49 | 4218. | 979950.85 | 980351.12 | .11 | 1.10 | -134.36 | -146.07 | N224 |
| B1-06 | 41. | 54.69 | 118. | 42.58 | 4218. | 979949.93 | 980351.18 | .11 | 1.20 | -135.25 | -146.95 | N224 |
| B1-07 | 41. | 54.74 | 118. | 42.67 | 4222. | 979949.02 | 980351.24 | .22 | 1.36 | -135.84 | -147.54 | N224 |
| B1-08 | 41. | 54.78 | 118. | 42.77 | 4217. | 979948.83 | 980351.30 | .42 | 1.64 | -136.19 | -147.85 | N224 |
| B1-09 | 41. | 54.82 | 118. | 42.86 | 4214. | 979948.51 | 980351.37 | .75 | 2.01 | -136.37 | -148.00 | N224 |

| STAT NO | LATITUDE DEG | LATITUDE MIN | LONGITUDE DEG | LONGITUDE MIN | ELEV FT | OBSERVED GRAVITY | THEORETICAL GRAVITY | TERRAIN COR INNER | TERRAIN COR TOTAL | COMPLETE BOUGUER 2.45 | BOUGUER 2.67 | CODE |
|---|---|---|---|---|---|---|---|---|---|---|---|---|
| B1-10 | 41. | 54.86 | 118. | 42.96 | 4214. | 979948.27 | 980351.44 | .03 | 1.09 | -137.56 | -149.26 | N224 |
| B1-11 | 41. | 54.90 | 118. | 43.05 | 4214. | 979948.09 | 980351.50 | .05 | 1.16 | -137.73 | -149.43 | N224 |
| B1-12 | 41. | 54.94 | 118. | 43.15 | 4214. | 979948.01 | 980351.55 | .12 | 1.29 | -137.76 | -149.44 | N224 |
| B1-13 | 41. | 54.98 | 118. | 43.25 | 4220. | 979947.94 | 980351.61 | .09 | 1.32 | -137.48 | -149.18 | N224 |
| B1-14 | 41. | 55.02 | 118. | 43.34 | 4228. | 979947.47 | 980351.66 | .20 | 1.49 | -137.33 | -149.03 | N224 |
| B1-15 | 41. | 55.06 | 118. | 43.45 | 4252. | 979945.88 | 980351.73 | .51 | 1.82 | -137.19 | -148.93 | N224 |
| B1-16 | 41. | 55.10 | 118. | 43.54 | 4276. | 979944.45 | 980351.79 | 1.04 | 2.36 | -136.64 | -148.41 | N224 |
| B1-17 | 41. | 55.14 | 118. | 43.62 | 4324. | 979941.51 | 980351.84 | 1.48 | 2.73 | -136.27 | -148.15 | N224 |
| B1-18 | 41. | 55.18 | 118. | 43.72 | 4376. | 979937.93 | 980351.90 | 2.29 | 3.47 | -135.98 | -147.94 | N224 |
| B2-1E | 41. | 54.40 | 118. | 40.92 | 4545. | 979938.44 | 980350.73 | 1.08 | 2.05 | -124.98 | -137.53 | V324 |
| B2-2E | 41. | 54.30 | 118. | 40.77 | 4670. | 979931.46 | 980350.59 | 1.03 | 1.88 | -124.11 | -137.03 | V324 |
| B2-3E | 41. | 54.23 | 118. | 40.67 | 4869. | 979919.20 | 980350.49 | .95 | 1.81 | -123.86 | -137.33 | V324 |
| B2-4E | 41. | 54.16 | 118. | 40.54 | 4928. | 979915.61 | 980350.38 | .99 | 1.87 | -123.56 | -137.20 | V324 |
| B2-5E | 41. | 54.06 | 118. | 40.40 | 5048. | 979908.03 | 980350.24 | .95 | 2.03 | -123.34 | -137.29 | V324 |
| B2-10 | 41. | 54.98 | 118. | 41.83 | 4254. | 979953.37 | 980351.61 | .14 | 1.18 | -130.05 | -141.85 | N224 |
| B2-09 | 41. | 54.92 | 118. | 41.74 | 4269. | 979952.87 | 980351.52 | .14 | 1.18 | -129.50 | -141.34 | N224 |
| B2-08 | 41. | 54.86 | 118. | 41.65 | 4289. | 979951.92 | 980351.44 | .13 | 1.17 | -129.11 | -141.01 | N224 |
| B2-07 | 41. | 54.81 | 118. | 41.58 | 4309. | 979951.39 | 980351.34 | .16 | 1.20 | -128.27 | -140.22 | N224 |
| B2-06 | 41. | 54.76 | 118. | 41.50 | 4329. | 979950.13 | 980351.27 | .13 | 1.17 | -128.18 | -140.20 | N224 |
| B2-05 | 41. | 54.70 | 118. | 41.40 | 4351. | 979949.14 | 980351.19 | .23 | 1.29 | -127.60 | -139.67 | N224 |
| B2-04 | 41. | 54.64 | 118. | 41.32 | 4379. | 979948.00 | 980351.10 | .24 | 1.31 | -126.90 | -139.04 | N224 |
| B2-03 | 41. | 54.60 | 118. | 41.25 | 4406. | 979946.99 | 980351.04 | .25 | 1.31 | -126.16 | -138.38 | N224 |
| B2-02 | 41. | 54.54 | 118. | 41.16 | 4430. | 979946.24 | 980350.95 | .28 | 1.35 | -125.27 | -137.56 | N224 |
| B2-01 | 41. | 54.50 | 118. | 41.09 | 4473. | 979944.02 | 980350.90 | .30 | 1.32 | -124.78 | -137.20 | N224 |
| B2-11 | 41. | 55.03 | 118. | 41.90 | 4240. | 979953.77 | 980351.68 | .13 | 1.18 | -130.58 | -142.34 | N224 |
| B2-12 | 41. | 55.08 | 118. | 41.99 | 4227. | 979954.09 | 980351.76 | .07 | 1.14 | -131.20 | -142.94 | N224 |
| B2-13 | 41. | 55.14 | 118. | 42.08 | 4216. | 979954.30 | 980351.84 | .05 | 1.14 | -131.74 | -143.45 | N224 |
| B2-14 | 41. | 55.19 | 118. | 42.16 | 4214. | 979953.75 | 980351.91 | .03 | 1.13 | -132.47 | -144.17 | N224 |
| B2-20 | 41. | 55.52 | 118. | 42.68 | 4241. | 979951.30 | 980352.41 | .37 | 1.76 | -133.16 | -144.89 | N224 |
| B2-21 | 41. | 55.57 | 118. | 42.77 | 4273. | 979949.40 | 980352.48 | .75 | 2.16 | -132.79 | -144.57 | N224 |
| B2-22 | 41. | 55.62 | 118. | 42.86 | 4329. | 979945.79 | 980352.57 | 1.34 | 2.27 | -132.83 | -144.75 | N224 |
| B2-19 | 41. | 55.47 | 118. | 42.60 | 4223. | 979951.98 | 980352.34 | .25 | 1.60 | -133.68 | -145.37 | N224 |

| STAT NO | LATITUDE DEG | LATITUDE MIN | LONGITUDE DEG | LONGITUDE MIN | ELEV FT | OBSERVED GRAVITY | THEORETICAL GRAVITY | TERRAIN COR INNER | TERRAIN COR TOTAL | COMPLETE 2.45 | BOUGUER 2.67 | CODE |
|---|---|---|---|---|---|---|---|---|---|---|---|---|
| B2-18 | 41. | 55.42 | 118. | 42.51 | 4216. | 979951.47 | 980352.27 | .05 | 1.33 | -134.85 | -146.53 | N224 |
| B2-17 | 41. | 55.36 | 118. | 42.42 | 4213. | 979951.59 | 980352.18 | .03 | 1.24 | -134.88 | -146.56 | N224 |
| B2-16 | 41. | 55.32 | 118. | 42.33 | 4213. | 979952.14 | 980352.12 | .02 | 1.19 | -134.30 | -145.99 | N224 |
| B2-15 | 41. | 55.22 | 118. | 42.24 | 4214. | 979952.91 | 980351.98 | .03 | 1.14 | -133.41 | -145.10 | N224 |
| M2P17 | 41. | 48.48 | 118. | 51.71 | 4799. | 979882.10 | 980341.89 | .85 | 2.36 | -156.25 | -169.48 | V324 |
| M2165 | 41. | 48.32 | 118. | 51.75 | 4768. | 979883.81 | 980341.66 | .58 | 2.15 | -156.45 | -169.61 | V324 |
| M2-17 | 41. | 48.34 | 118. | 51.84 | 4813. | 979882.05 | 980341.69 | .77 | 2.39 | -155.19 | -168.46 | V324 |
| M2-16 | 41. | 48.36 | 118. | 51.65 | 4737. | 979885.18 | 980341.72 | .65 | 2.16 | -157.06 | -170.14 | N224 |
| M2155 | 41. | 48.34 | 118. | 51.57 | 4703. | 979886.02 | 980341.69 | .39 | 1.86 | -158.63 | -171.64 | N224 |
| M2-15 | 41. | 48.38 | 118. | 51.46 | 4676. | 979887.10 | 980341.75 | .26 | 1.66 | -159.46 | -172.40 | N224 |
| M2145 | 41. | 48.42 | 118. | 51.36 | 4650. | 979888.34 | 980341.80 | .24 | 1.58 | -159.98 | -172.86 | N224 |
| M2-14 | 41. | 48.46 | 118. | 51.26 | 4625. | 979889.69 | 980341.86 | .20 | 1.50 | -160.38 | -173.19 | N224 |
| M2135 | 41. | 48.50 | 118. | 51.14 | 4599. | 979891.09 | 980341.92 | .16 | 1.40 | -160.77 | -173.51 | N224 |
| M2-13 | 41. | 48.48 | 118. | 51.03 | 4575. | 979892.26 | 980341.89 | .09 | 1.28 | -161.14 | -173.83 | N224 |
| M2125 | 41. | 48.47 | 118. | 50.92 | 4550. | 979893.49 | 980341.87 | .04 | 1.18 | -161.60 | -174.23 | N224 |
| M2-12 | 41. | 48.46 | 118. | 50.80 | 4529. | 979894.66 | 980341.86 | .03 | 1.11 | -161.79 | -174.37 | N224 |
| M2115 | 41. | 48.46 | 118. | 50.70 | 4514. | 979895.43 | 980341.86 | .03 | 1.07 | -161.99 | -174.53 | N224 |
| M2-11 | 41. | 48.45 | 118. | 50.58 | 4492. | 979896.77 | 980341.84 | .03 | 1.04 | -162.02 | -174.49 | N224 |
| M2105 | 41. | 48.44 | 118. | 50.46 | 4473. | 979898.08 | 980341.83 | .02 | 1.00 | -161.91 | -174.35 | N224 |
| M2-10 | 41. | 48.45 | 118. | 50.35 | 4457. | 979899.12 | 980341.84 | .02 | .97 | -161.92 | -174.31 | N224 |
| M2-9+ | 41. | 48.44 | 118. | 50.24 | 4444. | 979900.00 | 980341.83 | .02 | .94 | -161.91 | -174.26 | N224 |
| M2-09 | 41. | 48.44 | 118. | 50.12 | 4433. | 979900.71 | 980341.83 | .02 | .91 | -161.89 | -174.22 | N224 |
| M2-08 | 41. | 48.42 | 118. | 49.90 | 4411. | 979902.23 | 980341.80 | .02 | .87 | -161.77 | -174.04 | N224 |
| M3-17 | 41. | 49.25 | 118. | 51.52 | 4676. | 979886.48 | 980343.05 | .72 | 2.22 | -160.88 | -173.79 | N224 |
| M316+ | 41. | 49.24 | 118. | 51.41 | 4643. | 979888.35 | 980343.03 | .41 | 1.84 | -161.41 | -174.25 | N224 |
| M3-16 | 41. | 49.22 | 118. | 51.32 | 4636. | 979888.49 | 980343.00 | .25 | 1.62 | -161.89 | -174.73 | N224 |
| M315+ | 41. | 49.21 | 118. | 51.24 | 4615. | 979889.35 | 980342.98 | .17 | 1.47 | -162.48 | -175.28 | N224 |
| M3-15 | 41. | 49.19 | 118. | 51.13 | 4603. | 979889.95 | 980342.95 | .08 | 1.30 | -162.73 | -175.51 | N224 |
| M314+ | 41. | 49.18 | 118. | 51.04 | 4589. | 979890.65 | 980342.94 | .10 | 1.26 | -162.93 | -175.66 | N224 |
| M3-13 | 41. | 49.14 | 118. | 50.94 | 4582. | 979890.95 | 980342.88 | .07 | 1.17 | -163.13 | -175.85 | N224 |
| M3-12 | 41. | 49.26 | 118. | 50.78 | 4544. | 979892.80 | 980343.06 | .06 | 1.09 | -163.90 | -176.53 | N224 |
| M3-11 | 41. | 49.35 | 118. | 50.60 | 4511. | 979894.78 | 980343.19 | .04 | .99 | -164.23 | -176.77 | N224 |

| STAT NO | LATITUDE DEG | LATITUDE MIN | LONGITUDE DEG | LONGITUDE MIN | ELEV FT | OBSERVED GRAVITY | THEORETICAL GRAVITY | TERRAIN COR INNER | TERRAIN COR TOTAL | COMPLETE 2.45 | BOUGUER 2.67 | CODE |
|---|---|---|---|---|---|---|---|---|---|---|---|---|
| M3-10 | 41. | 49.41 | 118. | 50.39 | 4479. | 979896.77 | 980343.27 | .05 | .93 | -164.36 | -176.81 | N224 |
| M3-09 | 41. | 49.40 | 118. | 50.16 | 4450. | 979899.09 | 980343.26 | .04 | .86 | -163.95 | -176.33 | N224 |
| M3-08 | 41. | 49.34 | 118. | 49.95 | 4425. | 979901.16 | 980343.17 | .05 | .83 | -163.35 | -175.66 | N224 |
| M3-07 | 41. | 49.34 | 118. | 49.72 | 4404. | 979902.92 | 980343.17 | .07 | .81 | -162.95 | -175.20 | N224 |
| M3-06 | 41. | 49.30 | 118. | 49.50 | 4386. | 979904.34 | 980343.11 | .10 | .81 | -162.57 | -174.78 | N224 |
| M3-05 | 41. | 49.27 | 118. | 49.26 | 4368. | 979905.84 | 980343.07 | .08 | .77 | -162.20 | -174.36 | N224 |
| M3-04 | 41. | 49.25 | 118. | 48.99 | 4351. | 979907.27 | 980343.05 | .05 | .72 | -161.91 | -174.02 | N224 |
| M3-03 | 41. | 49.24 | 118. | 48.74 | 4330. | 979908.96 | 980343.03 | .02 | .68 | -161.52 | -173.58 | N224 |
| M3-02 | 41. | 49.27 | 118. | 48.50 | 4314. | 979910.33 | 980343.07 | .00 | .65 | -161.21 | -173.23 | N224 |
| M3-01 | 41. | 49.36 | 118. | 48.32 | 4307. | 979911.05 | 980343.20 | .00 | .63 | -161.08 | -173.08 | N224 |
| DB | 41. | 59.61 | 118. | 38.02 | 4214. | 979945.94 | 980358.53 | .04 | 2.08 | -146.05 | -157.67 | B121 |
| R-1 | 41. | 57.10 | 118. | 37.52 | 4217. | 979939.34 | 980354.79 | .01 | .85 | -149.85 | -161.58 | F524 |
| R-2 | 41. | 57.57 | 118. | 37.22 | 4204. | 979938.86 | 980355.48 | .02 | .86 | -151.83 | -163.53 | X224 |
| R-3 | 41. | 56.94 | 118. | 38.68 | 4213. | 979947.41 | 980354.54 | .09 | 1.21 | -141.48 | -153.16 | B124 |
| R-4 | 41. | 56.68 | 118. | 36.06 | 4227. | 979934.61 | 980354.15 | .10 | .97 | -153.20 | -164.95 | D424 |
| R-5 | 41. | 57.00 | 118. | 34.65 | 4324. | 979926.64 | 980354.62 | .08 | 1.05 | -155.48 | -167.49 | F524 |
| R-6 | 41. | 56.16 | 118. | 37.22 | 4254. | 979936.61 | 980353.37 | .07 | .97 | -148.72 | -160.54 | B124 |
| R-7 | 41. | 53.84 | 118. | 36.88 | 4439. | 979922.70 | 980349.91 | .06 | .81 | -147.70 | -160.05 | B124 |
| A01 | 41. | 55.30 | 118. | 46.13 | 4379. | 979928.56 | 980352.09 | .02 | .52 | -148.06 | -160.27 | G734 |
| A02 | 41. | 56.21 | 118. | 45.87 | 4538. | 979918.80 | 980353.45 | .02 | .62 | -149.11 | -161.76 | C844 |
| A03 | 41. | 57.01 | 118. | 45.16 | 4860. | 979901.57 | 980354.64 | .13 | 1.02 | -146.94 | -160.45 | C844 |
| A04 | 41. | 57.32 | 118. | 44.28 | 5166. | 979893.36 | 980355.11 | .51 | 1.73 | -135.75 | -150.06 | G623 |
| A05 | 41. | 58.04 | 118. | 44.02 | 5515. | 979874.19 | 980356.19 | .22 | 1.99 | -133.84 | -149.11 | C844 |
| A06 | 41. | 58.71 | 118. | 44.23 | 5300. | 979883.45 | 980357.19 | .46 | 1.81 | -139.24 | -153.92 | C844 |
| A07 | 41. | 59.11 | 118. | 43.44 | 5840. | 979856.06 | 980357.79 | .17 | 2.54 | -132.66 | -148.79 | C844 |
| A08 | 41. | 57.47 | 118. | 44.07 | 5349. | 979883.98 | 980355.34 | .91 | 2.42 | -133.23 | -148.00 | X123 |
| A09 | 41. | 57.24 | 118. | 43.57 | 5671. | 979864.20 | 980354.99 | 1.38 | 4.72 | -130.34 | -145.82 | C844 |
| A10 | 41. | 56.94 | 118. | 43.52 | 5723. | 979859.19 | 980354.54 | 1.72 | 6.04 | -130.39 | -145.91 | C844 |
| A11 | 41. | 52.40 | 118. | 46.68 | 4238. | 979921.00 | 980347.75 | .01 | .46 | -160.19 | -172.01 | B124 |
| A12 | 41. | 52.80 | 118. | 48.89 | 4255. | 979921.23 | 980348.34 | .01 | .42 | -159.53 | -171.40 | C824 |
| A13 | 41. | 53.48 | 118. | 50.94 | 4287. | 979912.60 | 980349.37 | .01 | .47 | -167.12 | -179.08 | B124 |
| A14 | 41. | 53.44 | 118. | 53.28 | 4318. | 979899.99 | 980349.30 | .01 | .73 | -177.48 | -189.50 | B124 |

| STAT NO | LATITUDE DEG | LATITUDE MIN | LONGITUDE DEG | LONGITUDE MIN | ELEV FT | OBSERVED GRAVITY | THEORETICAL GRAVITY | TERRAIN COR INNER | TERRAIN COR TOTAL | COMPLETE 2.45 | BOUGUER 2.67 | CODE |
|---|---|---|---|---|---|---|---|---|---|---|---|---|
| A15 | 41. | 54.15 | 118. | 55.39 | 4350. | 979899.70 | 980350.37 | .00 | .83 | -176.73 | -188.83 | B124 |
| A16 | 41. | 54.50 | 118. | 57.64 | 4497. | 979893.66 | 980350.90 | .15 | 1.26 | -173.67 | -186.15 | B124 |
| A17 | 41. | 54.19 | 118. | 55.53 | 4351. | 979898.63 | 980350.43 | .00 | .84 | -177.80 | -189.92 | B124 |
| A18 | 41. | 57.61 | 118. | 43.73 | 5831. | 979852.15 | 980355.55 | 2.89 | 6.83 | -130.96 | -146.71 | C844 |
| A19 | 41. | 56.65 | 118. | 43.39 | 5622. | 979864.84 | 980354.11 | 4.38 | 8.57 | -128.36 | -143.38 | C844 |
| A20 | 41. | 56.24 | 118. | 43.65 | 5795. | 979847.80 | 980353.49 | 4.95 | 11.19 | -131.50 | -146.80 | C844 |
| A21 | 41. | 55.91 | 118. | 43.74 | 5541. | 979865.99 | 980352.99 | 1.44 | 5.92 | -133.61 | -148.62 | C844 |
| A22 | 41. | 55.61 | 118. | 44.07 | 5460. | 979867.37 | 980352.55 | 3.49 | 7.72 | -135.23 | -149.87 | X124 |
| A23 | 41. | 55.09 | 118. | 37.84 | 4372. | 979936.43 | 980351.77 | .68 | 1.62 | -139.31 | -151.42 | C844 |
| A24 | 41. | 54.07 | 118. | 38.52 | 4409. | 979934.44 | 980350.26 | .17 | 1.19 | -137.85 | -150.09 | X234 |
| A25 | 41. | 53.18 | 118. | 38.63 | 4474. | 979926.02 | 980348.91 | .29 | 1.27 | -140.77 | -153.18 | X124 |
| A26 | 41. | 52.56 | 118. | 38.33 | 4528. | 979914.96 | 980347.99 | .01 | .97 | -147.79 | -160.38 | G624 |
| A27 | 41. | 52.71 | 118. | 40.80 | 4850. | 979914.84 | 980348.22 | .82 | 1.73 | -127.25 | -140.66 | C844 |
| A28 | 41. | 56.88 | 118. | 47.18 | 4439. | 979916.43 | 980354.45 | .01 | .49 | -158.81 | -171.19 | G624 |
| A29 | 41. | 57.14 | 118. | 46.20 | 4588. | 979912.22 | 980354.84 | .03 | .66 | -153.92 | -166.71 | C824 |
| A30 | 41. | 48.57 | 118. | 46.06 | 4244. | 979916.49 | 980342.02 | .00 | .95 | -158.15 | -169.94 | X624 |
| A31 | 41. | 45.60 | 118. | 50.00 | 4454. | 979899.75 | 980337.59 | .04 | 1.12 | -157.07 | -169.45 | C824 |
| A32 | 41. | 45.94 | 118. | 49.12 | 4511. | 979896.89 | 980338.10 | .09 | 1.09 | -156.90 | -169.43 | C824 |
| A33 | 41. | 46.35 | 118. | 47.90 | 4496. | 979896.30 | 980338.71 | .02 | 1.09 | -159.05 | -171.54 | C824 |
| A34 | 41. | 46.80 | 118. | 47.00 | 4426. | 979901.00 | 980339.40 | .11 | 1.22 | -159.35 | -171.64 | C824 |
| A35 | 41. | 46.27 | 118. | 44.61 | 4346. | 979908.54 | 980338.59 | .11 | 2.54 | -154.79 | -166.74 | C824 |
| A36 | 41. | 47.27 | 118. | 44.35 | 4281. | 979915.67 | 980340.10 | .06 | 2.13 | -153.62 | -165.42 | C824 |
| A37 | 41. | 47.37 | 118. | 55.32 | 6195. | 979786.76 | 980340.24 | .58 | 3.52 | -161.22 | -178.26 | C844 |
| A38 | 41. | 47.49 | 118. | 54.81 | 5890. | 979808.29 | 980340.42 | .28 | 2.34 | -160.10 | -176.39 | C844 |
| A39 | 41. | 47.38 | 118. | 54.43 | 6010. | 979798.41 | 980340.26 | 2.57 | 5.39 | -159.49 | -175.86 | G734 |
| A40 | 41. | 48.19 | 118. | 54.54 | 6075. | 979795.51 | 980341.45 | .14 | 2.45 | -162.20 | -179.00 | C844 |
| A41 | 41. | 49.16 | 118. | 54.35 | 5975. | 979802.63 | 980342.91 | .03 | 2.07 | -163.16 | -179.70 | C824 |
| A42 | 41. | 48.92 | 118. | 54.52 | 6018. | 979798.32 | 980342.55 | .12 | 2.17 | -164.31 | -180.98 | C824 |
| A43 | 41. | 48.82 | 118. | 54.01 | 5950. | 979803.79 | 980342.41 | .09 | 2.24 | -162.91 | -179.38 | C844 |
| A44 | 41. | 48.76 | 118. | 53.72 | 6095. | 979797.59 | 980342.31 | .63 | 3.68 | -158.59 | -175.35 | G744 |
| A45 | 41. | 48.57 | 118. | 53.31 | 5968. | 979805.40 | 980342.02 | .21 | 3.35 | -158.78 | -175.20 | C844 |
| A46 | 41. | 47.11 | 118. | 54.25 | 5518. | 979833.32 | 980339.84 | .89 | 2.69 | -157.53 | -172.75 | C824 |

| STAT NO | LATITUDE DEG | LATITUDE MIN | LONGITUDE DEG | LONGITUDE MIN | ELEV FT | OBSERVED GRAVITY | THEORETICAL GRAVITY | TERRAIN COR INNER | TERRAIN COR TOTAL | COMPLETE 2.45 | BOUGUER 2.67 | CODE |
|---|---|---|---|---|---|---|---|---|---|---|---|---|
| A47 | 41. | 49.47 | 118. | 44.56 | 4230. | 979922.93 | 980343.37 | .01 | 1.17 | -153.73 | -165.47 | X624 |
| A48 | 41. | 52.07 | 118. | 53.95 | 4616. | 979885.12 | 980347.26 | .98 | 2.48 | -170.00 | -182.70 | X824 |
| A49 | 41. | 56.92 | 118. | 42.59 | 4678. | 979931.75 | 980354.51 | .64 | 2.13 | -127.00 | -139.92 | C834 |
| DE01 | 41. | 56.58 | 118. | 40.92 | 4214. | 979960.80 | 980354.00 | .04 | 1.48 | -127.24 | -138.91 | |
| DE03 | 41. | 55.62 | 118. | 42.90 | 4375. | 979943.12 | 980352.57 | .46 | 1.73 | -133.15 | -145.25 | |
| DE04 | 41. | 54.58 | 118. | 44.02 | 4215. | 979944.79 | 980351.02 | .71 | 1.77 | -139.94 | -151.59 | |
| DE05 | 41. | 54.73 | 118. | 44.08 | 4327. | 979939.23 | 980351.23 | .97 | 1.85 | -138.61 | -150.57 | |
| DE06 | 41. | 53.84 | 118. | 44.82 | 4751. | 979906.54 | 980349.91 | 2.56 | 3.83 | -141.53 | -154.51 | |
| DE07 | 41. | 53.87 | 118. | 44.09 | 4214. | 979941.84 | 980349.95 | .04 | .77 | -142.79 | -154.52 | |
| DE08 | 41. | 53.03 | 118. | 44.69 | 4219. | 979942.09 | 980348.70 | .06 | .64 | -141.10 | -152.85 | |
| DE09 | 41. | 53.00 | 118. | 44.29 | 4215. | 979938.59 | 980348.65 | .01 | .63 | -144.81 | -156.55 | |
| DE10 | 41. | 55.82 | 118. | 40.69 | 4288. | 979957.02 | 980352.86 | .71 | 2.21 | -124.56 | -136.38 | |
| DE11 | 41. | 55.82 | 118. | 41.18 | 4208. | 979959.82 | 980352.86 | .10 | 1.49 | -127.45 | -139.10 | |
| DE13 | 41. | 54.95 | 118. | 40.70 | 4418. | 979947.59 | 980351.56 | .97 | 2.26 | -124.48 | -136.66 | |
| DE14 | 41. | 54.95 | 118. | 41.72 | 4266. | 979953.09 | 980351.56 | .40 | 1.45 | -129.27 | -141.09 | |
| DE15 | 41. | 53.88 | 118. | 42.32 | 4245. | 979950.59 | 980349.96 | .20 | 1.30 | -131.63 | -143.40 | |
| DE16 | 41. | 52.64 | 118. | 42.28 | 4247. | 979949.95 | 980348.11 | .19 | 1.54 | -130.07 | -141.83 | |
| DE17 | 41. | 52.10 | 118. | 41.73 | 4378. | 979942.68 | 980347.30 | .56 | 2.51 | -127.42 | -139.46 | |
| DE18 | 41. | 52.10 | 118. | 42.90 | 4214. | 979947.00 | 980347.30 | .01 | 1.22 | -134.58 | -146.27 | |
| DE19 | 41. | 52.12 | 118. | 44.10 | 4219. | 979938.70 | 980347.33 | .01 | .74 | -143.03 | -154.78 | |
| DE20 | 41. | 55.53 | 118. | 42.70 | 4248. | 979951.54 | 980352.43 | .30 | 1.69 | -132.60 | -144.34 | |
| DE21 | 41. | 55.46 | 118. | 42.64 | 4225. | 979952.01 | 980352.32 | .12 | 1.48 | -133.64 | -145.34 | |
| DE22 | 41. | 55.31 | 118. | 42.56 | 4211. | 979951.32 | 980352.11 | .05 | 1.30 | -135.19 | -146.86 | |
| DE23 | 41. | 55.24 | 118. | 42.50 | 4212. | 979951.13 | 980352.00 | .03 | 1.21 | -135.30 | -146.99 | |
| DE24 | 41. | 55.13 | 118. | 42.59 | 4216. | 979950.83 | 980351.84 | .03 | 1.16 | -135.24 | -146.94 | |
| DE25 | 41. | 55.39 | 118. | 42.42 | 4212. | 979951.73 | 980352.22 | .03 | 1.26 | -134.87 | -146.55 | |
| DE26 | 41. | 54.99 | 118. | 42.68 | 4212. | 979949.77 | 980351.62 | .04 | 1.12 | -136.33 | -148.02 | |
| DE27 | 41. | 54.82 | 118. | 42.80 | 4215. | 979948.41 | 980351.37 | .02 | 1.03 | -137.38 | -149.09 | |
| DE28 | 41. | 54.68 | 118. | 43.00 | 4189. | 979947.00 | 980351.16 | .02 | 1.06 | -140.16 | -151.79 | |
| DE29 | 41. | 55.18 | 118. | 42.29 | 4214. | 979952.38 | 980351.90 | .02 | 1.13 | -133.86 | -145.56 | |
| DE30 | 41. | 55.08 | 118. | 42.15 | 4216. | 979953.77 | 980351.76 | .06 | 1.14 | -132.24 | -143.94 | |
| DE31 | 41. | 55.00 | 118. | 41.90 | 4240. | 979953.63 | 980351.64 | .15 | 1.21 | -130.69 | -142.45 | |

| STAT NO | LATITUDE DEG | LATITUDE MIN | LONGITUDE DEG | LONGITUDE MIN | ELEV FT | OBSERVED GRAVITY | THEORETICAL GRAVITY | TERRAIN COR INNER | TERRAIN COR TOTAL | COMPLETE 2.45 | BOUGUER 2.67 | CODE |
|---|---|---|---|---|---|---|---|---|---|---|---|---|
| DE32 | 41. | 56.68 | 118. | 41.72 | 4303. | 979953.09 | 980354.15 | .07 | 1.58 | -129.41 | -141.32 | |
| DE33 | 41. | 57.02 | 118. | 42.83 | 5004. | 979910.32 | 980354.66 | .79 | 2.27 | -128.04 | -141.86 | |
| CS 8 | 41. | 55.88 | 118. | 53.43 | 4362. | 979906.98 | 980352.95 | .03 | .51 | -172.36 | -184.52 | G534 |
| CS 9 | 41. | 57.17 | 118. | 52.80 | 4458. | 979903.89 | 980354.89 | .04 | .48 | -171.38 | -183.81 | G534 |
| CS 10 | 41. | 57.95 | 118. | 52.25 | 4442. | 979907.96 | 980356.05 | .04 | .63 | -169.34 | -181.71 | G534 |
| CS11 | 41. | 53.78 | 118. | 45.57 | 4245. | 979935.71 | 980349.82 | .20 | .72 | -147.64 | -159.46 | G524 |
| CS12 | 41. | 55.01 | 118. | 47.03 | 4273. | 979930.53 | 980351.66 | .02 | .47 | -153.13 | -165.05 | F424 |
| CS15 | 41. | 58.97 | 118. | 42.38 | 5370. | 979889.48 | 980357.59 | .38 | 2.08 | -129.74 | -144.60 | G534 |
| CS16 | 41. | 58.28 | 118. | 47.35 | 4487. | 979912.88 | 980356.55 | .03 | .65 | -162.06 | -174.56 | G534 |
| CS17 | 41. | 59.08 | 118. | 47.58 | 4483. | 979913.41 | 980357.74 | .03 | .74 | -162.91 | -175.39 | G534 |
| CS18 | 41. | 59.58 | 118. | 47.72 | 4460. | 979915.41 | 980358.48 | .28 | 1.16 | -162.70 | -175.09 | X434 |
| CS19 | 41. | 59.58 | 118. | 49.41 | 4515. | 979913.43 | 980358.48 | .15 | .80 | -161.56 | -174.12 | F434 |
| CS20 | 41. | 58.02 | 118. | 48.55 | 4351. | 979917.70 | 980356.16 | .02 | .58 | -165.45 | -177.58 | F434 |
| CS21 | 41. | 56.24 | 118. | 50.54 | 4340. | 979914.90 | 980353.49 | .08 | .46 | -166.40 | -178.50 | F434 |
| CS22 | 41. | 54.36 | 118. | 51.90 | 4330. | 979908.41 | 980350.68 | .01 | .44 | -170.73 | -182.80 | F434 |
| CS23 | 41. | 52.54 | 118. | 58.33 | 5224. | 979860.75 | 980347.97 | .57 | 1.26 | -158.77 | -173.29 | F434 |
| CS24 | 41. | 51.58 | 118. | 57.65 | 5334. | 979852.98 | 980346.52 | .11 | .87 | -158.56 | -173.41 | G634 |
| CS25 | 41. | 50.65 | 118. | 57.05 | 5721. | 979825.03 | 980345.14 | .13 | 1.43 | -160.30 | -176.19 | G634 |
| CS26 | 41. | 50.25 | 118. | 56.05 | 6059. | 979801.14 | 980344.54 | .19 | 2.53 | -161.36 | -178.10 | F434 |
| CS27 | 41. | 49.34 | 118. | 54.70 | 6126. | 979793.38 | 980343.17 | .12 | 2.54 | -163.53 | -180.46 | G634 |
| CS28 | 41. | 47.75 | 118. | 55.15 | 6195. | 979786.78 | 980340.80 | .48 | 3.19 | -162.82 | -179.90 | G634 |
| CS30 | 41. | 46.14 | 118. | 55.58 | 5556. | 979831.44 | 980338.41 | .36 | 2.26 | -156.76 | -172.12 | G634 |
| CS32 | 41. | 46.92 | 118. | 45.82 | 4282. | 979910.59 | 980339.57 | .02 | 1.57 | -159.41 | -171.26 | F434 |
| CS33 | 41. | 49.45 | 118. | 43.38 | 4309. | 979927.13 | 980343.34 | .02 | 1.89 | -144.64 | -156.54 | X434 |
| CS34 | 41. | 48.96 | 118. | 42.20 | 4630. | 979903.41 | 980342.60 | 1.20 | 4.86 | -144.75 | -157.31 | Q634 |
| CS35 | 41. | 49.95 | 118. | 42.40 | 4472. | 979918.57 | 980344.09 | .52 | 3.40 | -142.33 | -154.57 | F434 |
| CS36 | 41. | 50.77 | 118. | 44.25 | 4221. | 979933.04 | 980345.32 | .01 | .97 | -147.09 | -158.82 | F424 |
| CS 37 | 41. | 50.72 | 118. | 45.45 | 4227. | 979928.96 | 980345.24 | .01 | .70 | -150.96 | -162.73 | F434 |
| CS 39 | 41. | 49.95 | 118. | 50.05 | 4394. | 979903.59 | 980344.09 | .02 | .78 | -164.61 | -176.84 | G634 |
| CS 40 | 41. | 51.57 | 118. | 49.67 | 4314. | 979911.93 | 980346.51 | .00 | .52 | -163.96 | -175.99 | G634 |
| CS 41 | 41. | 51.82 | 118. | 48.08 | 4249. | 979920.60 | 980346.89 | .03 | .48 | -159.79 | -171.64 | F434 |
| CS 42 | 41. | 48.32 | 118. | 59.50 | 4958. | 979864.70 | 980341.66 | .05 | .86 | -165.58 | -179.38 | G434 |

| STAT NO | LATITUDE DEG | LATITUDE MIN | LONGITUDE DEG | LONGITUDE MIN | ELEV FT | OBSERVED GRAVITY | THEORETICAL GRAVITY | TERRAIN COR INNER | TERRAIN COR TOTAL | COMPLETE 2.45 | BOUGUER 2.67 | CODE |
|---|---|---|---|---|---|---|---|---|---|---|---|---|
| CS 43 | 41. | 45.70 | 118. | 59.50 | 5231. | 979840.38 | 980337.75 | .26 | 1.54 | -168.23 | -182.74 | F334 |
| CS 49 | 41. | 38.25 | 118. | 59.91 | 5991. | 979793.89 | 980326.62 | .03 | .94 | -156.41 | -173.10 | G334 |
| CS 53 | 41. | 35.85 | 118. | 57.37 | 6070. | 979774.73 | 980323.03 | .52 | 1.92 | -166.12 | -182.94 | B124 |
| CS 54 | 41. | 39.50 | 118. | 54.66 | 4703. | 979867.71 | 980328.48 | .03 | 1.54 | -164.78 | -177.82 | N234 |
| CS140 | 41. | 58.43 | 118. | 39.55 | 4220. | 979953.96 | 980356.77 | .12 | 2.50 | -136.28 | -147.87 | N424 |
| CS141 | 41. | 45.65 | 118. | 34.56 | 4590. | 979888.85 | 980337.68 | .16 | 2.14 | -159.40 | -172.06 | G524 |
| CS143 | 41. | 46.93 | 118. | 38.03 | 5730. | 979824.14 | 980339.59 | 1.34 | 4.68 | -152.09 | -167.74 | Q734 |
| CS144 | 41. | 47.39 | 118. | 39.68 | 6010. | 979814.80 | 980340.27 | .40 | 3.23 | -145.87 | -162.42 | Q734 |
| CS145 | 41. | 39.25 | 118. | 38.88 | 5451. | 979837.54 | 980328.11 | .95 | 4.82 | -144.61 | -159.46 | G524 |
| CS146 | 41. | 39.13 | 118. | 40.94 | 6330. | 979772.87 | 980327.93 | 1.41 | 7.45 | -151.48 | -168.58 | G524 |
| CS147 | 41. | 38.67 | 118. | 35.92 | 4385. | 979899.88 | 980327.24 | .72 | 4.57 | -148.56 | -160.46 | C724 |
| CS148 | 41. | 38.14 | 118. | 35.08 | 4174. | 979909.54 | 980326.45 | .02 | 2.67 | -153.11 | -164.57 | F424 |
| CS149 | 41. | 38.24 | 118. | 31.32 | 4162. | 979909.28 | 980326.60 | .01 | .60 | -156.18 | -167.77 | X424 |
| CS251 | 41. | 56.86 | 118. | 48.59 | 4329. | 979920.09 | 980354.43 | .06 | .51 | -162.78 | -174.86 | F424 |
| CS252 | 41. | 55.23 | 118. | 48.77 | 4342. | 979922.35 | 980351.99 | .01 | .33 | -157.43 | -169.56 | F434 |
| CS253 | 41. | 54.33 | 118. | 49.82 | 4338. | 979915.99 | 980350.63 | .01 | .33 | -162.69 | -174.80 | Q534 |
| CS254 | 41. | 55.48 | 118. | 48.26 | 4281. | 979929.03 | 980352.35 | .02 | .43 | -154.85 | -166.80 | G524 |
| CS255 | 41. | 55.36 | 118. | 48.58 | 4327. | 979924.48 | 980352.18 | .01 | .35 | -156.43 | -168.50 | G424 |
| CS256 | 41. | 55.26 | 118. | 47.60 | 4283. | 979930.37 | 980352.03 | .01 | .43 | -153.07 | -165.02 | G434 |
| CS257 | 41. | 56.42 | 118. | 47.15 | 4406. | 979919.82 | 980353.77 | .01 | .47 | -157.61 | -169.89 | G534 |
| CS258 | 41. | 50.45 | 118. | 46.55 | 4245. | 979920.51 | 980344.84 | .00 | .60 | -157.94 | -169.77 | B134 |
| CS260 | 41. | 44.75 | 118. | 51.65 | 4392. | 979899.03 | 980336.32 | .19 | 1.50 | -160.85 | -173.01 | B124 |
| CS261 | 41. | 42.35 | 118. | 54.78 | 4473. | 979886.33 | 980332.73 | .02 | 1.77 | -164.64 | -177.01 | N234 |
| CS262 | 41. | 40.53 | 118. | 54.83 | 4467. | 979877.38 | 980330.03 | .15 | 2.04 | -171.02 | -183.35 | N234 |
| CS264 | 41. | 41.35 | 118. | 52.45 | 4561. | 979879.30 | 980331.25 | .01 | 1.55 | -164.87 | -177.51 | G424 |
| CS266 | 41. | 51.90 | 118. | 40.92 | 5033. | 979900.81 | 980347.00 | .29 | 1.84 | -129.21 | -143.14 | G634 |
| CS267 | 41. | 50.89 | 118. | 39.13 | 4940. | 979889.93 | 980345.49 | 1.50 | 4.11 | -142.34 | -155.82 | F424 |
| CS268 | 41. | 49.87 | 118. | 36.90 | 5438. | 979843.28 | 980343.98 | .49 | 3.45 | -156.81 | -171.74 | G424 |

# APPENDIX II

Wet bulk density measurements were made on all samples except for some tuffs which disintegrated when they were saturated. The following procedure was used to make the density measurements:

1. Weigh unsaturated (dry) sample in air to obtain $W_{d,a}$.
2. Evacuate the samples in a partial vaccuum for 3 to 6 hours.
3. Flood the evacuated samples with water, allowing them to soak for 3 to 6 hours.
4. Weigh the saturated sample in air to obtain $W_{s,a}$, and immersed in water to obtain $W_{s,i}$.

The "dry" bulk density is the weight of the rock in air, with air in the pore space, divided by the total rock volume. For wet density calculations the pore space contains water. The difference between the weight in air and the weight in water of a sample, in grams, equals the volume of the sample in cubic centimeters (Archimedes Principle). However, errors in rock volume determinations are caused by leakage of water in or out of the pore space.

Whenever possible, saturated rocks were used for volume determinations. Hence the equations become (following the notation indicated above):

$$\text{Dry density, } P_d = \frac{W_{d,\,a}}{W_{s,\,a} - W_{s,\,i}}$$

and

$$\text{Wet density, P or } P_W = \frac{W_{s,\,a}}{W_{s,\,a} - W_{s,\,i}}$$

Note that $W_{d,a} - W_{d,i}$ could just as well be used in the denominator for the volume of sample, and it was for the samples that could not be saturated.

Also note that since porosity is volume of pore space divided by total rock volume:

$$\text{Porosity, } \phi = \frac{W_{s,a} - W_{d,a}}{\text{rock volume}} = Pw - Pd$$

Tables 7 and 8 present the individual density determinations.

# TABLE 7
# BALTAZOR AREA
# DENSITIES

| ROCK TYPE | SAMPLE NO. | SAMPLE LOCATION DEG-MIN | DEG-MIN | DENSITY G/CC | POROSITY (%) |
|---|---|---|---|---|---|
| BASALT | B3-24 | 41-56.52 | 118-42.51 | 2.88 | 2.2 |
| " | RA20 | 41-56.24 | 118-43.65 | 2.77 | 6.2 |
| " | RA07 | 41-59.11 | 118-43.44 | 2.69 | 3.6 |
| " | BZ10 | 41-54.3 | 118-41.6 | 2.78 | 4.4 |
| " | BZ33 | 41-55.0 | 118-40.8 | 2.83 | 3.4 |
| " | BZ6 | 41-54.3 | 118-42.0 | 2.73 | 3.3 |
| " | BZ125 | 41-54.5 | 118-44.0 | 2.78 | 1.3 |
| " | RA10 | 41-56.94 | 118-43.52 | 2.87 | 1.6 |
| " | ASHDOWN | 41-50.0 | 118-41.7 | 2.91 | 2.1 |
| VESICULAR BASALT | RA10A | 41-56.94 | 118-43.52 | 2.37 | 27.7 |
| " | BZ8 | 41-54.3 | 118-41.9 | 2.43 | 20.2 |
| " | BZ1 | 41-53.7 | 118-42.5 | 2.19 | 10.5 |
| INTERMEDIATE VOLC. | RA18 | 41-57.61 | 118-43.73 | 2.58 | 15.4 |
| RHYOLITE | BZ111 | 41-57.0 | 118-42.5 | 2.44 | 9.3 |
| " | R3 | 41-55.0 | 118-43.5 | 2.50 | 5.8 |
| " | RA22 | 41-55.61 | 118-44.07 | 2.38 | 12.1 |
| " | RA03A | 41-57.01 | 118-45.16 | 2.21 | 32.2 |
| " | R2 | 41-55. | 118-43.5 | 2.48 | 5.7 |
| " | B2-22 | 41-55.62 | 118-46.86 | 2.30 | 15.4 |
| " | B1-17 | 41-55.14 | 118-43.62 | 2.46 | 8.0 |
| WELDED TUFF | RA03 | 41-57.01 | 118-45.16 | 2.33 | 12.4 |
| " | BZ62 | 41-56.0 | 118-45.0 | 2.31 | 18.1 |
| " | BZ15D | 41-54.6 | 118-42.2 | 2.25 | 10.6 |
| " | BZ16 | 41-54.6 | 118-42.2 | 2.55 | 3.4 |
| " | BZ115 | 41-57. | 118-44. | 2.42 | 8.6 |
| " | RA36A | 41-47.27 | 118-44.35 | 2.32 | 5.6 |
| " | BZ88 | 41-56. | 118-43. | 2.64 | 1.9 |
| " | BZ60 | 41-56. | 118-45. | 2.30 | 10.7 |
| TUFF | A04 | 41-57.32 | 118-44.28 | 1.72 | 44.4 |
| PLUTONIC ROCKS | B2-3E | 41-54.23 | 118-40.67 | 2.59 | 4.1 |
| " | BZ113A | 41-57. | 118-42.2 | 2.68 | 3.1 |
| " | BZ112 | 41-57.3 | 118-42.2 | 2.64 | 4.9 |
| " | BZ30 | 41-54.2 | 118-40.5 | 2.77 | 4.3 |
| " | RA36B | 41-47.27 | 118-44.35 | 2.59 | 2.2 |
| " | ASHDOWN G | 41-50. | 118-41.7 | 2.57 | 3.3 |
| " | RA26X | 41-52.56 | 118-38.33 | 2.52 | 7.3 |
| " | RA26 | 41-52.56 | 118-38.33 | 2.55 | 3.2 |
| " | B2-5E | 41-54.06 | 118-40.40 | 2.60 | 3.4 |
| METAMORPHIC ROCKS | ASHDOWN SCH | 41-50. | 118-41.7 | 2.77 | 2.3 |
| " | SCH A | 41-50. | 118-41.7 | 2.65 | 6.5 |
| " | SCH SC | 41-50. | 118-41.7 | 2.75 | 4.1 |

# TABLE 8
# PAINTED HILLS AREA
# DENSITIES

| ROCK TYPE | SAMPLE NO. | SAMPLE LOCATION DEG-MIN | DEG-MIN | DENSITY DRY | WET | POROSITY (%) |
|---|---|---|---|---|---|---|
| RHYOLITE | RA44A | 41-48.76 | 118-53.72 | | 2.33 | 4.3 |
| " | RA37 | 41-47.37 | 118-55.32 | | 2.27 | 12.0 |
| " | A81 | 41-48.7 | 118-52.5 | | 2.27 | 11.3 |
| " | RA39B | 41-47.38 | 118-54.43 | | 2.07 | 16.0 |
| " | M1-14 | 41-47.02 | 118-52.76 | | 2.25 | 22.0 |
| " | M1-9+5 | 41-46.82 | 118-51.85 | | 2.30 | 14.5 |
| " | RA44 | 41-48.76 | 118-53.72 | | 2.24 | 9.4 |
| " | RA38C | 41-47.49 | 118-54.81 | | 2.27 | 7.1 |
| " | RA45B | 41-48.57 | 118-53.31 | | 2.18 | 19.4 |
| " | RA39A | 41-47.38 | 118-54.43 | | 2.25 | 6.3 |
| " | RA39C | 41-47.38 | 118-54.43 | | 2.11 | 19.5 |
| " | RA44B | 41-48.76 | 118-53.72 | | 2.29 | 10.7 |
| " | RA38D | 41-47.49 | 118-54.81 | | 2.22 | 7.5 |
| " | RA38D | 41-47.49 | 118-54.81 | | 2.22 | 7.5 |
| " | RA44A | 41-48.76 | 118-53.72 | | 2.34 | 5.3 |
| " | RA45A | 41-48.57 | 118-53.31 | | 2.20 | 21.5 |
| " | RA38B | 41-47.49 | 118-54.81 | | 2.24 | 8.2 |
| " | RA44C | 41-48.76 | 118-53.72 | | 2.34 | 8.9 |
| " | RA45B | 41-48.57 | 118-53.31 | | 2.21 | 18.1 |
| " | RA38A | 41-47.49 | 118-54.81 | | 2.28 | 10.2 |
| " | RA44 | 41-48.76 | 118-53.72 | | 2.32 | 6.9 |
| WELDED TUFF (HEMATIZED) | M1-11 | 41-46.97 | 118-52.08 | | 2.31 | 14.5 |
| TUFF | A37 | 41-48.7 | 118-52.5 | | 1.92 | 26.1 |
| " | M2-17C | 41-48.34 | 118-51.84 | | 1.89 | 24.4 |
| " | A78 | 41-48.7 | 118-52.5 | | 1.96 | 17.7 |
| " | M2-17A | 41-48.34 | 118-51.84 | | 2.05 | 13.6 |
| " | A85 | 41-48.7 | 118-52.5 | 1.52 | | |
| " | RA45A | 41-48.57 | 118-54.81 | 1.60 | | |
| " | M2-17PC | 41-48.48 | 118-51.71 | 1.58 | | |
| " | RA45 | 41-48.57 | 118-54.81 | | 1.91 | 53.9 |
| " | RA45B | 41-48.57 | 118-54.81 | 1.45 | | |
| TUFF, HEMATIZED | M2-17B | 41-48.34 | 118-51.84 | 2.07 | | |
| " | M2-17 | 41-48.34 | 118-51.84 | 2.06 | | |
| " | F-1 | 41-48.7 | 118-52.5 | 1.99 | | |
| " | M2-17C | 41-48.34 | 118-51.84 | 2.17 | | |
| " | M2-17PA | 41-48.48 | 118-51.71 | 1.75 | | |
| TUFFACEOUS CONGLOMERATE | A42 | 41-48.7 | 118-52.5 | | 1.76 | 32.3 |
| TUFFACEOUS CONGLOMERATE (HEMATIZED) | A20 | 41-48.7 | 118-52.5 | | 2.29 | 3.4 |

# APPENDIX III

## Resistivity Numerical Model Output

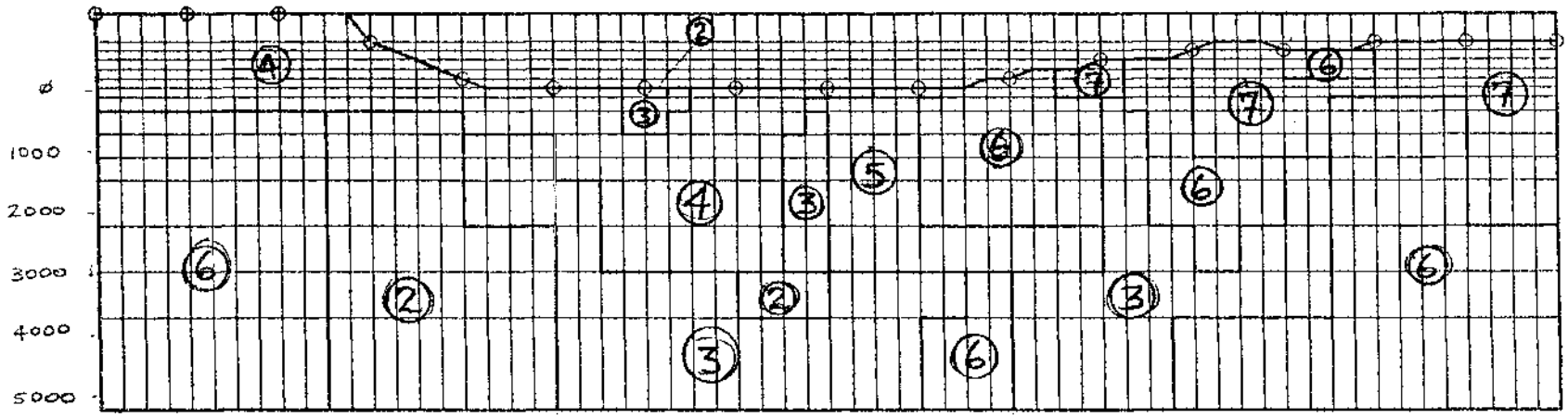


Line B1 (R1)

(2) 5 Ω-m
(3) 15 Ω-m
(4) 22 Ω-m
(5) 60 Ω-m
(6) 110 Ω-m
(7) 180 Ω-m

APPARENT RESISTIVITY - COMPUTED

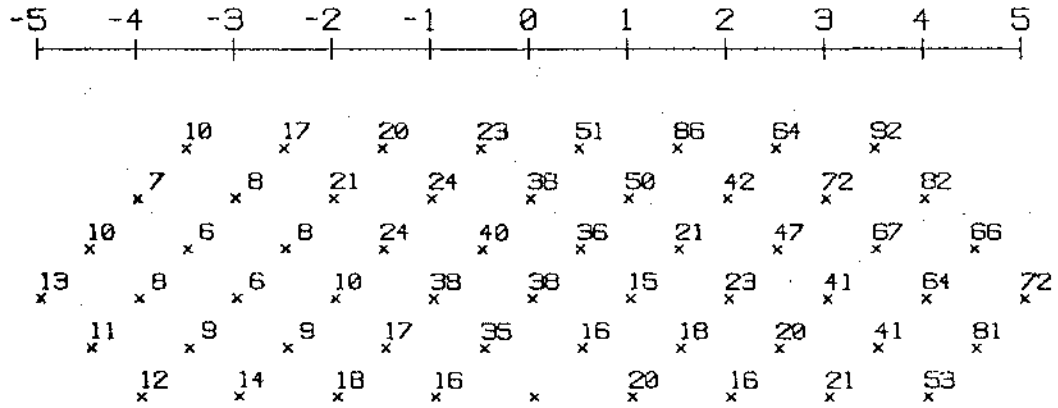

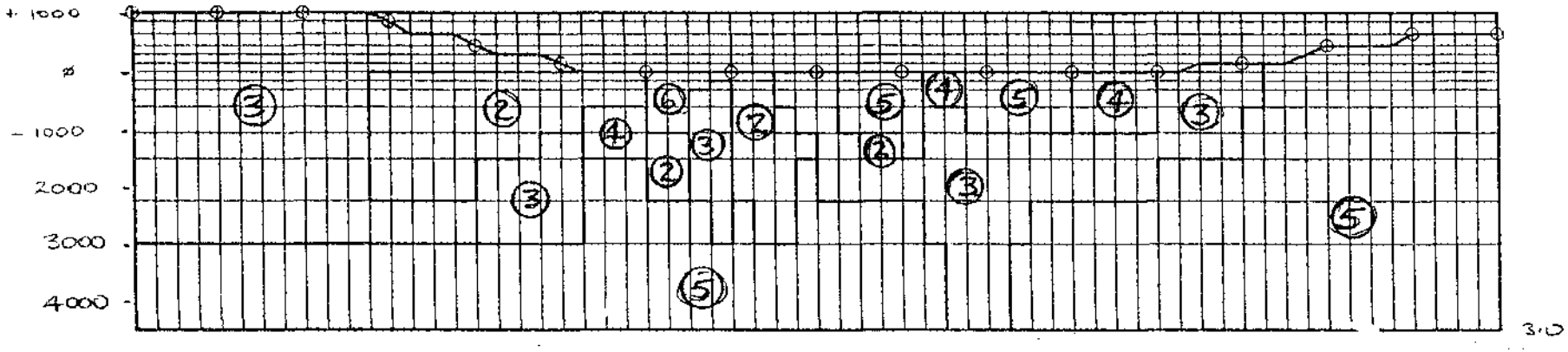


LINE BZ CRZ

② 5 Ω-M

③ 25 Ω-M

④ 40 Ω-M

⑤ 90 Ω-M

⑥ 2 Ω-M

APPARENT RESISTIVITY - COMPUTED

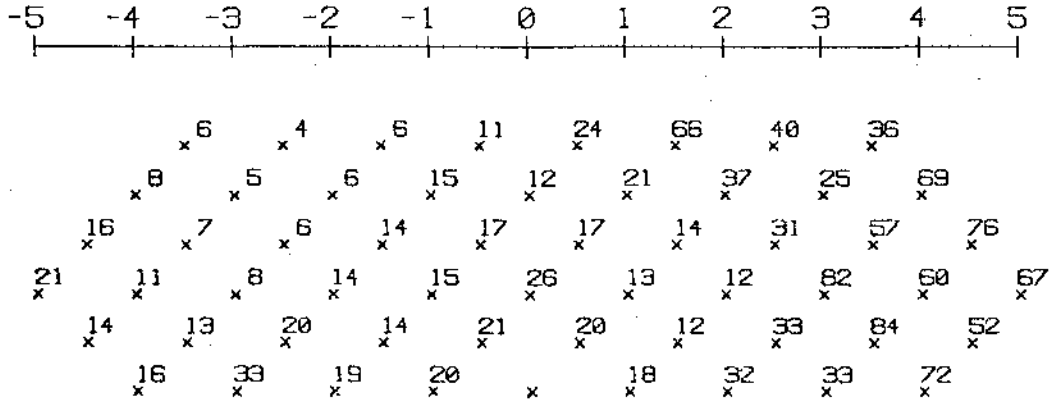

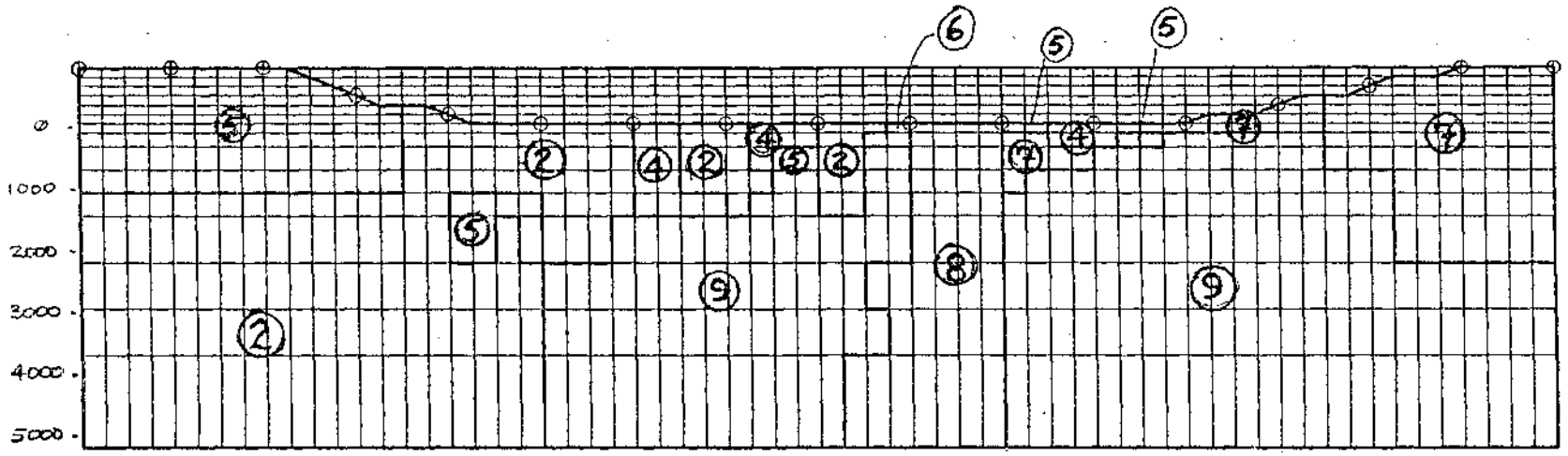


Line B3 (R3)

(2) 7 Ω-m
(3) 10 Ω-m
(4) 25 Ω-m
(5) 40.0 Ω-m
(6) 70 Ω-m
(7) 250 Ω-m
(8) 27.5 Ω-m
(9) 700 Ω-m

APPARENT RESISTIVITY - COMPUTED

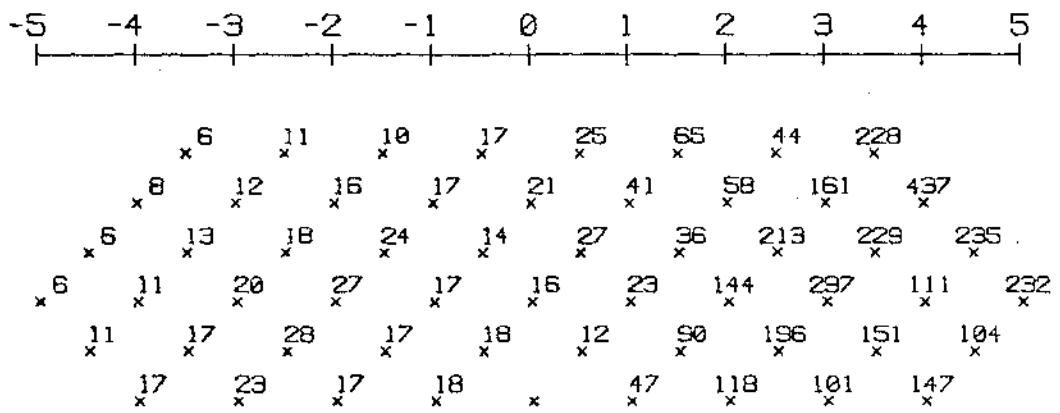

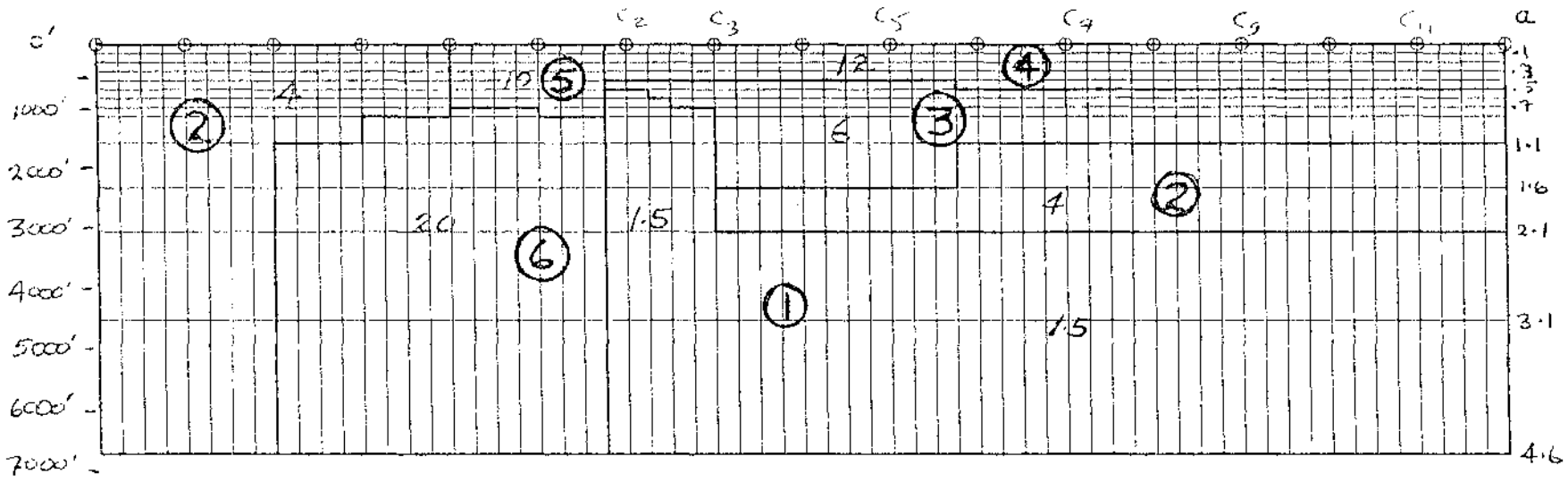


LINE R4

① 1.5 Ω-m

② 4 Ω-m

③ 6 Ω-m

④ 12 Ω-m

⑤ 10 Ω-m

⑥ 20 Ω-m

APPARENT RESISTIVITY - COMPUTED

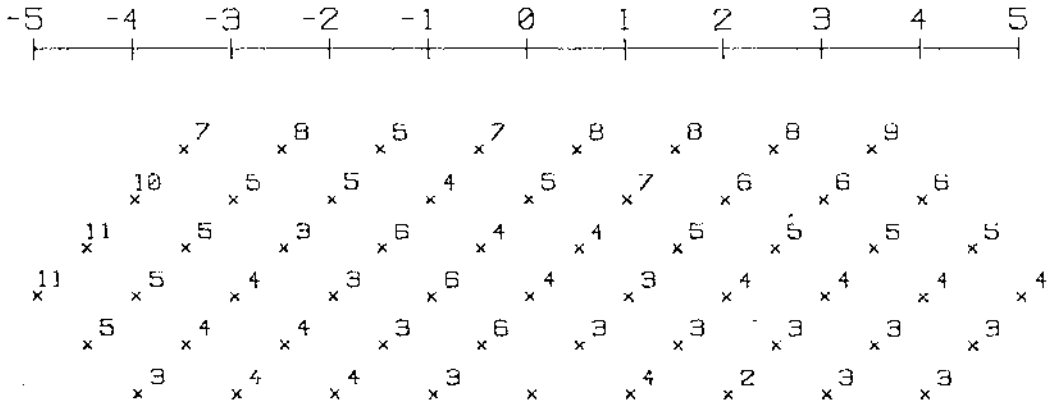

## REFERENCES


Bonham, H. F., 1969, Geology and mineral deposits of Washoe and Storey Counties, Nevada: Nevada Bureau of Mines and Geology, Bull. 70.

Bryant, G. T., 1969, The general geology of the northernmost part of the Pine Forest Mountains, Humboldt County, Nevada: Oregon State Univ., unpub. Master's thesis.

Burnham, R., 1971, The geology of the southern part of the Pueblo Mountains, Humboldt County, Nevada: Oregon State Univ., unpub. Master's thesis.

Carrier, D. L., 1979, Gravity and heat flow studies at Twin Peaks; an area of late Tertiary silicic volcanism in Millard County, Utah: unpub. M.S. thesis, Univ. of Utah, 120 p.

Clark, S. P., Jr. (Ed.), 1966, Handbook of physical constants: Geological Society of America, Memoir 97.

Corwin, R. F., and Hoover, D.B., 1979, The self-potential method in geothermal exploration: Geophysics, v. 44, no. 2, p. 226-246.

EPPC, 1979, 27 shallow thermal gradient holes-temp. and lithology: Univ. Utah Rsch. Inst., Earth Science Lab., OFR.

EEPC, 1980, Deep thermal gradient study of 3 holes to 1500 ft; temp. logs, drilling and completion histories, location map: Univ. Utah Rsch. Inst., Earth Science Lab., OFR.

Fox, R. C., Hohmann, G.W., and Rijo, L., 1978, Topographic effects in resistivity surveys: Univ. Utah Research Inst., Earth Science Laboratory, report no. 11, 105 p.

Gabbert, S. C., 1980, Gravity survey of parts of Millard, Beaver and Iron counties, Utah: unpub. M.S. thesis, Univ. Utah, 107 p.

Gardner, M. C., and Koenig, J.B., 1978, Photogeologic interpretation of the Baltazor-McGee (Painted Hills) geothermal prospects, Humboldt county, Nevada: Univ. Utah Rsch. Inst., Earth Science Lab. OFR.

Graichen, R. E., 1972, Geology of a northern part of the Pine Forest Mountains, northwestern Nevada: Oregon State Univ., unpub. Master's thesis.

Healy, D. L., 1966, Gravity and seismic study of Yucca Flat, Nevada Test Site, Nye County, Nevada, in Mining Geophysics (vol. 1): Society of Exploration Geophysicists, p. 84-93.

Hose, R. E. and Taylor, B. E., 1974, Geothermal systems of northern Nevada: U.S. Geol. Survey Open-File Report 74-271.

Hulen, J., 1979, Geology and alteration of the Baltazor Hot Springs and Painted Hills thermal areas, Humboldt County, Nevada: Univ. Utah Rsch. Inst., Earth Science Lab., report no. 27.

Killpack, T. J., and Hohmann, G. W., 1979, Interactive dipole-dipole resistivity and IP modeling of arbitrary two-dimensional structures (IP2D users guide and documentation): Univ. Utah Rsch. Inst., Earth Science Laboratory, report no. 15, 107 p.

Klein, C. W. and Koenig, J. B., 1977, Geothermal interpretation of groundwaters, Continental Lake region, Humboldt County, Nevada: Univ. Utah Rsch. Inst., Earth Science Lab., OFR.

Langenkamp, D., 1977, Temperature-gradient map of the Baltazor-McGee Mountain area, Humboldt County, Nevada: Univ. Utah Rsch. Inst., Earth Science Lab., OFR.

Lawrence, R. D., 1976, Strike-slip faulting terminates the Basin and Range province in Oregon: Geol. Soc. Amer. Bull. vol. 87, p. 846-850.

Long, C. L. and Senterfit, M., 1977, Audio-magnetotelluric data log and station location map for Baltazor Known Geothermal Resource Area, Nevada: U.S. Geological Survey OFR 77-65B, 5 p.

Mabey, D. R., 1960, Regional gravity survey of part of the Basin and Range Province in Geological Survey Research 1960: U.S. Geological Survey Prof. paper 400-B, p. 283-285.

Mining Geophysical Surveys, Inc., 1980, Resistivity and self-potential survey, Baltazor-McGee geothermal prospects, Humboldt County, Nevada: Univ. Utah Rsch. Inst., Earth Science Lab., OFR.

Montgomery, J. R., 1973, A regional gravity survey of western Utah: Univ. Utah, unpublished Ph.D. dissertation, 142 p.

Nettleton, L. L., 1976, Gravity and magnetics in oil prospecting: McGraw-Hill, New York.

Nutter, C., 1980, GRAV2D: an interactive 2 1/2 dimensional gravity modeling program (user's guide and documentation for Rev. 1): Univ. Utah Rsch. Inst., Earth Science Lab., report no. 42.

Peterson, D. L., and Hoover, D. B., 1977, Principal facts for a gravity survey of Baltazor Known Geothermal Resource Area, Nevada: U.S. Geological Survey, OFR, 77-67C, 4 p.

Plouff, D., 1977, Preliminary documentation for a FORTRAN program to compute gravity terrain corrections based on topography digitized on a geographic grid: U.S. Geol. Survey open-file report 77-535.

Plouff, D., Robbins, S. L., and Holden, K. D., 1976, Principal facts for gravity observations in the Charles Sheldon Antelope Range, Nevada - Oregon: U.S. Geological Survey, OFR, 76-601, 22 p.

Ratte, J. C., and others, 1979, Mineral resources of the Gila Primitive Area and Gila Wilderness, Catron and Grant Counties, New Mexico: U.S. Geological Survey Bulletin 1451, 229 p.

Rijo, L., 1977, Modeling of electric and electromagnetic data: Ph.D. Dissertation, Univ. Utah, Dept. of Geology and Geophysics, 242 p.

Ross, H. P., 1979, Numerical modeling and interpretation of dipole-dipole resistivity and IP profiles, Cove Fort - Sulphurdale KGRA, Utah: Univ. Utah Rsch. Inst., Earth Science Lab., report no. 26.

Rowe, W. A., 1971, Geology of the south-central Pueblo Mountains, Oregon-Nevada: Oregon State Univ., unpub. Master's thesis.

Sass, J. H., Lachenbruch, A. H., Munroe, R. J., Greene, G. W., and Moses, T. H., 1971, Heat flow in the western United States: Journ. Geophys. Research, v. 76, no. 26, p. 6376-6413.

Scintrex Mineral Surveys, Inc., 1972, Aeromagnetic Map of the Baltzaor-McGee Geothermal Prospects: Univ. Rsch. Inst. Utah, Earth Science Lab., OFR.

Senturion Sciences, Inc. 1977, Northwestern Nevada microearthquake survey report: Univ. Utah Rsch. Inst., Earth Science Lab., OFR.

Serpa, L. F., 1980, Detail gravity and aeromagnetic surveys in the Black Rock Desert Area, Utah: M.S. Thesis, Univ. Utah, 211 p.

Sill, W. R., and Johng, D. S., 1979, Self potential survey, Roosevelt Hot Springs, Utah: Univ. of Utah DOE/DGE Rpt. IDO/78-1701. a.2.3.

Smith, J. D., 1973, Geologic map of the Duffer Peak quadrangle, Humboldt County, Nevada: U.S. Geol. Survey Misc. Invest. Map I-606.

Snow, J. H., 1978, A study of structural and tectonic patterns as interpreted from gravity and aeromagnetic data: unpub. M.S. Thesis, Univ. Utah, 206 p.

Swick, C. H., 1942, Pendulum gravity measurements and isostatic reductions: U.S. Coast and Geodetic Survey Spec. Pub. 232.

Ward, S. H., and Sill, W. R., 1976, Dipole-dipole resistivity surveys, Roosevelt Hot Springs KGRA: NSF final rep., v. 2, grant GI-43741, Univ. Utah, 29 p.

Wendell, W. G., 1969, The structure and stratigraphy of the Virgin Valley-McGee Mountain area, Humboldt County, Nevada: Oregon State Univ., unpub. Master's thesis.

Willden, R., 1961, Preliminary geologic map of Humboldt county, Nevada: U.S. Geol. Survey Misc. Field Studies Map MF-236.

Willden, R., 1964, Geology and Mineral deposits of Humboldt County, Nevada: Nev. Bur. Mines and Geol., Bull. 59.

# VITA

| | |
|---|---|
| Name | Ronald K. Edquist |
| Birthdate | November 12, 1951 |
| Birthplace | Kenosha, Wisconsin |
| High School | Mary D. Bradford High School<br>Kenosha, Wisconsin |
| University | |
| 1969-1970 | Wisconsin State University<br>at Platteville<br>Platteville, Wisconsin |
| 1970-1974 | University of Alaska<br>Fairbanks, Alaska |
| Degrees | |
| 1974 | B.Sc. Mining Engineering<br>B.Sc. Geological Engineering<br>University of Alaska<br>Fairbanks, Alaska |
| Graduate Study | |
| 1977-1978 | Michigan Technological University<br>Houghton, Michigan |
| 1978-1980 | University of Utah<br>Salt Lake City, Utah |
| Professional Society | Society of Exploration Geophysicists |
| Professional Positions | Chief Engineer, Ground Preparation, Alaska Gold Co., Inc., Nome, Alaska, 1974-1977; Research Assistant, Department of Geology and Geophysics, University of Utah, Salt Lake City, Utah, 1980 |